

# A study on the removal of common analgesics from waste water, using zeolites Clinoptilolite and Beta

Laura J. Snelgrove BSc(Hons)

A thesis submitted in partial fulfilment for the requirements for the degree of Masters  
by research at the University of Central Lancashire

January 2017



STUDENT DECLARATION FORM

**Concurrent registration for two or more academic awards**

Either

\*I declare that while registered as a candidate for the research degree, I have not been a registered candidate or enrolled student for another award of the University or other academic or professional institution

Or

~~\*I declare that while registered for the research degree, I was with the University's specific permission, a \*registered candidate/\*enrolled student for the following award:~~

---

**Material submitted for another award**

Either

\*I declare that no material contained in the thesis has been used in any other submission for an academic award and is solely my own work

Or

~~\*I declare that the following material contained in the thesis formed part of a submission for the award of~~

---

*\* delete as appropriate*

**Collaboration**

Where a candidate's research programme is part of a collaborative project, the thesis must indicate in addition clearly the candidate's individual contribution and the extent of the collaboration. Please state below:

**Signature of Candidate** Laura Jean Snelgrove

**Type of Award** Masters By Reseach

**School** School of Physical and Computational Sciences

## Acknowledgments

I am using this opportunity to express my gratitude to Dr. Jennifer Readman and Chris Smalley, along with my friends and family who supported me. I am thankful for their aspiring guidance, invaluable constructive criticism and friendly advice during the project work.

## Abstract

Over the last few decades the use of pharmaceuticals has increased to a high level. Used by both humans and animals, pharmaceutical active compounds (PACs) are not completely metabolised inside their bodies. Consequently, PACs are excreted through urine or faeces and together, with the products of metabolisation, they enter wastewaters as biologically active substances. Pharmaceuticals form a large group of compounds that are often polar molecules, therefore, are usually soluble in water. Thus, many PACS cannot be completely removed from wastewaters; hence, are found globally in a wide range of environmental samples including: sewage treatment plant effluents, surface, ground and even in drinking water.

The amounts of PACs detected in the environment are usually very low; they are often detected in trace concentrations (ng/L). However, the long-term discharge of PACS may cause potential risk to both aquatic and terrestrial organisms. Therefore, this research focuses on the removal of the common analgesics; acetaminophen and ibuprofen using zeolites as the absorbent. Zeolites have attracted great attention as they are affordable materials that can be modified so to adjust or even tailor their adsorptive possibilities. The zeolites clinoptilolite and beta (BEA) were used as the absorbents and were ion-exchanged with Cu(II), Fe(III) and  $\text{NH}_4^+$  ions, with the aim of removing acetaminophen and ibuprofen from water. IR, XRD, HPLC and BET experiments were performed to measure uptake of the pharmaceuticals. It was found that both zeolites were able to adsorb the pharmaceuticals in question, however, HPLC results showed clinoptilolite to be the better adsorbent. The best uptake was exhibited by Cu-exchanged clinoptilolite with the highest adsorption affinity towards ibuprofen. It is believed that ibuprofen degraded during the adsorption experiments to produce ions that form stable complexes with the cations.

# Contents

## Chapter 1: Introduction

- 1.1 Introduction      pg.18
  
- 1.2 Occurrence of Pharmaceuticals      pg. 22
  
- 1.3 Advances in Analytical and Detection Methods      pg.23
  
- 1.4 The Fate in the Environment receiving Pharmaceutical Active Compounds      pg.24
  - 1.4.1 Adverse Effects on Organisms in the Environment      pg.24
  - 1.4.2 Feminisation of Fish      pg.26
  
- 1.5 Removal of Pharmaceutical Waste from water      pg.27
  - 1.5.1 Waste Water from the Pharmaceutical Industry      pg.28
  - 1.5.2 Recovery Processes      pg.28
  - 1.5.3 Activated Carbon      pg.29
  - 1.5.4 Advanced oxidation processes      pg.29
    - 1.5.4.1 *Ozone/Hydrogen Peroxide Treatment*      pg.30
    - 1.5.4.2 *Electrochemical Oxidation/Degradation*      pg.30
  - 1.5.5 Conclusion      pg.31
  
- 1.6 The Removal of PACs from Wastewater by Adsorption      pg.32
  
  
- 1.7 Introduction to Zeolites      pg.32
  - 1.7.1 Zeolites as Ion-Exchangers      pg.34
  - 1.7.2 Zeolites as Molecular Sieves      pg.35
  - 1.7.3 Other Applications and Uses of Zeolites      pg.37
  - 1.7.4 Clinoptilolite      pg.38
  - 1.7.5 Applications of Clinoptilolite      pg.40
    - 1.7.5.1 *Surfactant Modified Clinoptilolite*      pg.40
    - 1.7.5.2 *Removal of Pollutants by Ion-exchange and adsorption*      pg.40
  - 1.7.6 Zeolite Beta      pg.41
  
- 1.8 Porous Silicates as Pharmaceutical Adsorbents      pg.42
  
- 1.9 Drug Molecules Used in This Research      pg.45
  - 1.9.1 Ibuprofen      pg.45
  - 1.9.2 Acetaminophen      pg.47

1.10 Introduction to Drug Adsorption pg.49

1.11 Research Proposal pg.50

## Chapter 2: Experimental Techniques

2.1 Powder X-Ray Diffraction pg.52

2.1.1 XRD Experimental pg.56

2.2 An Introduction to High Performance Liquid Chromatography pg.58

2.2.1 HPLC Experimental pg.60

2.3 An Introduction to Infra-Red Spectroscopy pg.61

2.3.1 IR Experimental pg.62

2.4 Introduction to Solid State Nuclear Magnetic Resonance (MAS NMR) pg.63

2.4.1 MAS NMR Experimental pg.64

2.5 An Introduction to Scanning Electron Microscope pg.65

2.6 An Introduction to Energy Dispersive X-ray Spectroscopy pg.66

2.6.1 SEM Experimental pg.67

2.7 BET Isotherm pg.68

2.7.1 BET Experimental pg.69

2.8 The Zeolites and Pharmaceuticals used in this Research Project pg.70

## Chapter 3: Results and Discussion

3.1 Adsorption by Clinoptilolite pg.71

3.1.1 HPLC Results pg.71

3.1.2 IR Results pg.72

3.1.3 Acetaminophen XRD Results pg.73

3.1.4 Na-Ibuprofen XRD Results pg.79

3.2 Adsorption by Japanese Clinoptilolite	pg.83
3.2.1 HPLC Results	pg.83
3.2.2 XRD Results for Acetaminophen	pg.84
3.2.3 XRD Results for Na-Ibuprofen	pg.88
3.3 Ion-Exchange of Clinoptilolite	pg.92
3.3.1 SEM-EDX Results	pg.92
3.3.2 HPLC Results	pg.94
3.3.3 XRD Results for Cu-exchanged Clinoptilolite Samples	pg.95
3.4 Adsorption using Zeolite Beta	pg.106
3.4.1 Ion-exchange	pg.106
3.4.2 HPLC Results	pg.108
3.4.3 XRD results for BEA-NH <sub>4</sub> Ion-exchanged with Fe	pg.110
3.5 <sup>29</sup> -Si NMR Results	pg.116
3.6 BET Results	pg.118
<b>Chapter 4: Conclusion and Future work</b>	<b>pg.120</b>
<b>Chapter 5: References</b>	<b>pg.124</b>

# List of Tables

*Table 1.1 - A table reporting a few examples of pharmaceuticals found in the environment and their impact on the environment*      pg.25

*Table 2.1 -The HPLC parameters used for quantifying adsorption of acetaminophen and Na-ibuprofen*  
pg.60

*Table 2.2 – Parameters used for all <sup>29</sup>Si MAS NMR*    pg.64

*Table 2.3 – The names of the zeolites used and the company they were bought from*      pg.70

*Table 2.4 – List of chemicals used for cation exchange and the company they were bought from*    pg.70

*Table 3.1.1 – Percentage of drug uptake by clinoptilolite determined by HPLC*    pg.71

*Page Table 3.1.2 – Intensity changes of peak 2 and 3, relative to peak 1, for all for the three XRD patterns in Figure 3.1.2*    pg.74

*Table 3.1.3 – The  $R_{wp}$  values of the Pawley fits in figure 3.1.5*    pg.76

*Table 3.1.4 – Intensity changes of peak 2 and 3, relative to peak 1, for all for the three XRD patterns in Figure 3.1.6*      pg.80

*Table 3.1.5 – The  $R_{wp}$  values of the Pawley fits in figure 3.1.7*    pg.80

*Table 3.2.1 – Percentage of drug uptake by Japanese clinoptilolite determined by HPLC*    pg.84

*Table 3.2.2 – Intensity changes of peak 2, 3 and 4, in respect to peak 1, for all for the three XRD patterns in Figure 3.2.1*    pg.84

*Table 3.2.3 – The  $R_{wp}$  values of the Pawley fits in figure 3.2.3*    pg.86

*Table 3.2.4 – Intensity changes of peak 2, 3 and 4, relative to peak 1, for all of the three XRD patterns in Figure 3.2.4*      pg.89

*Table 3.2.5 – The  $R_{wp}$  values of Pawley fits in figure 3.2.6*      pg.90

Table 3.3.1 – Results of EDX analyses for each of the four clinoptilolite samples in wt%. The chemical compositions correspond to average values obtained from 5 area measurements (1-2mm<sup>2</sup>) pg.93

Table 3.3.2- Results of EDX analyses for each of the four Japanese clinoptilolite samples in wt%. The chemical compositions correspond to average values obtained from 5 area measurements (1-2mm<sup>2</sup>) pg.93

Table 3.3.3 – Percentage uptake of Acetaminophen by clinoptilolite samples determined by HPLC pg.94

Table 3.3.4 – Percentage uptake of Acetaminophen by Japanese clinoptilolite samples determined by HPLC pg.94

Table 3.3.5 – Percentage uptake of Na-ibuprofen by clinoptilolite samples determined by HPLC pg.95

Table 3.3.6 – Percentage uptake of Na-ibuprofen by clinoptilolite samples determined by HPLC pg.95

Table 3.3.7 – Intensity changes of peak 2, 3 and 4, relative to peak 1, for all of the three XRD patterns in Figure 3.3.4 pg.98

Table 3.3.8 – Intensity changes of peak 2, 3 and 4, relative to peak 1, for all of the three XRD patterns in Figure 3.3.1 pg.98

Table 3.3.9 - The  $R_{wp}$  values of the Pawley fits in figure 3.3.11 pg.103

Table 3.3.10 - The  $R_{wp}$  values of the Pawley fits in figure 3.3.12 pg.103

Table 3.4.1- Results of EDX analyses for each of the four BEA-H samples in wt%. The chemical compositions correspond to average values obtained from 5 area measurements (1-2mm<sup>2</sup>) pg.107

Table 3.4.2- Results of EDX analyses for each of the three BEA-NH<sub>4</sub> samples in wt%. The chemical compositions correspond to average values obtained from 5 area measurements (1-2mm<sup>2</sup>) pg.107

Table 3.4.3 – Percentage uptake of Na-Ibuprofen by Beta Hydrogen (X) samples determined by HPLC pg.109

Table 3.4.4 – Percentage uptake of Na-Ibuprofen by Beta Ammonia (Y) samples determined by HPLC pg.109

Table 3.4.5 – Percentage uptake of Acetaminophen by Beta Hydrogen (X) samples determined by HPLC pg.109

Table 3.4.6 – Percentage uptake of Acetaminophen by Beta Ammonia (Y) samples determined by HPLC pg.109

Table 3.4.7 - The  $R_{wp}$  values of the Pawley fits in figure 3.4.3 pg.111

Table 3.5.1. – Si:Al results for the four initial zeolites as supplied without modification pg.116

*Table 3.6.1 – BET results showing the micropore volume (cm<sup>3</sup>/g) for the following samples: 1) Moroccan clinoptilolite standard, 2) Moroccan clinoptilolite adsorbed with acetaminophen and 2) Moroccan clinoptilolite adsorbed with Na-ibuprofen pg.118*

*Table 3.6.2 –BET results showing the micropore volume (cm<sup>3</sup>/g) for the following samples: 1) Japanese clinoptilolite standard, 2) Japanese clinoptilolite adsorbed with acetaminophen and 2) Japanese clinoptilolite adsorbed with Na-ibuprofen pg.118*

# List of Figures

Figure 1.1 – A diagram showing the concentrations detected for PACs in different parts of the environment pg.20

Figure 1. 2- Diagram to show how in a zeolite each “T” atom (in blue) is co-ordinated to four atoms. Then each oxygen atom (in red) is bonding to two “T” atoms. Pg.33

Figure 1.3 - The structure of the natural occurring zeolite Clinoptilolite pg.39

Figure 1.4 - Framework structures of (a) polymorph A, (b) polymorph B, and (c) polymorph C of zeolite beta, showing the different stackings of the 12-ring pores as (a) ABAB. . . , (b) ABCABC. . . , and (c) AA. . . pg.41

Figure 1.5 – Image of zeolite Y pg.44

Figure 1.6 - Chemical structure of Na-Ibuprofen, Na is represented by the purple atom, O is represented by the red atoms and C is represented by the grey atoms. pg.45

Figure 1.7- Chemical structure of Acetaminophen, oxygen is represented by the red atoms, nitrogen is represented by the purple atom and carbon is represented by the grey atoms pg.47

Figure 2.1 – Diagram of Bragg’s law pg.53

Figure 2.2 -The configuration of a typical HPLC system pg.59

Figure 2.3 - The positions of <sup>29</sup>Si NMR peaks in silicates as a function pg.64

Figure 3.1.1 – Comparison of IR Spectra of clinoptilolite before and after adsorption pg.72

Figure 3.1.2 – Comparison of the XRD pattern of clinoptilolite adsorbed with acetaminophen against the XRD pattern of the clinoptilolite standard and the XRD pattern of clinoptilolite with zero mixing time. XRD patterns and peaks labelled with reference to table 3.1.2 pg.73

Figure 3.1.3– Polyhedral image of clinoptilolite looking along the c-axis p g.75

Figure 3.1.4 – Change in the unit cell lattice parameters of clinoptilolite before and after adsorption (1) clinoptilolite with no mixing, 2) clinoptilolite standard, 3) clinoptilolite mixed with acetaminophen for 24 hours pg.76

Figure 3.1.5 – Pawley fits obtained for 1) clinoptilolite with zero hours mixing 2) clinoptilolite standard 3) clinoptilolite mixed with acetaminophen for 24 hours pg.78

Figure 3.1.6 – Comparison of the XRD pattern of clinoptilolite adsorbed with Na-ibuprofen against the XRD pattern of the clinoptilolite standard and the XRD pattern of clinoptilolite with zero mixing time. XRD patterns and peaks labelled with reference to table 3.1.4 pg.80

Figure 3.1.7 – Pawley fits for 1) Clinoptilolite with zero hours mixing time 2) Clinoptilolite standard 3) Clinoptilolite with Na-ibuprofen pg.81

Figure 3.1.8– Change in the unit cell lattice parameters of Clinoptilolite before and after adsorption (1) Clinoptilolite with no mixing, 2) Clinoptilolite standard, 3) Clinoptilolite mixed with Na-Ibuprofen for 24 hours) pg.82

Figure 3.2.1 – Comparison of the XRD pattern of Japanese clinoptilolite adsorbed with acetaminophen against the XRD pattern of the Japanese clinoptilolite standard and the XRD pattern of Japanese clinoptilolite with zero mixing time. XRD patterns and peaks labelled with reference to table 3.2.2 pg.84

Figure 3.2.2 – Change in the unit cell lattice parameters of Japanese clinoptilolite before and after adsorption (1) Japanese clinoptilolite with no mixing, 2) Japanese clinoptilolite standard, 3) Japanese clinoptilolite mixed with acetaminophen for 24 hours) pg.85

Figure 3.2.3 – Pawley fits obtained for 1) Japanese clinoptilolite mixed for 0 hours 2) Japanese clinoptilolite standard 3) Japanese clinoptilolite mixed with acetaminophen for 24 hours pg.87

Figure 3.2.4 – Comparison of the XRD pattern of Japanese clinoptilolite adsorbed with Na-ibuprofen against the XRD pattern of the Japanese clinoptilolite standard and the XRD pattern of Japanese clinoptilolite with zero mixing time. XRD patterns and peaks labelled with reference to table 3.2.4 pg.89

Figure 3.2.5 – Change in the unit cell lattice parameters of Japanese clinoptilolite before and after adsorption (1) Japanese clinoptilolite with no mixing, 2) Japanese clinoptilolite standard, 3) Japanese clinoptilolite mixed with Na-ibuprofen for 24 hours) pg.90

Figure 3.2.6 – Pawley fits obtained for 1) Japanese clinoptilolite mixed for 0 hours 2) Japanese clinoptilolite Standard 3) Japanese clinoptilolite mixed with Na-ibuprofen for 24 hours pg.91

Figure 3.3.1 – Comparison of the XRD pattern of clinoptilolite Cu-exchanged adsorbed with acetaminophen against the XRD pattern of the clinoptilolite Cu-exchanged standard, and the XRD pattern of clinoptilolite with zero mixing time. XRD patterns and peaks labelled with reference to table 3.3.8 pg.97

Figure 3.3.2 – Comparison of the XRD pattern of clinoptilolite Cu-exchanged adsorbed with Na-ibuprofen against the XRD pattern of the clinoptilolite Cu-exchanged standard, the XRD pattern of clinoptilolite with zero mixing time and the XRD pattern of Na-ibuprofen. Pg.97

Figure 3.3.3 – Comparison of the XRD pattern of Japanese clinoptilolite Cu-exchanged adsorbed with Na-ibuprofen against the XRD pattern of the Japanese clinoptilolite Cu-exchanged standard, the XRD pattern of Japanese clinoptilolite with zero mixing time and the XRD pattern of Na-ibuprofen. Pg.99

Figure 3.3.4 – Comparison of the XRD pattern of Japanese clinoptilolite Cu-exchanged adsorbed with acetaminophen against the XRD pattern of the Japanese clinoptilolite Cu-exchanged standard, and the XRD pattern of Japanese clinoptilolite with zero mixing time. XRD patterns and peaks labelled with reference to table 3.3.7 pg.99

Figure 3.3.5 – Identification of new peaks found in the diffraction pattern of Japanese clinoptilolite Cu-exchanged adsorbed with Na-ibuprofen. The diffraction pattern of Copper propionate is represented by the blue lines and the green lines represent the diffraction pattern from clinoptilolite pg.100

Figure 3.3.6 – Change in the unit cell lattice parameters of Cu-exchanged clinoptilolite before and after adsorption (1) Cu-exchanged clinoptilolite with no mixing, 2) Cu-exchanged, clinoptilolite standard, 3) Cu-exchanged, clinoptilolite mixed with acetaminophen for 24 hours pg.101

Figure 3.3.7 – Change in the unit cell lattice parameters of Cu-exchanged clinoptilolite before and after adsorption (1) Cu-exchanged clinoptilolite with no mixing, 2) Cu-exchanged, clinoptilolite standard, 3) Cu-exchanged, clinoptilolite mixed with Na-ibuprofen for 24 hours pg.101

Figure 3.3.8 – Change in the unit cell lattice parameters of Cu-exchanged, Japanese clinoptilolite before and after adsorption (1) Cu-exchanged, Japanese clinoptilolite with no mixing, 2) Cu-exchanged, Japanese clinoptilolite standard, 3) Cu-exchanged, Japanese clinoptilolite mixed with acetaminophen for 24 hours pg.102

Figure 3.3.9 – Change in the unit cell lattice parameters of Cu-exchanged, Japanese clinoptilolite before and after adsorption (1) Cu-exchanged, Japanese clinoptilolite with no mixing, 2) Cu-exchanged, Japanese clinoptilolite standard, 3) Cu-exchanged, Japanese clinoptilolite mixed with Na-ibuprofen for 24 hours pg.102

Figure 3.3.10 – Pawley fits for 1) clinoptilolite, Cu-exchanged, 0 hours mixing time, 2) clinoptilolite, Cu-exchanged, standard, 3) clinoptilolite, Cu-exchanged, 24 hour mix with acetaminophen, 4) clinoptilolite, 24 hour mix with Na-ibuprofen pg.104

Figure 3.3.11 - Pawley fits for 1) Japanese clinoptilolite, Cu-exchanged, 0 hours mixing time, 2) Japanese Clinoptilolite, Cu-exchanged, standard, 3) Japanese clinoptilolite, Cu-exchanged, 24 hour mix with acetaminophen, 4) Japanese clinoptilolite, 24 hour mix with Na-ibuprofen pg.105

Figure 3.4.1– Change in the unit cell lattice parameters of Fe-exchanged, BEA-NH<sub>4</sub> before and after adsorption (1) Fe-exchanged, BEA-NH<sub>4</sub> with no mixing, 2) Fe-exchanged, BEA-NH<sub>4</sub> standard, 3) Fe-exchanged, BEA-NH<sub>4</sub> mixed with acetaminophen for 24 hours pg.110

Figure 3.4.2– Change in the unit cell lattice parameters of Fe-exchanged, BEA-NH<sub>4</sub> before and after adsorption (1) Fe-exchanged, BEA-NH<sub>4</sub> with no mixing, 2) Fe-exchanged, BEA-NH<sub>4</sub> standard, 3) Fe-exchanged, BEA-NH<sub>4</sub> mixed with Na-ibuprofen for 24 hours pg.111

Figure 3.4.3– Pawley fits obtained for (1) Fe-exchanged, BEA-NH<sub>4</sub> with no mixing, 2) Fe-exchanged, BEA-NH<sub>4</sub> standard, 3) Fe-exchanged, BEA-NH<sub>4</sub> mixed with acetaminophen for 24 hours and 4) Fe-exchanged, BEA-NH<sub>4</sub> mixed with Na-ibuprofen for 24 hours pg.112

Figure 3.4.4 – Identification of new peaks found in the diffraction pattern of Na-ibuprofen adsorbed by BEA-NH<sub>4</sub>, ion-exchanged with Fe. The diffraction pattern of copper acetate hydroxide hydrate e is represented by the blue lines pg.113

Figure 3.4.5 – Comparison of the diffraction pattern of BEA-NH<sub>4</sub>, Fe-exchanged adsorbed with Na-ibuprofen against the XRD pattern of BEA-NH<sub>4</sub>, Fe-exchanged, standard, the diffraction pattern of BEA-NH<sub>4</sub>, Fe-exchanged, with zero mixing time, and the diffraction pattern of Na-ibuprofen pg.114

Figure 3.4.6 – Comparison of the diffraction pattern of BEA-NH<sub>4</sub>, Fe-exchanged adsorbed with Acetaminophen against the diffraction pattern of BEA-NH<sub>4</sub>, Fe-exchanged, standard and the diffraction pattern of BEA-NH<sub>4</sub>, Fe-exchanged, with zero mixing time pg.115

# List of Equations

*Equation 1.1 – showing an equation expressing ion-exchange at equilibrium* pg.35

*Equation 2.1- Equation for Bragg's law* pg.52

*Equation 2.2 – The equation used to calculate the intensity of a given peak within a diffraction* pg.54

*Equation 2.3 – Scherrer equation* pg.55

*Equation 2.4 – The weight profile R-factor ( $R_{wp}$ ) equation* pg.56

*Equation 2.5 – Equation for wavenumber* pg.61

*Equation 2.6 – The equation for wavelength* pg.61

*Equation 2.7 – Planks law equation* pg.62

*Equation 2.8- The BET equation expressed in linear form* pg.69

*Equation 3.1 – Equation for Si:Al ratio* pg.116

# List of Abbreviations

PACs	Pharmaceutically Active Compounds
BEA	Beta
CECs	Contaminants of Emerging Concern
EPs	Emerging Pollutants
ERA	Environmental Risk Assessment
EQs	Environmental Quality Standard
GC	Gas Chromatography
GC-MS	Gas Chromatography, Mass Spectrometry
GC-MS/MS	Gas Chromatography, Tandem Mass Spectrometry
LC-MS	Liquid Chromatography, Mass Spectrometry
LC-MS/MS	Liquid Chromatography, Tandem Mass Spectrometry
FDA	Food and Drug Administration
EE2	Ethinyl Estradiol
AOPs	Advanced Oxidation Processes
NF	Nanofiltration
AC	Activated Carbon
TOC	Total Organic Carbon
BDD	Boron Doped Diamond
IZA	International Zeolite Association
HDTMA	Hexa-decyl-tri-methyl-ammonium
ERY	Erythromycin
CBZ	Carbamazepine
FLX	Levofloxacin

NSAID	Nonsteroidal Anti-Inflammatory Drug
XRD	X-ray Diffraction
R <sub>wp</sub>	Weight Profile R-factor
HPLC	High Performance Liquid Chromatography
IR	Infra-red
FT	Fourier Transformation Method
NMR	Nuclear Magnetic Resonance
MAS	Mass Angle Spinning
SEM	Scanning Electron Microscope
TEM	Transmission Electron Microscope
EDX	Energy Disperse X-ray Spectroscopy
BET	Brunauer, Emmett and Teller
BEA-H	Beta, Hydrogen Form
BEA- NH <sub>4</sub>	Beta, Ammonium Form

# Chapter 1: Introduction

## 1.1 Introduction

Pharmaceutical products have increased both the quality of life and life expectancy across the globe. In the last decade, low traces of pharmaceuticals, typically at levels in the ng/L have been detected in the environment [1]. The presence of pharmaceutical substances in water has raised concerns among stakeholders, such as drinking-water regulators, governments, water suppliers and the public. In the long term, pharmaceuticals in the aquatic environment may cause potential risk towards both aquatic and terrestrial organisms. Moreover, continuous discharge of pharmaceuticals may have physiological effects on humans and animals even in very low (trace) concentrations. It has been proven that pharmaceuticals in the environment are persistent or pseudo-persistent [2,3] and toxic to organisms [4,5,6]. They also have the potential for bioaccumulation in organisms of different trophic levels [7,8], causing aquatic toxicity, development of resistance in pathogenic microbes, genotoxicity and endocrine disruption [9,10,11,12]. Therefore, pharmaceutically active compounds (PACs) are classified as “contaminants of emerging concern” (CECs), [9] or “emerging pollutants” (EPs). Although these chemicals have been released into the environment since they first started production, they have only been recently discovered in the environment [13] becoming an important threat to wildlife and also creating problems for the drinking water industry.

Pharmaceuticals form a large group of synthetic or natural compounds used in human and veterinary medicine, as well as, aquaculture and agricultural products. They are not necessarily a class of substances, as they have no chemical, physical, structural or biological similarities connecting them, meaning there is no overall class of chemicals that pharmaceuticals can be ordered into. However, the large quantities produced and used has

led to the continual release of a wide array of pharmaceutical chemicals into our environment. Often being polar molecules, PACs are usually soluble in water. Therefore, many PACs cannot be completely removed from wastewaters and as a result they can be found in a wide range of environmental samples including the sewage treatment plant effluents [9,14,15], ground and even drinking water, all over the world [16, 17, 18, 19].

PACs in humans and animal drugs are not completely metabolised inside their bodies. Consequently, PACs are excreted through urine or faeces and together with their metabolites enter into wastewaters as biologically active substances. Therefore, PACs in water sources and drinking-water are often present at trace concentrations. Also, PACs are released during manufacturing, as well as by disposal of unused or expired drugs [9,10,20].

The main sources of waste from pharmaceutical and personal care products are prescription and over-the-counter drugs, fragrances, cosmetics, veterinary drugs and vitamin supplements. Humans are exposed to these PACs through their drinking water or from bioaccumulation in the food chain. As illustrated in figure 1.1, sources and pathways have been well identified, with the main route of release from human and animal excretion. Hospitals play a large contributing factor as their sewage effluents and medical waste include a large array of different PACs. Pharmaceuticals can also enter the environment through wastewater effluent, treated sewage sludge, industrial waste, medical waste from health-care and veterinary facilities, landfill leachate and biosolids [21].

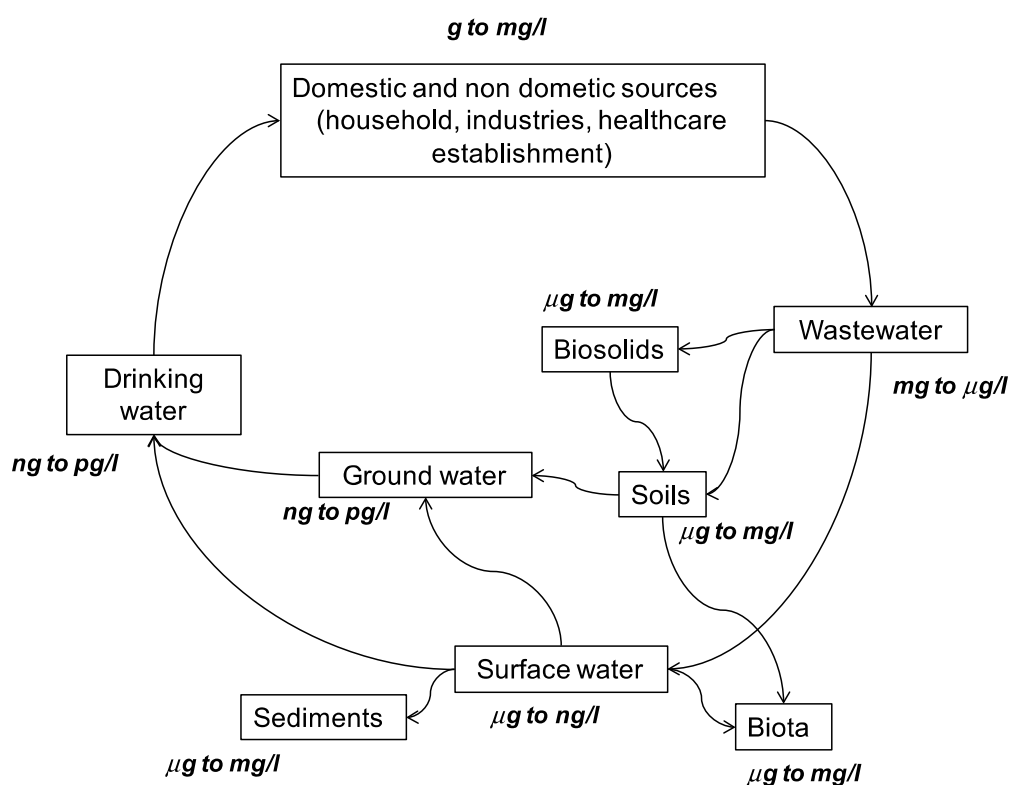


Figure 1.1 – A diagram showing the concentrations detected for PACs in different parts of the environment [22]

Regulations regarding pharmaceutical residues in the environment are quite limited in spite there being several good procedures in place. Following the European Guidelines, the Environmental Risk Assessment (ERA) of pharmaceuticals can identify “substances of concern” before market authorisation, but, this procedure is not applied to “old” pharmaceuticals already in use. Even with the gaps in the ERA legislations identified, they still have not addressed issues in other legislations, such as the Groundwater Directive, relating to antimicrobial resistance in the environment.

In 2008, the European Commission recognised that pharmaceutical residues are polluting waters and soils and this is seen as an emerging environmental problem and a public health concern. Then in another communication in 2011, the European Commission proposed an

action plan against the rising threats from antimicrobial resistance. It was also noted in the communication that the antimicrobials polluting the environment are contributing to the acceleration of the emergence and spread of resistant microorganisms.

In 2012, on the basis of data regarding risks to the aquatic environment, particularly to fish, the commission proposed the inclusion of three pharmaceutical substances, 17-alpha ethinylestradiol, 17-beta estradiol and diclofenac, in the list of Priority Substances under the Water Framework Directive, but on a special "watch list", meaning they will be monitored but not yet have an Environmental Quality Standard (EQS) set for them. The European Commission has also committed to developing a strategic approach on pharmaceuticals in the environment. This might include legislative and non-legislative solutions, such as development of improved source-control approaches and end-of-pipe solutions, and improved data-sharing to ensure a consistent basis for ERA [23].

## 1.2 Occurrence of Pharmaceuticals

The worldwide pharmacopeia has approximately 3500 pharmaceutical molecules listed and over 10% of these compounds have been detected in aquatic and terrestrial environments. With this being said, there is no routine monitoring programmes to test drinking water for pharmaceuticals. Generally, data collected are from ad hoc surveys or targeted research projects. Data collected show that pharmaceuticals have mainly been detected and measured in surface water [24,25,26] and wastewater effluents [27,28,29,30], ground water, marine water, drinking water [31,32,33,34,35], biosolids [36,37], sediments [38,39], soils [40,41,42] and biota [22,43,44,45].

Antibiotics and anti-inflammatories have been measured and detected in sewage treatment effluents and surface waters worldwide. In general, results gathered show that PACs belonging to this therapeutic class are present, more than 40% of the time, in collected samples with concentrations for half of them  $<0.1 \mu\text{gL}^{-1}$ . Ibuprofen, carbamazepine, diclofenac and sulfamethoxazole are the PACs detected in effluents at the highest concentration, as they are sold in highest quantities. In fact, they have been measured and recorded in water samples from around 70% of the different countries where water has been sample [46]. Whereas, acetylsalicylic acid has been detected at much lower concentrations compared to salicylic acid in the aquatic environment. This is because salicylic acid is the degradation product from a number of compounds, including acetylsalicylic acid [22,47].

Other analgesics and anti-inflammatories at lower concentrations have been detected in sewage effluents samples, surface waters, ground water samples and drinking water samples. PACs such as fenoprofen, indomethacin, ketoprofen and phenazone [48,49,50,51,52] have been detected in both sewage effluents sample and surface water samples. Whilst, diclofenac, dimethylaminophenazone, phenazone and propyphenazone were detected in groundwater

samples [53,54,55,56,57,58]. However, in drinking water analgesics and anti-inflammatories measured were not detected above the limits of detection [59,60,61].

### 1.3 Advances in Analytical and Detection Methods

There has been a continuous improvement in analytical techniques over the last decade. The improvements allow for the identification and quantification of a broad range of substances at concentrations levels as low as ng/L. In recent years, it has become possible to simultaneously analyse 3 times the number of compounds, increasing from around 30 compounds per analysis, to around 80-100 compounds [22].

The increase in reported detections of very low concentrations of pharmaceuticals in water is mainly attributable to technological advances. Analytical instruments such as Gas Chromatography (GC) have had major improvements in both sensitivity and accuracy, allowing us to determine target compounds in the ng/L. GC with mass spectrometry (GC-MS) or tandem mass spectrometry (GC-MS/MS) and liquid chromatography with mass spectrometry (LC-MS) or tandem mass spectrometry (LC-MS/MS) are commonly used analytical instruments for the detection of pharmaceutical compounds in water and wastewater. The method and instrument used is dependent on the physical and chemical properties of the target compound. For example, LC-MS/MS analysis is more suitable for measuring target compounds that are more polar and highly soluble in water, whereas GC-MS/MS is better for more volatile target compounds [62].

With improved analytical detection methods and instruments, we are able to learn more about the fate and occurrence of pharmaceuticals in the environment, including the water cycle. However, it is important to recognise that detection of these compounds does not directly correlate to human health risks, as the risks would have to be verified by available human risk assessment methods. In addition, there is currently no standardised practice or protocol for

the sampling and analytical determination of pharmaceuticals in water or any other environmental media that ensures the comparability and quality of the data generated.

## 1.4 The Fate in the Environment receiving Pharmaceutical Active Compounds

Before the late 1990s any environmental impact caused from the pharmaceutical industry was considered to arise solely from the manufacturing facilities i.e. from well-controlled emissions. It was appreciated that the pharmaceutical products themselves were biologically active, as Richardson and Bowron in the mid-1980s predicted the presence of pharmaceutical residues in surface waters [63]. However, it was not until 1994 where clofibric acid was identified in German rivers by Stan and his colleagues [64].

None the less, the occurrence of PACs in the environment has become a worldwide issue of increasing concern. As PACs are increasingly used in large amounts in human and veterinary medicine around the world, many of them may end up in the aquatic environment. These findings have raised questions about how this mixture of human and veterinary medicines in the aquatic environment impact organisms in the environment and on human health [65].

### 1.4.1 Adverse Effects on Organisms in the Environment

The US Food and Drug administration (FDA) do not allow products on the market until environmental risk assessments has been performed. These environmental risk assessments investigate the potential effects pharmaceuticals have on aquatic and terrestrial organisms. Risk assessments include the studies of potential negative effects on fish, daphnids, algae, bacteria, earthworms, plants and dung invertebrates. The majority of the data collected is publically accessible. However, the effects observed in these risk assessment tests are from concentrations much higher than those that are in measured in the environment. They tend to use standard eco-toxicity tests that tend to focus on mortality as the end point. For the aquatic tests, the risk assessments only measure the water compartment and do not consider

the potential pharmaceutical residing in sediments. Therefore, less is known about the subtle effects that PACs can have on organisms in the environment, for example, growth, fertility or behaviour.

With PACs being continuously being released into the environment, aquatic and terrestrial organisms are exposed for much longer durations than those used in the FDA's standard tests. Therefore, researchers are looking into some of the subtler effects caused by long-term, low-level exposure from PACs. A wide range of impacts reported so far are listed in table 1.1. The case study below is a well-known example of PACs having adverse effects on wildlife [66].

*Table 1.1 - A table reporting a few examples of pharmaceuticals found in the environment and their impact on the environment [66]*

Substance	Drug Class	Reported Effect
Fenfluramine	Anorectic	It enhances the release of serotonin (5-HT) in crayfish which triggers the release of an ovary-stimulating hormone. This results in larger oocytes with enhanced amounts of vitellin.
Carbamazepine	Analgesic	It inhibits the activity of basal EROD in cultures of rainbow trout hepatocytes.
Ibuprofen	Anti-Inflammatory	It stimulates the growth of cyanobacteria and inhibits the growth of aquatic plants.
17a-Ethinylestradiol	Steroid	It has endocrine-disrupting effects on fish, reptiles and invertebrates.
Tylosin	Antibacterial	Impacts the structure of soil microbial communities

### 1.4.2 Feminisation of Fish

Male wild fish in rivers and estuaries have been found with elevated concentrations of vitellogenin in their blood plasma or with a condition known as intersex, (intersex is a condition in which the reproductive ducts are feminised). Intersex fish were first found by accident in 1976 [67]. Since then, comprehensive field surveys have shown that intersex fish are widespread in British rivers [68]. They have also been reported from many other countries [69]. These feminised fish were associated with exposure to sewage effluents suggesting that estrogenic chemicals such as estrogens used in the birth control pill, ethinyl estradiol (EE2), are the cause. The discharge of estrogen into fresh water has caused male fish to produce vitellogenin, which is an egg-yolk that is produced in the liver of mature female fish. The implications of abnormal induction of vitellogenin in fish are not well known but high concentrations can lead to kidney failure [70].

Research conducted on various aquatic species, in particularly fish, where they were exposed under controlled conditions (known concentrations of EE2) showed that some aquatic organisms are exquisitely sensitive to EE2. Studies have also predicted the maximum concentration limit of estrogenic chemicals having no effect on fish to be less than 1 ng/L. Concentrations at 1 ng/L can cause some degree of feminisation, however, results have shown concentrations as low as 4 ng/L to cause severe feminisation [71,72,73].

The consequence of the feminisation of wild fish population is presently unclear. This is because it is not necessary for all male fish in a population to be able to breed successfully for the population to be sustained long term. Therefore, the effect on population levels may be small or even non-existent even if the concentrations of estrogenic chemicals in the aquatic environment are high enough to adversely affect a proportion of fish. However, this does not mean the population will not be compromised and the example of EE2 undoubtedly highlights the issue of PACs in the environment.

## 1.5 Removal of Pharmaceutical Waste from Water

Currently there is a growing awareness of PACs being found in different water mediums leading to adverse effects on the environment and human health. For that reason, it is important pharmaceuticals can be removed from waste water effectively and efficiently, in order to produce safe drinking water and to protect the environment. Due to rapid population growth, water treatment facilities deserve more investment, particularly into the treatment of wastewater. If waste water was treated appropriately it could be used as a large water resource to supply the needs of a growing economy. The greatest challenge in implementing this strategy is the adoption of low cost wastewater treatment technologies that will maximise the efficiency of utilising limited water resources and ensuring compliance with all health and safety standards regarding reuse of treated wastewater effluents.

A number of methods such as coagulation, filtration with coagulation, precipitation, ozonation, adsorption, ion-exchange, reverse osmosis and advanced oxidation processes (AOPs) have been used for the removal of organic pollutants from polluted water and waste water [74,75]. These methods have been found to be limited, since they often involve high investment and maintenance cost. Furthermore, AOPs have been found to effectively remove PACs but these processes can also lead to the formation of oxidation intermediates that are mostly unknown at this point. Whereas, physicochemical treatments, such as coagulation processes, are generally found to be unable to remove PACs. The main PACs which are known to pass through the treatment and remain in the wastewater include; analgesics, antibiotics, mood stabilisers, endocrine disruptors, contraceptives, stimulants, tranquilisers and statins [65,67].

### 1.5.1 Waste Water from the Pharmaceutical Industry

A wide range of water treatment and disposal methods are used in the pharmaceutical industry. It is very difficult to apply a standard water treatment system because wastewaters generated from the pharmaceutical industry vary not only in composition but also in quantity, depending on the raw materials and the processes used in the manufacturing of various pharmaceuticals. Also, the plant location brings in a variable relating to the quality of available water.

One of the most common technologies applied is the advanced oxidising process which is mainly to remove organic compounds which are sometimes non-biodegradable. Then the waste having enhanced biodegradability thus can be treated effectively by either an aerobic or anaerobic biological treatment method. However, there are many alternative treatment processes available to deal with the diverse range of waste produced from this industry, but they are specific to the waste the plant produces. Some of the methods that are used to remove PACs from wastewater are discussed below.

### 1.5.2 Recovery Processes

Recovery processes include the following techniques; reverse osmosis, nanofiltration and ultrafiltration. The pharmaceutical industry sees them as very important waste control techniques as they are able to recover PACs, along with other useful by-products, such as solvents, heavy metals and acid.

Amoxicillin is an antibiotic used to prevent and treat many different types of bacterial infections. Its recovery from the environment is very important due to it being widely used in human and veterinary medicine. Nanofiltration (NF) can be used to separate and recover amoxicillin from pharmaceutical wastewater in order to palliate the antibiotics harm to the environment. NF is a recently developed pressure driven membrane separation process, which has had an increasing number of applications within the last decade [76,77].

### 1.5.3 Activated Carbon

Organic compounds are easily adsorbed by activated carbon (AC) due to its high surface area (over 1000m<sup>2</sup>/g) along with the combination of a well-developed pore structure and its surface chemistry properties. A waste derivative of activated carbon has recently been used by Mestre *et al.* [78] to remove ibuprofen from water. This is an advantageous process as the AC is an abundant raw material. There are two types of AC; powdered AC or granular AC. Granular AC is usually recycled in fixed bed columns, whereas, powdered AC is usually fresh, thus being a more efficient process [79,80]. Even with the high efficiency of powdered AC they are not cost effective and when granular AC becomes saturated, disposal/regeneration also becomes an issue [81]. However, the major problem with powdered AC is the separation of the adsorbent from the treated water; therefore, a filtration unit has to be integrated with it. To overcome this problem, more recent studies are using AC along with other technologies, so that AC can be used as a pre-treatment [82]. Furthermore, it has also been published that AC adsorption may not always be successful in removing such organics [81].

### 1.5.4 Advanced oxidation processes

Most pharmaceuticals have a low biodegradability and the commonly employed treatment processes are not effective enough to completely remove these PACs from wastewater [83]. Thus, the discharge of these compounds into receiving waters has proven to be high enough to cause toxic effects to environmental organisms [84,85]. AOPs have shown to be able to breakdown PACs. AOPs can be broadly defined as aqueous-phase oxidation process based on the intermediate highly reactive species, such as hydroxyl radicals in the mechanisms, leading to the destruction of the target pollutant [86]. The main types of AOPs are heterogeneous and homogenous photocatalysis and this is dependent upon whether the treatment objective is transformation or destruction, together with the nature of the pharmaceutical effluent. The AOPs can be employed alone or coupled with other physiochemical and biological processes.

#### 1.5.4.1 Ozone/Hydrogen Peroxide Treatment

Ozone is a very strong oxidising agent that decomposes in water to form hydroxyl radicals, which are even stronger oxidising agents. The oxidising agents then induce an indirect oxidation or attacks certain functional groups of organic molecules through an electrophilic mechanism [86,87]. Pharmaceutical wastewater contains various organic compounds that exhibit resistance against biodegradation, such as; toluene, phenols, nitrophenols and nitroaniline.

In cases where treatment of pharmaceutical wastewater by AC adsorption is not financially feasible, ozone/hydrogen peroxide treatments appear to be better technologies. Ozonation has largely been employed in removal of antibiotics [88,89]. However, compounds with amide linkages are resistant to ozone [90]. To overcome this problem, combination of ozone with hydrogen peroxide treatments can be employed, for example, the combination has been successfully utilised for degradation of penicillin formulation wastewater [89,91,92].

#### 1.5.4.2 Electrochemical Oxidation/Degradation

The electrochemical method produces hydroxyl radicals ( $\cdot\text{OH}$ ) as the main oxidant. Hydroxyl radicals are the second strongest oxidising agent known after fluorine. Hydroxyl radicals are able to non-selectively react with most organic contaminants via hydroxylation or dehydration until the chemical decomposes. This is due to the hydroxyl radical having such a high standard reduction potential ( $E^\circ(\cdot\text{OH}/\text{H}_2\text{O})=2.8\text{ V vs SHE}$ ) [93]. The electrochemical method has shown complete degradation of pharmaceutical residues (simulated waste) such as; diclofenac, carbamazepine, propranolol, ibuprofen and ethinylestradiol. Dominquez *et al.* [94] showed a satisfactory removal of total organic carbon (TOC) by the use of a boron doped diamond (BDD) anode which showed higher corrosion stability.

It was also observed that by using BDD electrochemical treatment more than 97% TOC was removed from paracetamol and diclofenac spiked wastewater [95]. Whereas, the degradation

rate of the antibiotics was also enhanced with an increasing concentration of doping boron and decreasing electrode thickness.

#### 1.5.5 Conclusion

From the literature reviewed above, it can be seen most of the technologies mentioned are “removal” processes. However, there should be more of an emphasis on “recovery” technology research. At the time of writing, researchers have been trying to implement recovery options in order to recover important and valuable reagents, by-products and solvents which can be reused.

## 1.6 The Removal of PACs from Wastewater by Adsorption

Adsorption by solid adsorbents has the potential to be one of the most efficient methods for the removal of PACs from wastewater. Adsorption techniques have advantages over the techniques mentioned above because of its simple and low cost design. The adsorption process has had great deal of attention from researchers, as it can be used for the treatment of industrial wastewater from organic and inorganic pollutants. Natural adsorbents include charcoal, clays and zeolites, as they are relatively cheap, abundant in supply and can be modified to enhance their adsorption capabilities. The following section describes how the properties and characteristics of zeolites has allowed them to absorb PACs from water, with particular reference towards the zeolites beta and clinoptilolite.

## 1.7 Introduction to Zeolites

In 1756, natural zeolites were discovered by Alex Cronstedt a Swedish mineralogist. Zeolites are hydrated, crystalline microporous aluminosilicates. Alex Cronstedt found that when heating the mineral Stilbite large amounts of steam were released. This discovery led to the name zeolite, as 'Zeo' is the Greek word for boil and 'Lithos' means stone. However, zeolites useful properties such as adsorption and ion-exchange were not recognised until the 19<sup>th</sup> century. Their unique structural characteristics, such as the size of the pore window, the accessible void space, the dimensionality of the channel system, and the numbers and sites of cations, etc, have found roles in a variety of applications. Zeolites can be used in adsorption, catalysis, building industry, agriculture, soil remediation, and energy [96,97].

There are many zeolites that occur naturally as minerals; however, the majority have been made synthetically. At present, there are 200 different zeolite frameworks identified and recognised by the International Zeolite Association (IZA) [98]. Clinoptilolite, mordenite, phillipsite, chabazite, stilbite, analcime and laumontite are very common naturally occurring

zeolites. With clinoptilolite being the most abundant naturally occurring zeolite, it is the most widely used natural zeolite around the world.

The term “zeolite” is given to microporous, crystalline solid structures composed of aluminium, silicon and oxygen. The general chemical formula of zeolites is:



where **M** is (Na, K, Li) and/or (Ca, Mg, Ba, Sr), **n** is cation charge; **y/x** = 1–6, **p/x** = 1–4 [99].

Their structure is based on ‘vertex sharing’ TO<sub>4</sub> (T=Si or Al) tetrahedral units that form a three-dimensional four-connected framework with uniformly sized pores of molecular dimensions. These [SiO<sub>4</sub>] and [AlO<sub>4</sub>] tetrahedral units are the basic structural building units of a zeolite framework.

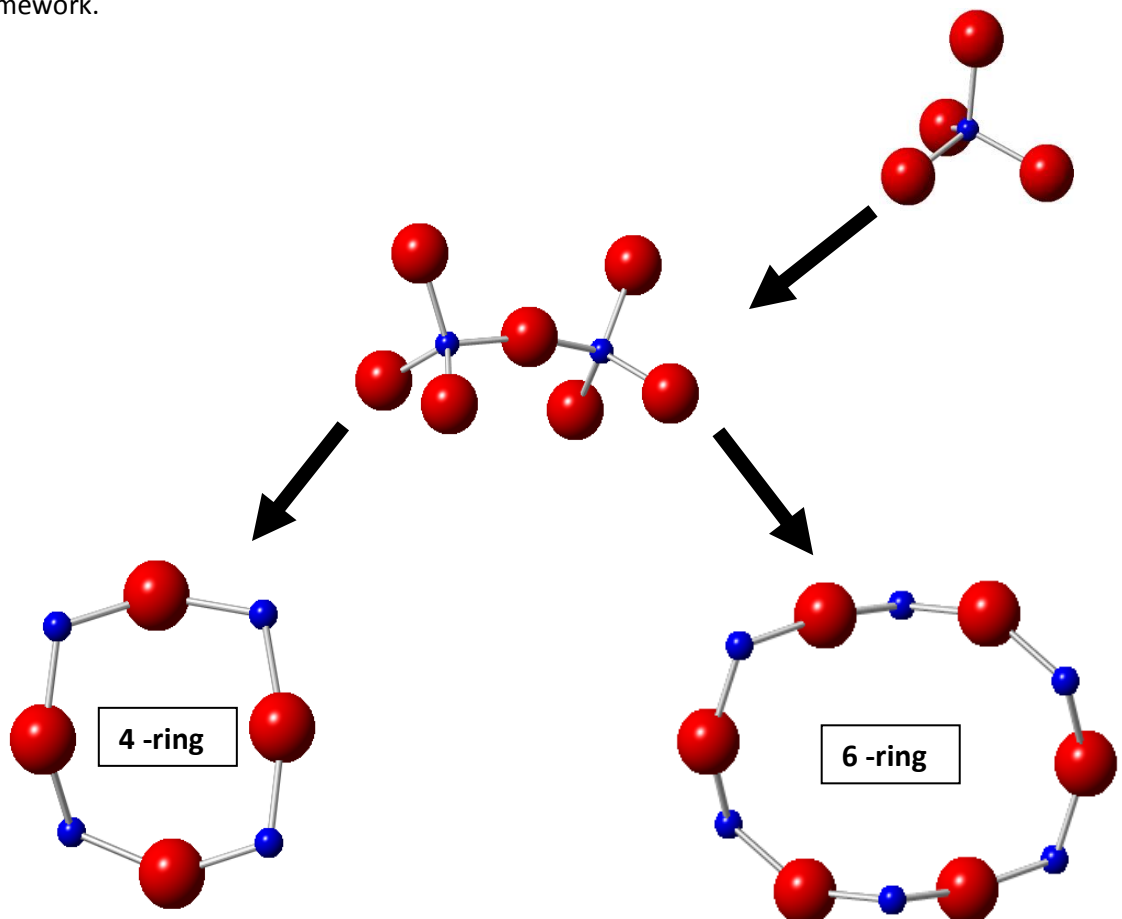


Figure 1.2 - Diagram to show how in a zeolite each “T” atom (in blue) is co-ordinated to four atoms. Then each oxygen atom (in red) is bonding to two “T” atoms.

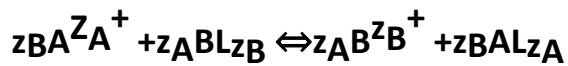
The distribution and arrangement of Si and Al atoms in the zeolite framework is difficult to determine. This is due to their similar ionic radii and electronic shell arrangement of ions. However, it is known that the linkage of two tetrahedral Al atoms is forbidden, this is known as the Löwenstein's rule. Löwenstein's rule dictates the ordering of  $[\text{SiO}_4]$  and  $[\text{AlO}_4]$  tetrahedra units in the framework, stating their distribution within a zeolite is not random. This means that one Al atom can only connect with four adjacent Si atoms (denoted as  $\text{Al}[4\text{Si}]$ ), whereas, a Si atom can link with either a Si atom or an Al atom. Moreover, the Si:Al ratio of a zeolite can vary from 1 to  $\infty$ . Changing the Si:Al ratio will alter the magnitude of the negative charge on the framework and will change the number of charge balancing cations needed, causing very little change to the structure.

The silicon-oxygen tetrahedral unit are electrically neutral, however, the substitution of Si(IV) with Al(III) creates a charge imbalanced framework, with a net negative charge. Therefore, each  $[\text{AlO}_4]^{5-}$  requires a charge balancing cation to ensure an overall neutral charge. These cations are located in the channels and cages of the zeolites structure, the number and location sites of these cations are of keen interest. This is due to their effects on the performance of zeolites, such as ion-exchange and their catalytic properties. However, there is still some limitation on the identification of the sites of cations, even with modern crystallographic techniques being applied to diffraction data [100].

### 1.7.1 Zeolites as Ion-Exchangers

The most significant characteristic of a zeolite is that they are capable of exchanging ions with external medium. The exchange of ions depends on several factors, including the framework structure, charge density of the anionic framework, the ion size and shape, as well as, the ionic charge and concentration of the external electrolyte solution [96]. Ion-exchange is stoichiometric and essentially a diffusion process, this means that the chemical kinetics usually has little relation to the process as a whole.

The equilibrium ion-exchange is expressed by the following equation:



*Equation 1.1 – showing an equation expressing ion-exchange at equilibrium*

where **L** is defined as a portion of zeolite framework unit with an overall negative charge and the  $z_A^+$  and  $z_B^+$  are the valences of the respective cations.

It was not until the early 1900's that ion exchange was first commercially exploited as a water softening technique. It was observed that the  $Na^+$  form of zeolite-A could produce soft water by ion-exchanging with  $Ca^{2+}$  and  $Mg^{2+}$  ions that are responsible for hard water. Like most ion-exchange reactions this process is completely reversible. Zeolite-A can be regenerated once all the  $Na^+$  ions have been exchanged by simply passing a brine solution through the bed of inactivated zeolite [101].

### 1.7.2 Zeolites as Molecular Sieves

The water molecules in the pores and channels of zeolites can be removed by dehydration to leave a porous crystalline structure. The dehydration has little to no effect on the anionic framework and results in large empty pores or “cages” that have a high affinity to re-adsorb water or other polar molecules. Therefore, zeolites can be used as a drying agent, as dehydration is a reversible process. However, it should be noted that the removal of water from zeolites can be more difficult for some zeolites than others. This is due to there being a positive correlation between framework density and energy required for water diffusion.

Molecular sieves are capable of adsorbing a considerable amount of water or other fluids. As they are aided by the enormous internal surface area and by strong ionic forces, such as electrostatic fields, due to the presence of  $Na^+$ ,  $Ca^{2+}$  and  $K^+$  cations. That being said molecular sieves can remove many gas or liquid impurities to very low levels (ppm or less). Especially if

the species being adsorbed is a polar compound, it can be adsorbed with high loading, even at very low concentrations of the fluid, due to presence of cations in the zeolites framework.

Another important feature of molecular sieve is their ability to separate liquids or gases by molecular size or polarity. For example, a molecular sieve would be able to separate straight chained hydrocarbon paraffins from branched chains, as the normal, straight chained, molecules are able to fit into the pores and the branched molecules cannot enter the pores and would pass through molecular sieve bed un-adsorbed [102]. The pore or “cage” size is dependent on the number of oxygen molecules in the rings with 8-, 10- and 12- membered rings having typical sizes of  $\sim 4.5 \text{ \AA}$ ,  $\sim 6.3 \text{ \AA}$  and  $\sim 8.0 \text{ \AA}$  respectively [103]. A useful way of tailoring the pore size is by ion-exchange. The charge balancing cations are partially blocking the pores and reducing the pores overall size, thus, exchanging ions would cause a change in the amount of space within a unit cell. This is an important feature as it is possible to synthesise zeolites with specific pore sizes, to allow adsorption of different molecule sizes, such as the example described above.

Another way to alter pore size is by changing the zeolites Si:Al ratio. The increase in the quantity of Si will decrease the size of the unit cell as the differences between bond lengths between Si-O and Al-O are around  $1.61 \text{ \AA}$  and  $1.75 \text{ \AA}$ . This difference in bond lengths will, therefore, alter the overall size of the zeolites cavities. Moreover, zeolites with higher quantities of Si will require a reduced amount of cations to balance the overall charge, this means the pore sizes are also less restricted by cations [104].

### 1.7.3 Other Applications and Uses of Zeolites

Zeolites are frequently used as heterogeneous catalysts in for chemical reactions in industry. Zeolites make very good catalysts as they can be fully recovered and recycled with great ease and incur a relatively low cost. This leads to less waste and fewer by-products, meaning that zeolites can be considered a greener alternative to common catalysts. Their cation exchanging properties also allow zeolites to have different catalytic properties by using different cations. Also zeolites can often function with higher activity or may combine several catalytic steps which may reduce the environmental impact [105]. Examples of zeolites being used a catalysts include; isomerisation [106], cracking [107,108,109] and hydrocarbon synthesis [110,111].

Zeolites also have been researched by the pharmaceutical industry as drug carriers, adjuvants in anticancer therapy, dietetic supplements and antimicrobial agents. The natural zeolite clinoptilolite has been used for all of above applications [112]. Clinoptilolite is non-carcinogenic to humans and studies show it is not significantly toxic in animals [113]. Because of this and its high resistance in acid media, clinoptilolite is the main constituent in a large number of currently marketed dietary supplements and is in some antacid formulations [114] .

There has been a lot of research into drug delivery systems with zeolites being the carriers. The reason being is that zeolites have very attractive features, such as: large surface areas, high pore volumes, abundant inner/outer surface chemistries, along with their good biocompatibility, thermal/chemical stability and resistance to corrosion under physiological conditions. Their easily modified pore size and volume, along with ease of synthesis, also means they can be customised to their desired purpose. Owing to these characteristics they have found wide application in adsorption, enzyme immobilization and drug delivery systems. In 2001, it was reported that MCM-41, a mesoporous material, was used to deliver ibuprofen [115].

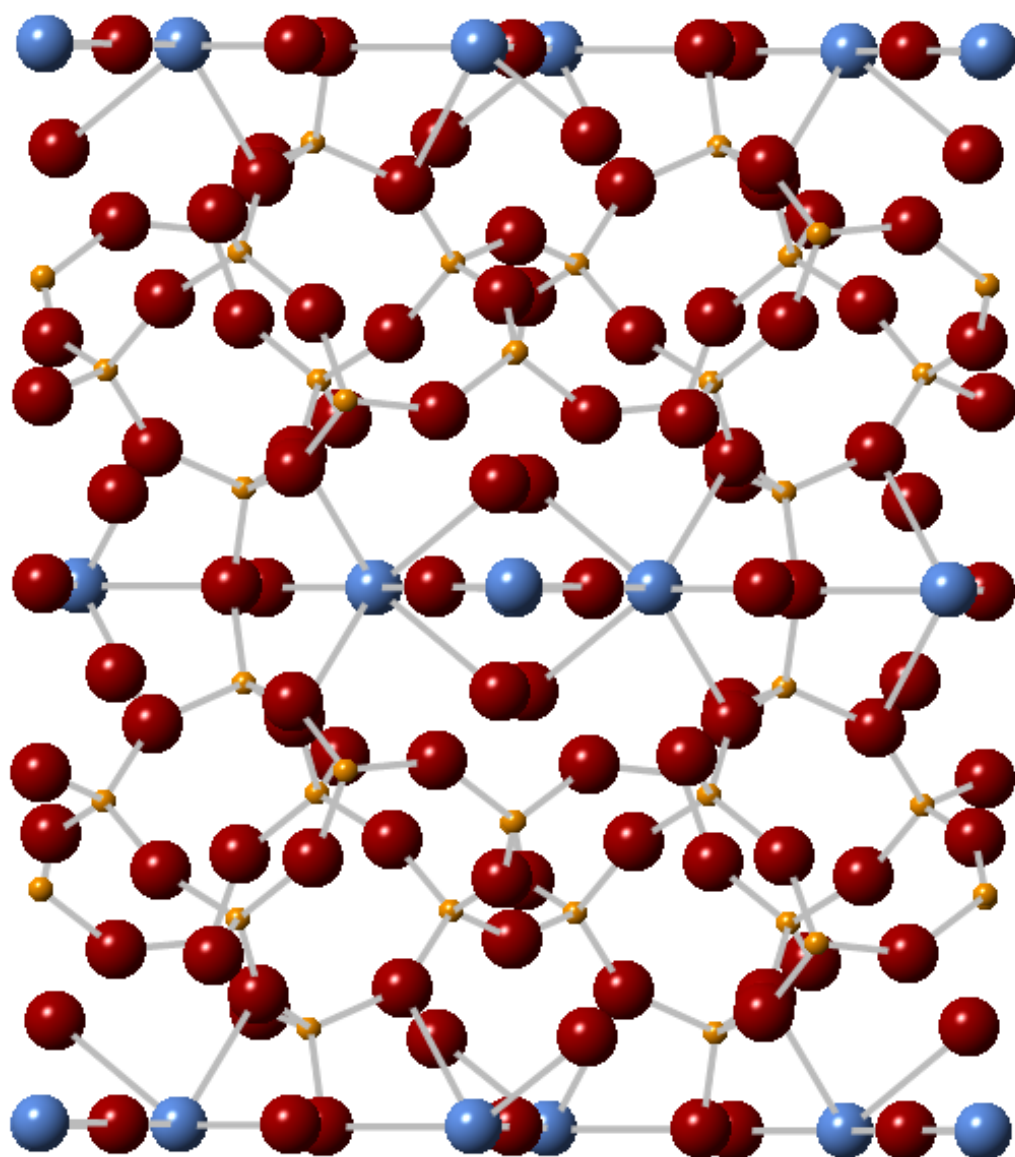
#### 1.7.4 Clinoptilolite

Clinoptilolite [Figure 1.3] is the most abundant natural zeolite [116] with the following chemical formula:



It is reported to have a monoclinic crystal structure with the space group of  $C2/m$ . Clinoptilolite has a tetrahedral framework labelled HEU and it forms a continuous composition series known to the group of zeolites called the heulandite group. This framework consists of three sets of intersecting channels all located in the (010) plane. There are two channels parallel to the  $c$ -axis, with the A channels consisting of strongly, compressed, ten-membered rings with an aperture of  $3.0 \times 7.6 \text{ \AA}$  and the B channels consisting of eight-membered rings with an aperture of  $3.3 \times 4.6 \text{ \AA}$ . The C channels consisting of eight membered rings with an aperture of  $2.6 \times 4.7 \text{ \AA}$  are parallel to the  $a$ -axis.

The two main sites containing the charge balancing cations are the A and B channels. The channels commonly contain the following ions;  $\text{Na}^+$ ,  $\text{Ca}^{2+}$ ,  $\text{K}^+$  and  $\text{Mg}^{2+}$ . Channel A contains  $\text{Na}^+$  along with  $\text{Ca}^{2+}$ , whereas, B channel containing  $\text{Ca}^{2+}$  is mostly  $\text{Na}^+$  free.  $\text{K}^+$  is found more centered in the C channel and in other nearby sites along with  $\text{Na}^+$ . The water molecules are found in the A and B channels. The water molecules in the B channel are coordinated to  $\text{Ca}^{2+}$  and are commonly fully occupied unlike the water molecules in the A channels where they are generally only partially occupied [117].



- Key:
-  Cations
  -  Oxygen
  -  Aluminium/Silicon

*Figure 1.3 - The structure of the natural occurring zeolite clinoptilolite*

### 1.7.5 Applications of Clinoptilolite

Clinoptilolite is a well-researched zeolite because of its porous bulk structure and its ability to have broad range of surfactants on its surface. It has been used as an absorber or as an ion exchanger in numerous studies to remove pollutants, deliver drugs, and be a dietetic supplement [118].

#### 1.7.5.1 Surfactant Modified Clinoptilolite

Clinoptilolites surface can be altered through treatment using cationic surfactants. The charge balancing cations on the surface of clinoptilolite can be replaced to convert the external surface from hydrophilic to hydrophobic, or change the external charge from negative to positive by covering the surface with a surfactant bilayer [119]. For these reasons, the use of surfactant modified zeolites is a very common in removal of various pollutants [120]. For example, high-molecular-weight quaternary amines, such as hexa-decyl-tri-methyl-ammonium (HDTMA) replaced the charge balanced cations on the surface of clinoptilolite forming a bilayer. The HDTMA enhances clinoptilolites sorption of  $\text{Cs}^+$  from nuclear waste [121].

#### 1.7.5.2 Removal of Pollutants by Ion-exchange and adsorption

An excess of nitrogen in the environment causes eutrophication of lakes and rivers. Ammoniacal nitrogen ( $\text{NH}_2\text{-NH}_2$ ) is a colourless, toxic gas, often found in industrial waste water and cause a sharp decrease of dissolved oxygen. The decrease in dissolved oxygen can cause eutrophication of lakes and rivers, hence, it is of great importance to remove ammonia from natural waters. The removal of the ammonium ions from aqueous solutions through adsorption using clinoptilolite is found to be very promising. The Tahoe-Truckee Sanitation Agency, California, extracted 507kg of  $\text{NH}_4^+$  from waste water a day by using clinoptilolite for ammonia exchange. Whereas, NASA used Ca-saturated clinoptilolite to remove ammonia from a wastewater system to establish long term human presence in space.

### 1.7.6 Zeolite Beta

Zeolite Beta is a mixture of related polymorphs [Figure 1.4] which was first reported in 1967, they are highly siliceous, large-porous, synthetic zeolites obtained by using tetra-ethyl-ammonium hydroxide as structure-directing agent. Their high thermal and chemical stability, together with the presence of strong acid sites on the surface has made zeolite beta an active and efficient catalysts for a wide spectrum of reactions in industry [122].

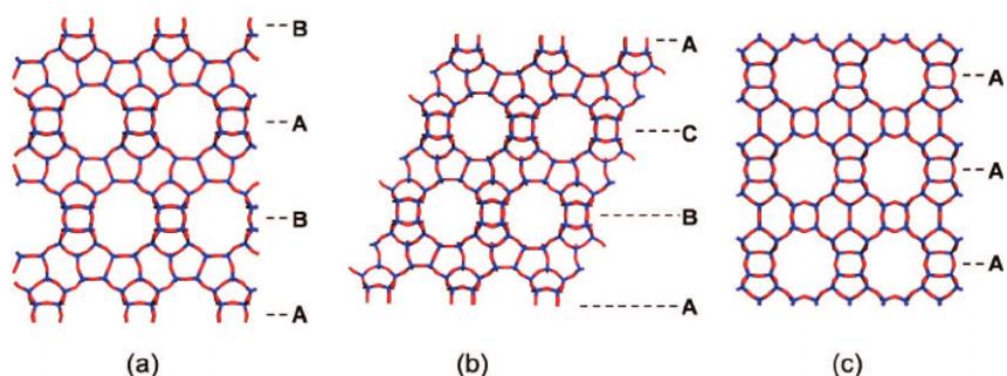


Figure 1.4 - Framework structures of (a) polymorph A, (b) polymorph B, and (c) polymorph C of zeolite beta, showing the different stackings of the 12-ring pores as (a) ABAB. . ., (b) ABCABC. . ., and (c) AA. . . [123]

Their framework consists of three polymorphs; A, B and C [Figure 1.4]. Polymorph A (\*BEA,  $P4_122$ ,  $a=12.632 \text{ \AA}$  and  $c=26.186 \text{ \AA}$ ), polymorph B ( $C2/c$ ,  $a=17.896 \text{ \AA}$ ,  $b=17.920 \text{ \AA}$ ,  $c=14.328 \text{ \AA}$ , and  $\beta=114.8^\circ$ ), and polymorph C (BEC,  $P4_2/mmc$ ,  $a=12.769 \text{ \AA}$  and  $c=12.977 \text{ \AA}$ ). Whilst the structure of polymorph C was determined using several different techniques, the structures of polymorphs A and B are still hypothetical [123]. The polymorphs have three-dimensional pore systems with 12-rings as the minimum constricting apertures, however, they are all built from the same tertiary building units just in different sequences. They can either be interconnected in a left (L) or right (R) hand fashion. Polymorph B has a uninterrupted sequence of (RRRR...) or (LLLL..), whereas, polymorph A has an alternative stacking sequence (RLRLR....). There is equal probability of either stacking sequences occurring, as a result of this, there is a random extent of interplanar stacking faults and to a lesser extent, intraplanar defects terminated by hydroxyl groups. The intergrowth of the polymorphs does not

significantly affect the volume of the pores but influences the tortuosity of the pore connectivity along the c direction. The high stacking fault densities produces complex X-ray diffraction patterns that have both sharp and broad features [124].

## 1.8 Porous Silicates as Pharmaceutical Adsorbents

The removal of contaminants by adsorption using natural materials such as zeolites has, has gained much interest during recent decades. H.M. Otker *et. al* [125], used clinoptilolite, a natural zeolite, to remove the veterinary antibiotic enrofloxacin. Enrofloxacin is a fluoroquinolone group antibiotic, which is widely used in poultry production in order to treat respiratory and enteric bacterial infections. Their results showed that the optimum uptake of enrofloxacin by clinoptilolite was obtained by decreasing pH and increasing temperature.

Clinoptilolite was used again in another study [126] in attempt to remove dexamethasone. Dexamethasone is a type of glucocorticoids, that cannot be removed efficiently from hospital wastewater using conventional on-site treatment methods. Dexamethasone can cause many adverse effects when it is contaminating the aquatic environment. Organisms exposed to this drug can be expected to have a weakened immune system and as a result of this, can be at high risk of suffering from an infectious disease. Their study showed that the removal efficiency was dependent on the solutions pH, initial concentration of dexamethasone, amount of adsorbent and contact time. Maximum removal of dexamethasone occurred at pH 4 along with 0.5g of Clinoptilolite.

An investigation into zeolite beta, with different Si:Al ratios (i.e. 25, 38 and 360), adsorbing the three pharmaceuticals; atenolol, hydrochlorothiazide and ketoprofen, from diluted aqueous solutions, was performed in 2013 [122]. The researchers investigated the effect of changing the ionic strength and the pH, before and after thermal treatment of the adsorbents. Analysis by X-ray diffraction and thermogravimetry confirmed the drug adsorption. The results showed that the adsorption capacity of beta zeolites was strongly dependent on both the solution pH

and the alumina content of the adsorbent. Atenolol was readily adsorbed on the less hydrophobic zeolite, under pH conditions in which electrostatic interactions were predominant. Whereas, the adsorption of ketoprofen was mainly driven by hydrophobic interactions. In addition, it was shown that thermal treatment, presence of cations or buffered solutions can significantly modify the adsorption characteristics of zeolite beta. Their results showed that by adding salt to the solution it was found that drug desorption was more favourable. This would be helpful once the zeolites had been removed from the treated water as it would allow for the drugs to be removed and the zeolites to be used multiple times.

MCM-41 and SBA-15 are both mesoporous silica sieves that are composed of uniform ordered structures, along with high pore volume and high surface area. They have both been investigated as adsorbents for the removal of pharmaceuticals from aqueous solution. In 2008 [127], MCM-41 was incorporated with nickel (II) complexes in attempt to remove naproxen. Their results indicated that the inclusion of the transition metal nickel onto the surface of MCM-41 improves the materials affinity towards naproxen in aqueous mediums.

Whereas, a different study in 2009 [128], used the mesoporous silica SBA-15 to adsorb the following pharmaceuticals; carbamazepine, clofibric acid, diclofenac, ibuprofen, and ketoprofen from aqueous solution. X-ray diffraction, transmission electron microscopy, N<sub>2</sub> adsorption-desorption measurement, and point of zero charge measurement, were used to synthesise and characterise the adsorbent SBA-15.

Their results showed that SBA-15 is a promising adsorbent for removal of pharmaceuticals from surface water and from pharmaceutical industrial wastewater. The highest removal rates achieved were in acidic media (pH 3-5), reaching 94.3% uptake of ketoprofen, closely followed by ibuprofen with 93.0%, diclofenac with 88.3%, carbamazepine with 85.2% and clofibric with the lowest of 49.0%. It was found that by increasing pH above 5 caused a decrease in the drug uptake. On the other hand, the researchers also confirmed that SBA-15 had low desorption

percentages, implying that the adsorbed pharmaceutical would not easily detach from the adsorbent to return to the treated water.

In 2012, a research study attempted to remove the three drugs; erythromycin (ERY), carbamazepine (CBZ) and levofloxacin (FLX) from water using three organo-philic zeolites; Y, mordenite (MOR), ZSM-5 [129]. Their results indicated that Zeolite Y [Figure 1.5] was the most efficient adsorbent, with the material being able to adsorb ERY and FLX at up to 5% and CBZ as much as 10% of its as-synthesised weight. X-ray diffraction patterns were analysed by the Rietveld method to determine the unit parameter variations and structural deformations of the zeolites after adsorption. The results showed that after adsorption of the tested antibiotics, that zeolite Y showed remarkable distortion in its framework, which caused a lowering in the symmetry of FLX and CBZ. Therefore, they concluded the drugs were adsorbed inside the channel system of zeolite Y. It was also noted that ERY is adsorbed inside the crystals of zeolite Y even if its dimensions appeared to be too large to pass through the 12-ring windows delimiting the large cage of this zeolite. Furthermore, the results also showed that CBZ is not adsorbed by either MOR or ZSM-5, even if the dimensions of the drug appear suitable for adsorption in the channel system of these microporous materials.

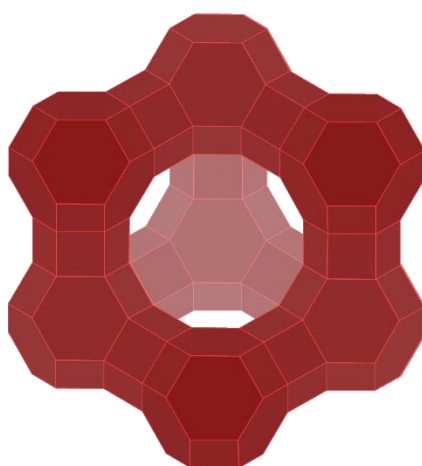


*Figure 1.5 – Image of zeolite Y*

## 1.9 Drug Molecules Used In This Research

Both ibuprofen and paracetamol are two of the most commonly detected PACs in waste water across the world. Ibuprofen was detected in 56 countries with a concentration range of 0.034  $\mu\text{L}^{-1}$  to 0.0506  $\mu\text{L}^{-1}$ , whereas, paracetamol was detected in 29 countries with an average concentration of 0.038  $\mu\text{L}^{-1}$ .

### 1.9.1 Ibuprofen

Ibuprofen is a common nonsteroidal anti-inflammatory drug (NSAID), treat minor pain, fever and inflammation [130]. In 2015, Nurofen (ibuprofen based pharmaceuticals) sold approximately £117.5 million of the drug [131]. Its chemical structure is shown in figure 1.6:

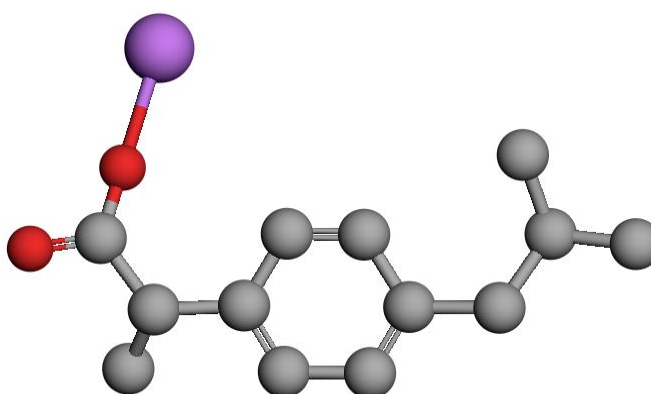


Figure 1.6 - Chemical structure of Na-ibuprofen, Na is represented by the purple atom, O is represented by the red atoms and C is represented by the grey atoms.

Ibuprofen metabolises in an organism's digestive system. Its metabolites include hydroxyibuprofen and carboxyibuprofen. It is important to understand that these two chemicals retain the same low level of toxicity as the parent compound [132]. One of the main routes for ibuprofen to enter the aquatic environment is excretion, with 90% of ingested ibuprofen being excreted by urine [133]. It is no surprise that 0.22  $\mu\text{g}\text{L}^{-1}$  of ibuprofen was identified in German sewage effluents [134]. In 2002, a research group tested 139 streams across the U.S for PACs. 9.5% of the streams tested had traces of ibuprofen (0.018-1.  $\mu\text{g}\text{L}^{-1}$ ) [135]. A different research group tested the same 139 streams 5 years later and found that

the concentrations of ibuprofen in the streams had increased to 0.90-2.11  $\mu\text{gL}^{-1}$  [136]. This has raised questions to whether ibuprofen is persisting in the environment and what effects it has on organisms in the aquatic ecosystem.

Several studies have looked into how concentrations of ibuprofen may affect aquatic life. One particular research group studied the growth effects of two aquatic species; *Synechocystis* and *Lemna minor*, using 1-100  $\mu\text{gL}^{-1}$  ibuprofen [137]. The strain of *Synechocystis* used was *Synechocystis* sp. PCC6803, which is a freshwater cyanobacteria. *Lemna minor* is a common duckweed which is also found in fresh water. Their results showed that ibuprofen strongly stimulated the growth of *Synechocystis* at all concentrations tested, with a 72% increase at 10  $\mu\text{gL}^{-1}$ . However, ibuprofen inhibited *Lemna minor* in a linear dose-dependent manner with a 25% growth reduction with an ibuprofen dosage of 1  $\mu\text{gL}^{-1}$ . The effects shown by ibuprofen on *Synechocystis* and *Lemna minor* growth may have potential implications to the ecosystem. As the loss of one organism in a small ecosystem could mean disaster for the other organisms in the same ecosystem. In the case of ibuprofen harming humans there is a growing concern with prolonged use of ibuprofen. Many health specialists are concerned that ibuprofen can cause gastrointestinal, cardiovascular, kidney and brain conditions [138].

### 1.9.2 Acetaminophen

Acetaminophen, also known as paracetamol, is one of the most prescribed drugs globally due to its antipyretic and analgesic properties [139,140,141,142]. Its chemical structure is shown in figure. The minimum concentration for a therapeutic effect on invertebrates is  $9.2\mu\text{L}^{-1}$  [143]. However, it is highly toxic at elevated doses and can cause hepatotoxic, a condition that can occur in both animals and humans [142,144,145,146].

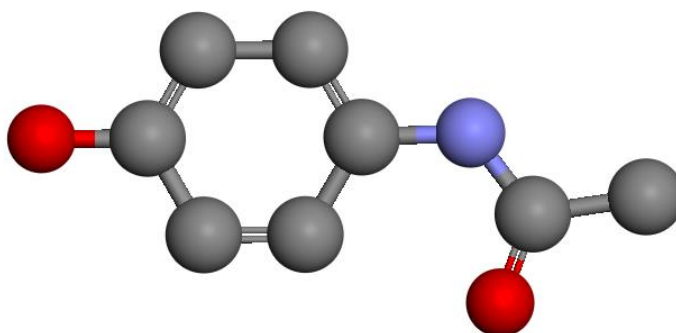


*Figure 1.7- Chemical structure of Acetaminophen, oxygen is represented by the red atoms, nitrogen is represented by the purple atom and carbon is represented by the grey atoms*

Paracetamol administered in normal dosages results in non-toxic metabolites that are promptly excreted. A higher dosage of paracetamol along with the unavailability of intracellular glutathione can result in toxic effects. Without glutathione the highly reactive, electrophilic metabolite of paracetamol (N-acetyl-p-benzoquinoneimine, NAOQI) will accumulate and cause toxic effects such as; DNA and RNA damage, oxidation of membrane lipids, modification of thiol groups on cellular proteins, resulting in necrosis and cellular death. Therefore, a saturated detoxification mechanism or a lack of a similar detoxification mechanism in non-target organisms are likely to exhibit the toxic effects [142,145,146,147,148].

The environment concern surrounding paracetamol stems from its common presence in the aquatic environment. Paracetamol degrades naturally in the environment by 57-99% within 28 days [149], however, it is the continuous discharge and the time taken to degrade that

causes paracetamol to persist in the environment. The persistence of paracetamol is well documented, with concentrations of up to  $6 \mu\text{L}^{-1}$  in European sewage plants [150],  $10 \mu\text{L}^{-1}$  in USA natural waters [151] and above  $65 \mu\text{L}^{-1}$  in the River Tyne, UK [152]. Despite this, the number of ecotoxicological studies on potential effects of paracetamol in wild organisms is still scarce.

## 1.10 Introduction to Drug Adsorption

Adsorption is “the preferential partitioning of substances from the gaseous or liquid phase onto the surface of a solid substrate”. The material being adsorbed onto the solid is known as the adsorbate and the solid which the adsorbate accumulates onto is called the adsorbent. This process is reversible as the physical adsorption is caused mainly weak van der Waals and electrostatic forces.

For a solid to provide large adsorption capacity it must have a large specific surface area, this can be created by having a large number of small sized pores between adsorption surfaces. The size of these pores determines the accessibility of the adsorbate to the adsorbent's internal surface. Therefore, the adsorbents can be ‘tuned’ for a particular separation process by being engineered to have specific pore sizes distribution [153].

Zeolites are hydrophilic adsorbents which have a high affinity towards polar substances such as water. With most PACs being polar it was for this reason zeolites have been explored for being a potential adsorbent.

## 1.11 Research Proposal

Pharmaceuticals have only recently been considered as CECs and as a result of this, have received a lot of attention from scientists. Pharmaceuticals have been detected in the aqueous environment with concentrations up to the g/L and as high as 100g/L in effluents from pharmaceutical manufacturers. Most pharmaceuticals are readily soluble in water due to their polar properties and consequently, they cannot be completely removed from wastewater. This is due to current wastewater treatments systems being based on filtration and hence, not designed to remove polar pharmaceuticals from water. Therefore, alternative treatment technologies that achieve efficient pharmaceutical removal need to be developed. Among the several technologies propose for the removal of pharmaceuticals from water, adsorption has been receiving special attention due to its simplicity, no production of undesirable by-products, low setup and operation cost [154].

In the last decade, zeolites have attracted great attention as they are affordable materials that are abundant and inexpensive. They have high surface area, large and uniform pore size, high pore volume and tailorable surfaces that make them good candidates for the adsorption removal of pharmaceuticals. The aim of this study, was to determine the adsorption capacities of natural zeolite clinoptilolite and the synthetic zeolite beta towards the two pharmaceuticals that are recognized as emerging contaminants of water: acetaminophen and Na-ibuprofen. Apart from their frequent occurrence in wastewaters, these pharmaceuticals were chosen because of their molecular structures. They both possess polar groups which can be expected to adsorbed on three-dimensional ordered solids that possess specific active sites [155].

Zeolite beta was chosen as an adsorbent as they are commercially ready, have a defective structure and large pores, which are ideal characteristics for the adsorption of drugs with moderate molecular dimensions. Although zeolite beta show great potential as pharmaceutical adsorbents, there has been relatively a few studies performed on these

materials unlike clinoptilolite which has been investigated as a potential adsorbent in numerous studies.

As the addition of specific cations can adjust and even tailor the adsorption affinities of the zeolites, both zeolites were ion-exchanged with: Cu(II), Fe(III) and  $\text{NH}_4^+$ . It is thought that the adsorption of acetaminophen and Na-ibuprofen, on the three-dimensionally order solids, that contain these specific cations, will occur as both pharmaceuticals possess polar groups. Acetaminophen contains one alcohol group and one amide group, and Na-ibuprofen contains a carboxylic group. It is thought that N- and O- donor groups will form stable complexes with Cu(II) ions. Whereas, the Fe(III) cations were introduced with the aim to strongly bind with the oxygen atoms present on the target drugs and the  $\text{NH}_4^+$  cation were exchanged with the aim to increase adsorption via hydrogen bonds.

To determine the adsorption properties of the zeolites, XRD, IR and HPLC will be used. If the pharmaceuticals are adsorbed, the analytical techniques IR and XRD would contain peaks representing the drug uptake. Whereas, HPLC would be used in attempt to quantify the percentage of drug adsorbed, in order to determine the best adsorbent.

# Chapter 2: Experimental Techniques

## 2.1 Powder X-Ray Diffraction (XRD)

Zeolites and other related microporous materials are made up of a range of structures and compositions. Since the earliest of days X-ray diffraction has been one of the main and useful analytical technique for structural characterisation. In 1912, Max von Laue discovered that the three dimensional array of atoms or molecules making up crystalline substances can act as a diffraction grating for X-ray wavelengths similar to the spacing of planes in a crystalline lattice [156]. X-ray diffraction is based on constructive interference of monochromatic X-rays with a crystalline sample. The diffraction pattern produced can be used to determine a structural model of which either the Laue equations or Bragg's law can be used.

The Laue equations are based on the idea that the 3-dimensional network of atoms behaved as a 3-dimensional diffraction grating. Despite Laue's approach being correct it was often not used as it was seen as too complicated. This led to advances in Bragg's law which relates the wavelength of electromagnetic radiation to the diffraction angle and the lattice spacings in a crystalline sample [Equation 2.1]. The equation for Bragg's law is the following:

$$n\lambda = 2d_{hkl} \sin \theta$$

*Equation 2.1- Equation for Bragg's law [157]*

where  $\lambda$  is the wavelength,  $n$  is the order of reflection,  $d_{hkl}$  is the perpendicular lattice plane distance and  $\sin \theta$  is the angle of incidence/reflection to the plane [157].

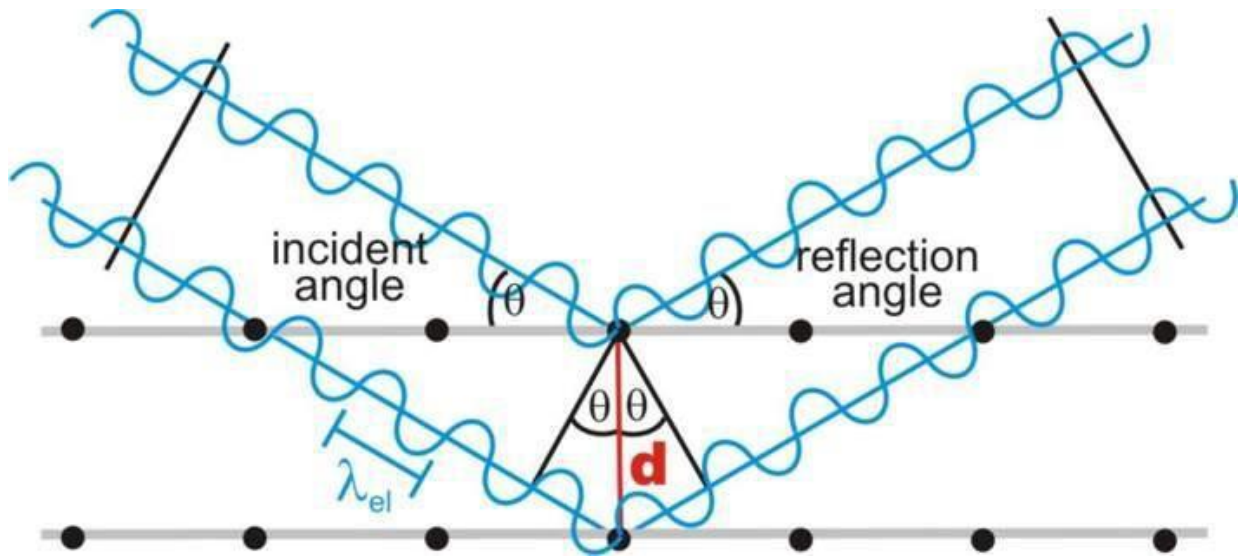


Figure 2.1 – Diagram of Bragg's law [158]

When X-rays interact with crystalline solids they are scattered in all directions due to the random orientation of microcrystallites. When the geometry of the incident X-rays impinging the sample satisfies Bragg's law (when two incident waves remain in phase), constructive interference occurs and a peak in intensity occurs. However, if the two waves are out of phase, this means no diffraction will occur as Bragg's law is not satisfied. Due to the random orientation of crystallites there will always be in phase waves which are satisfying Bragg's equation leading to a diffraction pattern being produced [159].

X-ray diffractometers consist of three main elements: X-ray tube, X-ray detector and a sample holder. X-rays are generated in a cathode ray tube by heating a filament to produce electrons and fired at a metal anode, commonly copper. X-rays are produced when the high energy electrons ionise coppers inner shell electrons to produce vacant orbitals. When this occurs electrons from a higher energy level drop down and release excess energy in the form of X-rays of a characteristic wavelength. The spectra produced consists of several components, with the most common being  $K\alpha$  and  $K\beta$ .  $K\alpha$  is made up of  $K\alpha_1$  and  $K\alpha_2$ , with  $K\alpha_1$  having a slightly shorter wavelength and twice the intensity. Monochromaters are filters and are required to produce the monochromatic X-rays needed for a diffraction pattern. The

monochromators are often used within diffractometers to select only  $K\alpha_1$  as the two spin states of electrons will provide radiation at  $\lambda=1.54051 \text{ \AA}$  ( $K\alpha_1$ ) and  $\lambda=1.54433 \text{ \AA}$  ( $K\alpha_2$ ) [160].

The scattering of X-rays by the electrons within a sample produces a diffraction pattern. The intensity of the patterns peaks can provide useful information such as the crystal structure and stacking faults of the sample. The equation for the intensity ( $I_{hkl}$ ) of a given peak within the diffraction pattern is as follows:

$$I_{hkl} = K(Lp)_{hkl} j_{hkl} F_{hkl}^2 e^{-2w} \bullet A_{hkl}$$

*Equation 2.2 – The equation used to calculate the intensity of a given peak within a diffraction*

**K** is the scale factor normalizing experimentally observed intensities with calculated intensities

**(Lp)<sub>hkl</sub>** is the Lorentz-Polarisation factor, this contains two parts, the Lorentz factor and the polarization factor

**j<sub>hkl</sub>** is the multiplicity of the [hkl] planes

**W** is the debye temperature correction factor

**A<sub>hkl</sub>** is the absorption factor

**F<sub>hkl</sub>** is the structure factor [161]

The structure factor ( $F_{hkl}^2$ ) proportional to the intensity of a peak in a diffraction pattern. With the structure factor being dependent on the type of atom and their location within a unit cell it can be assumed that the nature or location of atoms has changed if the relative intensity has changed. Therefore, measuring the change in intensity is very important when analysing diffraction patterns from ion-exchanged samples. Analysis of the intensity can help determine crystal structures as it can determine atomic positions, occupancy, temperature factors and texture.

XRD patterns can also be used as fingerprints for the identification of known minerals, however, other information is needed when dealing with unknown substances. For instance, peak position in terms of  $2\theta$  values can determine the unit cell dimensions, symmetry along with space groups by determining the positions of reflections. However, it is important to ensure consistency when preparing samples as high background readings can indicate scattering from the sample holder. High background readings can also be from amorphous material within a sample [162].

XRD patterns can also provide information on the size of the crystallites by using the Scherrer equation [Equation 2.3]. Scherrer equation states that peak width is inversely proportional to particle size, thus, sharp peaks implies large crystallites and broad peaks indicates small crystallites [156].

$$\mathbf{Size} \left( \text{\AA} \right) = \frac{k\lambda}{\Delta\theta \times \cos\theta}$$

*Equation 2.3 – Scherrer equation [156]*

### 2.1.1 XRD Experimental

Diffraction patterns were obtained using a Bruker D2 phaser powder diffractometer fitted with 0.6mm slits and a Lynxeye solid state detector fitted with 0.6 mm slits and a Lynxeye solid state detector fitted with a 1mm solar slits using CuK radiation ( $\lambda = 1.5418 \text{ \AA}$ ) and a Ni K $\beta$  filter, between 3-80° 2 $\theta$  with a 30 minute scan.

The X-ray diffraction patterns are analysed using the Pawley fit method. The Pawley fit method is a process in which the peaks observed in a XRD pattern are fitted by 2-theta values constrained by the size and symmetry of the unit cell. The structural refinement of the unit cell gives an indication of the “best fit possible”. By extracting the peak intensities before structural solution the software can determine the cell parameters [163]. A Pawley fit can also determine any changes made to zeolites unit cell parameters due to adsorption. For the X-ray diffraction patterns obtained the parameters were refined with a Pawley fit, using a Chebyshev background function and pseudo-Voight peak shape function. If the unit cell results change significantly after adsorption (the change is larger than the calculated error), then it is an indication that the drug has adsorbed into the pores rather than attached to the particles on the surface.

The Pawley fit method was also used to see if the unit cells of the samples fits well to the structural model. This was done by evaluating the weight profile R-factor ( $R_{wp}$ ) and also by visual examination of the fit for each XRD pattern collected. The  $R_{wp}$  is the most straightforward discrepancy index, with the following equation:

$$R_{wp}^2 = \frac{\sum_i w_i (y_{c,i} - y_{o,i})^2}{\sum_i w_i (y_{o,i})^2}$$

*Equation 2.4 – The weight profile R-factor ( $R_{wp}$ ) equation*

The equation follows direction from the square root of the quantity minimised, scaled by the weighted intensities [164]. It is regarded as the target of a correct structural refinement, thus the smaller the  $R_{wp}$  value the better [165].

## 2.2 An Introduction to High Performance Liquid Chromatography (HPLC)

Chromatography is a technique used to separate components in a mixture due to the differing time taken for each component carried in a mobile phase to travel through a stationary phase. Chromatography was first used in 1906 by a Russian botanist, Mikhail Tswett. He separated plant pigments such as chlorophylls and xanthophylls by passing them through a glass column packed with calcium carbonate [166].

High Performance Liquid Chromatography (HPLC) is characterised by the use of mobile phase being pumped through very small particles (stationary phase) at high pressure. It is the most common analytical separation tool that is used to identify, quantify or purify the components of a mixture. For HPLC the stationary phase is typically a column filled with surface-modified silica particles. The particles in the columns are extremely small with typical values of 5 microns. There are many different columns differing in particle sizes. It is the high-surface area stationary phase that maximises the interaction between the substance to be separated and the stationary phase, resulting in a better separation [167].

Analyte is the term used to refer to the molecule of interest that is being analysed. The time at which an analyte emerges from the column is known as the retention time. The retention time of each analyte depends on its chemical nature and the composition of the mobile phase. This is because as the sample is pumped through the column it interacts with the stationary phase through a combination of hydrophobic and van der Waals interactions [168].

The separation of the analytes happens inside the column and a detector “collects” this separation allowing us to see it [Figure 2.2]. There is no universal detector, however, a UV/VIS detector is a very common type of detector used for HPLC analysis and was used in the experimental explained below. A UV/VIS detector comes under the category of absorbance detectors. During the analysis, the samples goes through a flow cell. When UV light is irradiated on the flow cell, the analyte absorbs a part of the UV light. Therefore, the intensity of the UV light absorbed by the mobile phase with analyte and without analyte will differ. This difference in intensities determines the amount of analyte detected. The wavelength used depends on the type of sample being detected. The most commonly used wavelength is 254nm [169].

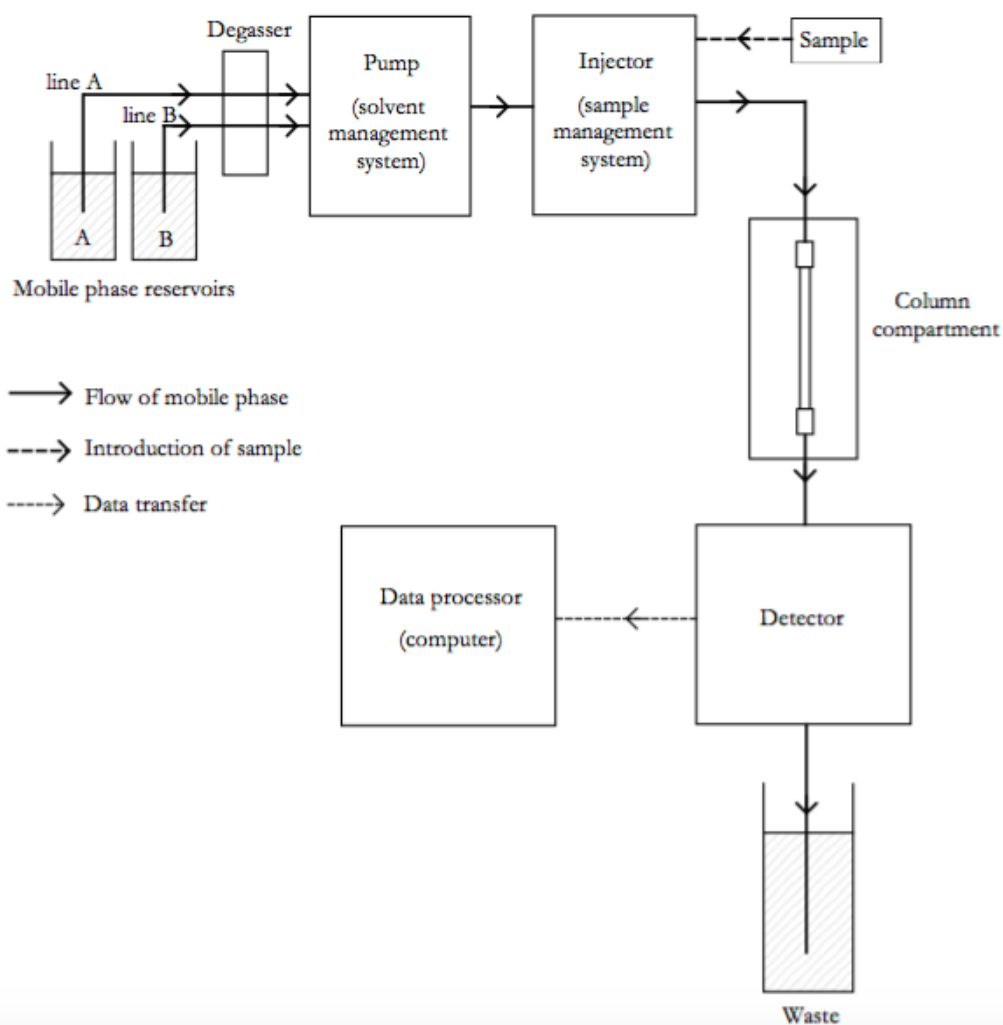


Figure 2.2 -The configuration of a typical HPLC system [166]

### 2.2.1 HPLC Experimental

PU-1580 intelligence HPLC with a Waters 486 absorbance detector was used to analyse samples. The HPLC parameters are stated in table 2.1.

*Table 2.1 -The HPLC parameters used for quantifying adsorption of acetaminophen and Na-ibuprofen*

Analyte	Run Time (minutes)	Wave length $\lambda$ (nm)	Flow Rate (mL/min)	Mobile Phase
Acetaminophen	7.00	254	1.00	40 Methanol: 60 Water: 1.6 Acetic Acid
Na-Ibuprofen	15.00	220	1.00	45 Water: 55 Acetonitrile: 0.045 Phosphoric Acid

## 2.3 An Introduction to Infra-Red Spectroscopy

Infra-red (IR) spectroscopy uses IR radiation which is a type of electromagnetic radiation. When an IR radiation wave interacts with a covalent bond which has an electrical dipole, the radiation energy is absorbed and the bond will start to vibrate. This type of analysis is performed on an IR spectrophotometer. Older spectrophotometers slowly scan through the whole IR spectrum, however, modern machines use the Fourier Transform (FT) method [170]. This method uses an interferometer instead of a diffraction grating. It analyses the sample using a single pulse from an IR laser and all frequencies reach the detector at the same time. The spectrum is obtained by a mathematical calculation and is then converted on a computer to a readable form. The spectrum produced normally has a 'plot' of % transmittance against wavenumber. Wavenumber is expressed as [171].

$$\text{Wavenumber (cm}^{-1}\text{)} = \frac{1}{\text{wavelength (cm)}}$$

*Equation 2.5 – Equation for wavenumber*

No two organic compounds have the same IR spectrum, therefore, an individual, pure compound can be identified by examination of its spectra [171]. The energy at which any peak in an absorption spectrum appears corresponds to the frequency of a vibration of a part of a sample molecule:

$$c = \nu\lambda$$

*Equation 2.6 – The equation for wavelength [171]<sup>1</sup>*

where,

**c** = velocity of light ( $3.00 \times 10^8 \text{ m s}^{-1}$ )

**v** = frequency (Hz)

**$\lambda$**  = wavelength (m)

and

$$\mathbf{E = hv}$$

*Equation 2.7 – Planks law equation*

where,

**E** = energy ( $\text{kJ mol}^{-1}$ )

**h** = Planck's constant ( $6.63 \times 10^{-34} \text{ J/s}$ )

**v** = frequency (Hz) [171]

### 2.3.1 IR Experimental

A Nicolet IR2000 FT-IR machine was used to determine whether the pharmaceuticals had been successfully adsorbed by the zeolites. A background scan is run first to remove  $\text{CO}_2$  peaks and other artefacts found in the air. A small sample is then placed onto a clean attenuated total reflection (ATR) cell sample plate to be scanned.

## 2.4 Introduction to Solid State Nuclear Magnetic Resonance (MAS NMR)

Nuclear magnetic radiation (NMR) is an extremely valuable technique for determining molecular structure and providing structural information on solids. NMR spectra for liquids give a number of sharp peaks, with their positions and intensities providing information on which atoms are bonded together, co-ordination numbers, next nearest neighbour etc. Whereas, NMR spectra, obtained from solids, provide broad featureless peaks. The broad featureless absorptions are caused by chemical shift anisotropy and dipolar coupling, due to the absence of molecular motion. Therefore, no useful information such as; chemical shifts and spin-spin coupling can be extracted from the broad line shapes [172].

Magic angle spinning (MAS) removes the anisotropies of the chemical shift and dipole-dipole interactions producing a liquid-type NMR spectrum that structural information can be obtained from. The solid sample is rapidly rotated at a frequency in the order of kHz and at the so-called 'magic angle' of  $54.74^\circ$  to the applied magnetic field. The fast rotation averages the chemical shift and the dipole-dipole interactions to the values they would have if they were in a liquid solvent [173], resulting spectra are composed of sharp peaks producing much structural information.

Lippma and others first applied MAS NMR to crystalline silicates and found that it determines the position of silicate anions when using  $^{29}\text{Si}$  NMR. The position of the peaks in the spectra can distinguish between isolated  $\text{SiO}_4$  tetrahedra and  $\text{SiO}_4$  tetrahedra linked by their corner oxygen atoms to 1, 2, 3 or 4  $\text{AlO}_4$  tetrahedra. A 'Q' value is assigned to represent the number of adjacent corner sharing  $\text{SiO}_4$  tetrahedra. Q values range from zero to four. An example of a solid with a Q value of zero is the orthosilicate  $\text{Mg}_2\text{SiO}_4$ .

The chemical shifts for a  $^{29}\text{Si}$  NMR spectra depends approximately on the  $Q$  values [Figure 2.3]. For each  $Q$  value, a range of chemical shifts are present which are relative to the internal standard tetramethylsilane (TMS) [172].

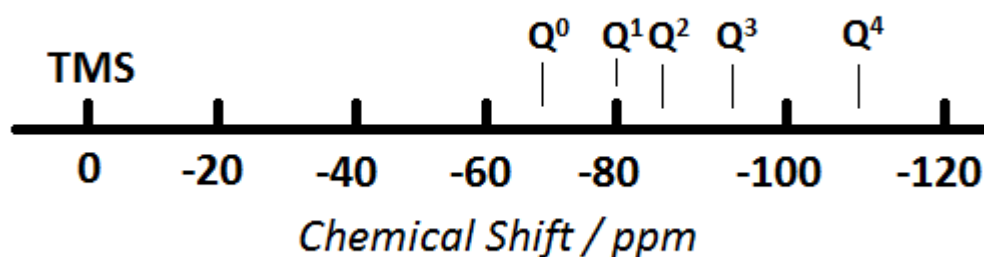


Figure 2.3 - The positions of  $^{29}\text{Si}$  NMR peaks in silicates as a function [172]

#### 2.4.1 MAS NMR Experimental

All  $^{29}\text{Si}$  MAS NMR results were obtained on a Bruker AB3, 400MHz ultra-shield, with the parameter settings in table 2.2.

Table 2.2 – Parameters used for all  $^{29}\text{Si}$  MAS NMR

<b>Pulse Programme</b>	Zg
<b>Spin Speed</b>	6 kHz
<b>Relaxation Delay</b>	10 sec
<b>Lamor frequency</b>	79.45 MHz
<b>Reference Standard</b>	TMS, 0ppm
<b>Number of Acquisitions</b>	1024

## 2.5 An Introduction to Scanning Electron Microscopy

A scanning electron microscope (SEM) is an analytical instrument commonly used to determine composition, morphology. SEM is similar to the transmission electron microscope (TEM) in that they both fire a beam of electrons at the sample. Therefore, the two microscopes share similar features such as; the electron gun, vacuum system and condenser lenses, however, SEM produces images differently to TEM. SEM can typically magnify a material from 10-300,000 times. By using the scale bar, which is shown on the SEM image, the size of the image can be calculated. SEM, therefore, can provide information on the size and the morphology of the zeolite and can show if the PACs adsorbed affect or damage the morphology of the zeolite.

The electrons are normally produced by a field emission gun that can produce high resolution images. These electrons are accelerated to an energy which is typically between 1-30 keV, this is considerably lower than TEM which uses energies around 100-300keV. The beam of electrons pass through two or three condenser lenses that de-magnify the electron beam before it hits the sample, this causes the beam to only have a diameter of 2-10nm. The position of the electron beam on the sample is digitally controlled and the resultant imaged is displayed on a computer screen. Moreover, the signals are produced can be electronically cleaned and amplified before being displayed [174].

The electrons passing through the sample are separated into various types as they emerge; being collected according to angle of scatter, or energy loss or both [175]. It is the diffracted electrons (elastic scattering) leaving the sample that produce the image. Elastic scattering is where the electron beam loses energy from electrons interactions with the sample surface atoms. The energy loss is caused by the sample surface atoms releasing secondary electrons. The release of secondary electrons is useful for imaging as there is a positive correlation between number of secondary electrons and brightness [174].

## 2.6 An Introduction to Energy Dispersive X-ray Spectroscopy

Energy dispersive X-ray spectroscopy (EDX) is used in conjunction with SEM as a chemical microanalysis technique. EDX can analyse samples as small as  $1\mu\text{m}$ . The sample emits X-rays when it is bombarded with electrons from the SEM's electron beam. The samples surface atoms eject electrons when it is hit by the electron beam. This results in empty electron vacancies to be filled by electrons from a higher state causing an X-ray to be emitted to balance the energy difference between the two electrons states. It is these X-rays which are detected by the EDX and are used to characterise the elemental composition of the sample, as the X-ray energy is characteristic of the element from which it was emitted from.

The EDX X-ray detector is typically a lithium-drifted silicon solid-state device that measures the relative abundance of emitted X-rays versus their energy. The detector creates a charge pulse that is proportional the energy of the X-ray that it receives. A charge-sensitive preamplifier is then used to convert charge pulses to voltage pulses, which still remain proportional to the energy of the X-ray. These signals are then sorted by voltage and their energies determined by a multichannel analyser. The computer displays each incident X-ray for further data evaluation [176].

### 2.6.1 SEM Experimental

A small amount of sample is adhered to an aluminium specimen holder using carbon conductive tape. It is important that the sample is electrically grounded to the sample holder to minimise specimen charging. If the sample is non-conductive, it can be coated with a 1-5nm layer of gold. This conductive layer increases beam stability and improves the image quality. In this experiment, the samples morphology was determined using an FEI Quanta 200 Scanning Electron Microscope with a secondary electron detector, Everhart-Thornly detector.

This experimental was done to determine the elemental composition of the zeolite before and after ion-exchange. Samples were coated with 1nm layer of gold and an average result was obtained from 5 area measurements (1-2 mm<sup>2</sup>).

## 2.7 BET Isotherm

By BET (Brunauer, Emmett and Teller) the specific surface area of a sample is measured. The samples are dried by purging nitrogen or by having elevated temperatures applied whilst being in a vacuum. Unless otherwise instructed standard measurement points are taken at  $P/P_0$  of 0.1, 0.2 and 0.3. The volume of gas adsorbed is correlated to the total surface area of the particles including the surface pores [177]. Traditionally nitrogen is used as the adsorbate gas and the calculations are based on the Langmuir adsorption isotherm with introduction of a number of simplified assumptions:

1. It is assumed that adsorption of the first adsorbate layer is to take place on an array of surface sites of uniform energy
2. Then the second layer of adsorption can only take place on top of first, third on top of second, fourth on top of third, etc. When  $P=P_0$  (the saturated vapour pressure of the adsorbate), an infinite number of layer form
3. It is also assumed, that at equilibrium, the rates of condensation and evaporation are the same for each individual layer
4. Finally, for the first adsorption layer the enthalpy of adsorption is the same as in the Langmuir case. Therefore, the BET equation is formed from the summation of the amount adsorbed in all layers [Equation 2.8].

$$\frac{P}{N_s(P_0 - P)} = \frac{1}{NC} + \frac{(C - 1)}{NC} \times \frac{P}{P_0}$$

Equation 2.8- The BET equation expressed in linear form

Where

$C = e^{(q_t - q_o)/RT}$  (is a constant)

$N$  = monolayer adsorption amount

$N_s$  = Adsorption amount at the equilibrium pressure (P) [178]

### 2.7.1 BET Experimental

Samples were degassed at 100°C under vacuum for 4 hours before being analysed by a Micromeritics ASAP 2010 Accelerate Surface Area and Porosimetry System.

## 2.8 The Zeolites and Pharmaceuticals used in this Research Project

The zeolites used as adsorbents are listed in table 2.3. The zeolites [Table 2.3] were examined by the analytical techniques: XRD and IR, before the adsorption experiments, the results obtained are referred to as “zero hour mixing time”. Standards for the adsorption experiments are performed by weighing out 0.25g of the zeolite [Table 2.3] and stirring with 250 mL of water for 24 hours. The standards are filtered out by using a centrifuge and dried in an oven before being analysed by XRD and IR.

*Table 2.3 – The names of the zeolites used and the company they were bought from*

<b>Zeolite Name</b>	<b>Supplier</b>
Moroccan Clinoptilolite	RS Minerals
Japanese Clinoptilolite	Newstone International
Beta Hydrogen	Alfa Chemicals
Beta Ammonia	Alfa Chemicals

The pharmaceuticals used for the adsorption experiments were acetaminophen and Na-ibuprofen. The acetaminophen was supplied as a powder from the chemical company, Sigma Aldrich and was used to make a 250 mL aqueous solutions (0.05M). Whereas, Nurofen Express tablets were obtained and crushed, in order to perform the Na-ibuprofen adsorption experiments with 250mL aqueous solutions of 0.005M.

All the zeolites in table 2.3 were ion-exchanged with different cations in order to adjust the adsorption affinities. For the ion-exchanges the following chemicals were used [Table2.4].

*Table 2.4 – List of chemicals used for cation exchange and the company they were bought from*

<b>Cation Obtained</b>	<b>Chemical Used</b>	<b>Supplier</b>
$\text{NH}_4^+$	$\text{NH}_4\text{NO}_3$	Sigma Aldrich
Cu (II)	$\text{Cu SO}_4 \cdot 6\text{H}_2\text{O}$	Sigma Aldrich
Fe(III)	$\text{Fe SO}_4 \cdot 7\text{H}_2\text{O}$	Alfa

# Chapter 3: Results and Discussion

## 3.1 Adsorption by Clinoptilolite

Clinoptilolite, obtained from a mine in Morocco and supplied by the RS minerals, was used as the adsorbent for the first two adsorption experiments. Solution i) was a 0.05M aqueous solution of acetaminophen and solution ii) was a 0.005M aqueous solution of Na-ibuprofen (Nurofen Express tablets). The two mixtures were stirred for 24 hours at room temperature. The following analytical techniques were used to determine the affinity of clinoptilolite towards the two pharmaceuticals; HPLC, XRD and IR.

### 3.1.1 HPLC Results

The HPLC results obtained [Table 3.1.1], show the remaining concentrations of the drugs in solution and the percentage of drug adsorbed by clinoptilolite. The results indicate clinoptilolite has a higher affinity towards the adsorption of Na-ibuprofen with a 53.93% drug uptake. Despite the difference in percentage drug uptake, the results both show that clinoptilolite has the ability to adsorb both pharmaceuticals.

*Table 3.1.1 – Percentage of drug uptake by clinoptilolite determined by HPLC*

<b>Drug Adsorbed</b>	<b>Drug Uptake (%)</b>	<b>Concentration Remaining in Solution (M)</b>
Acetaminophen	23.93	$3.8 \times 10^{-3}$
Na-Ibuprofen	53.92	$2.3 \times 10^{-4}$

### 3.1.2 IR Results

An IR spectroscopy scan of clinoptilolite before and after adsorption was performed, as seen in figure 3.1.1. If any organic media was adsorbed within the pores there would be peaks shown in the spectra, however, there is little to no changes between the three spectra. It was expected that the IR spectrum of clinoptilolite with acetaminophen to at least have an aromatic C=C bending at  $1700\text{-}1500\text{cm}^{-1}$ , along with an alcohol/phenol O-H stretch at  $3550\text{-}3200\text{cm}^{-1}$  to show that adsorption was successful. Whereas, if Na-ibuprofen was adsorbed the IR spectrum was expected to show alkyl C-H stretches at  $2950\text{-}2850\text{cm}^{-1}$  and an ester C=O stretch at  $1750\text{-}1735\text{cm}^{-1}$ . However, as none of these peaks are displayed on the IR spectra it was concluded that the amount of drug was so small it could not be detected by the IR. Therefore, IR spectroscopy was not used as again as an analytical technique to detect pharmaceutical adsorption.

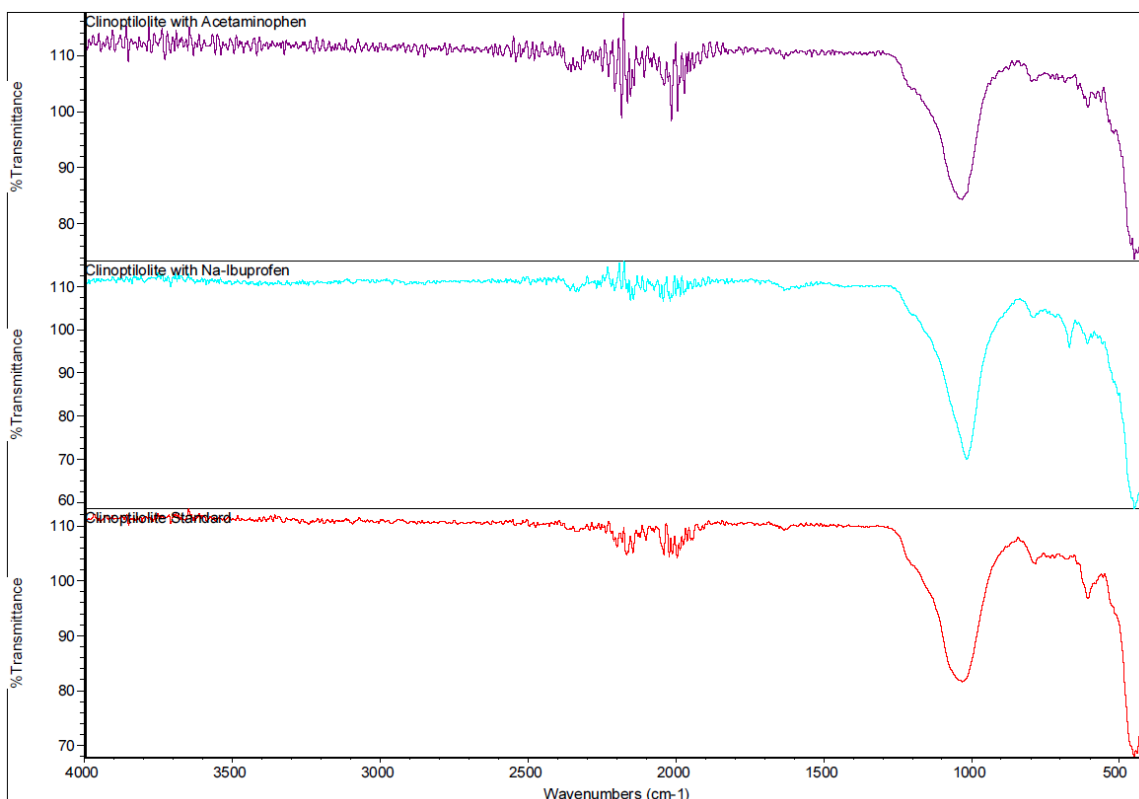


Figure 3.1.1 – Comparison of IR Spectra of clinoptilolite before and after adsorption

### 3.1.3 Acetaminophen XRD Results

It has been recognised that a change in the relative intensities of peak in a diffraction pattern can be due to molecules or ions occupying the pores of a zeolite. The diffraction patterns of clinoptilolite before and after adsorption of acetaminophen differ slightly in the peak positions and relative intensities [Figure 3.1.2].

The XRD patterns show a slight intensity change between 10 and 12° 2θ and between 20 and 25° 2θ [Figure 3.1.2]. The greatest intensity change is displayed by peak 3 [Table 3.1.2] [Figure 3.1.2] between XRD pattern A and C with peak 3 intensity decreasing by 24.11%. XRD patterns B and A [Figure 3.1.2] also exhibited changes in their peak intensities, with peak 3 showing a 11.5% decrease and peak 2 showing a 6.3% decrease.

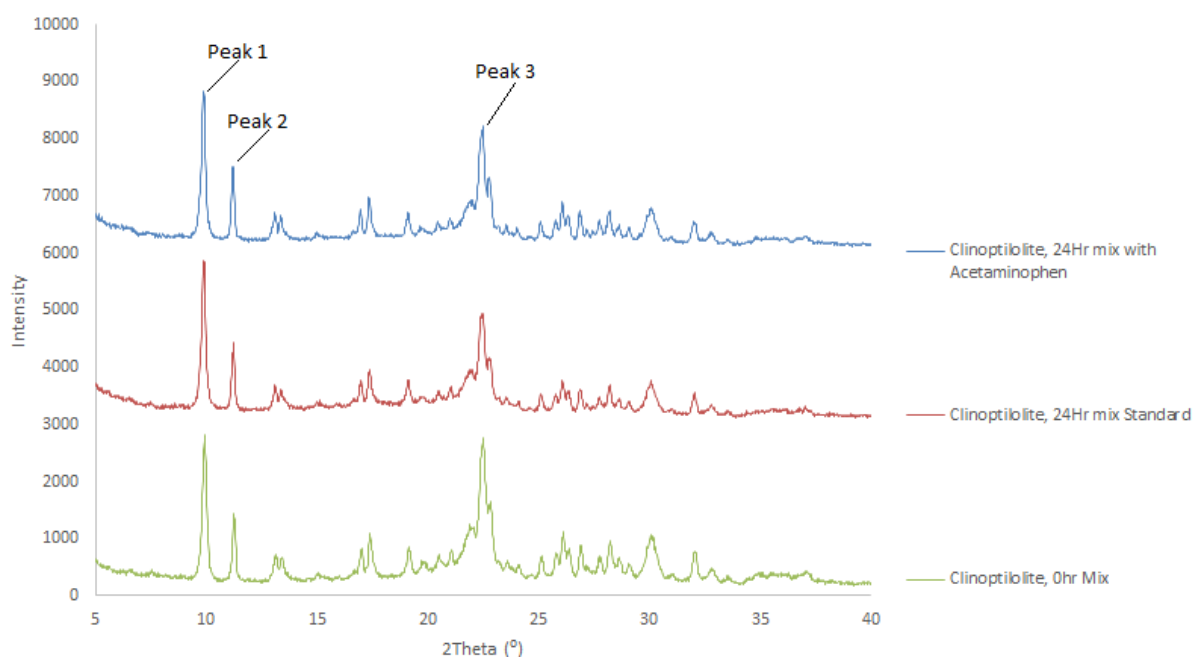


Figure 3.1.2 – Comparison of the XRD pattern of clinoptilolite adsorbed with acetaminophen against the XRD pattern of the clinoptilolite standard and the XRD pattern of clinoptilolite with zero mixing time. XRD patterns and peaks labelled with reference to table 3.1.2

Table 3.1.2 – Intensity changes of peak 2 and 3, relative to peak 1, for all for the three XRD patterns in Figure 3.1.2

	<b>Peak 1 Intensity (%)</b>	<b>Peak 2 Intensity (%)</b>	<b>Peak 3 Intensity (%)</b>
<b>Clinoptilolite with zero mixing time (A)</b>	100.0	46.3	92.9
<b>Clinoptilolite standard (B)</b>	100.0	44.6	62.4
<b>Clinoptilolite mixed with Acetaminophen (C)</b>	100.0	47.6	70.5

It is thought that the slight changes in peak intensities [Figure 3.1.2] [Table 3.1.2] are caused by the clinoptilolite adsorbing paracetamol into pores. To support this idea the XRD patterns [Figure 3.1.2] are analysed by the software Topas using the Pawley fit method. Pawley fit is a process in which the peaks observed in a XRD pattern are fitted by 2-theta values constrained by the size and symmetry of the unit cell. The structural refinement of the unit cell gives an indication of the “best fit possible”. By extracting the peak intensities before structural solution the software can determine the cell parameters [163]. A Pawley Fit can also determine any changes made to clinoptilolite unit cell parameters due to adsorption. For the following results the parameters were refined with a Pawley fit, using a Chebyshev background function and pseudo-Voigt peak shape function. If the unit cell results from clinoptilolite change significantly after adsorption (the change is larger than the calculated error), then it is an indication that the drug has adsorbed into the pores rather than attached to the particles on the surface.

Figure 3.1.3 shows that a change in lattice parameter along the  $a$  or  $b$ -axis would have a greater effect on the size and structure of the pores, more so than a change in lattice parameter along the  $c$ -axis. It is thought that any changes undertaken by the  $c$ -axis would be caused from the  $a$  and  $b$ -axis adjusting to enable the drug to adsorb.

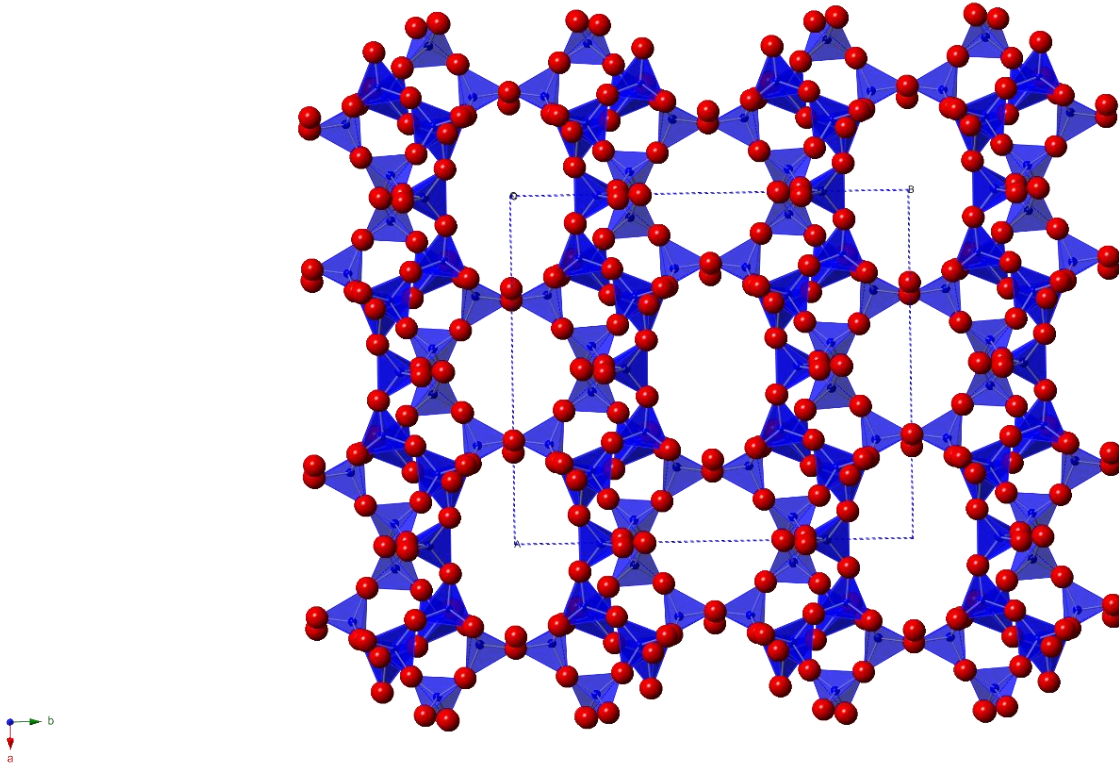


Figure 3.1.3– Polyhedral image of clinoptililite looking along the  $c$ -axis.

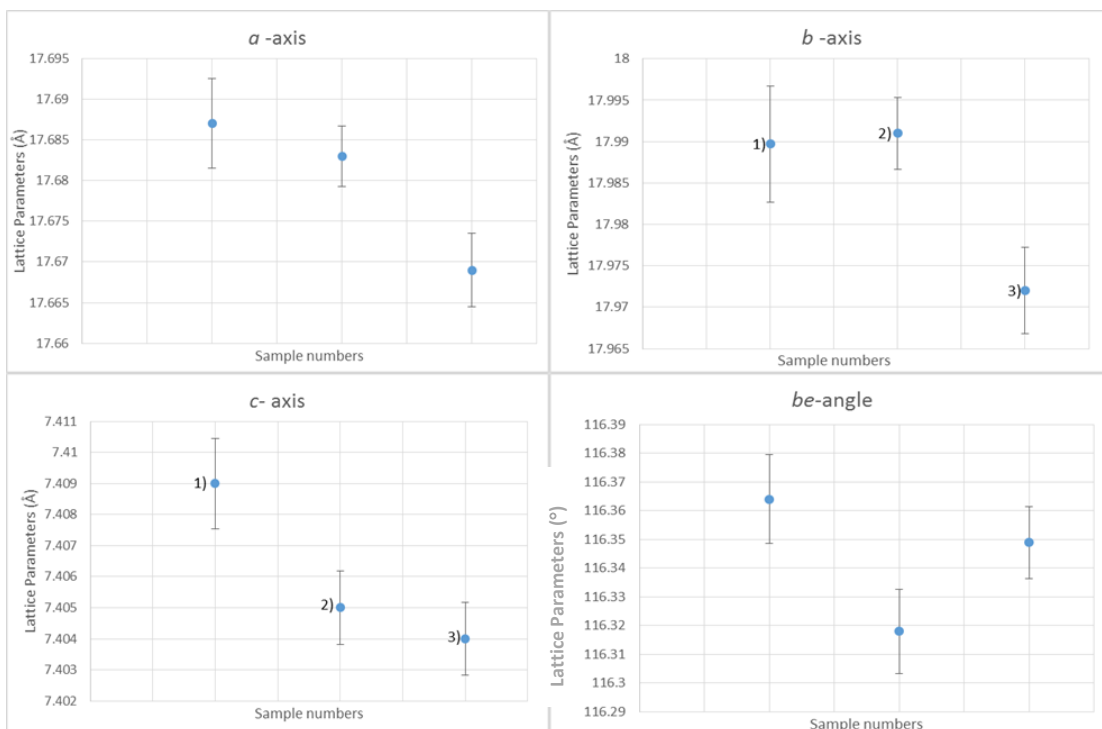


Figure 3.1.4 – Change in the unit cell lattice parameters of clinoptilolite before and after adsorption (1) clinoptilolite with no mixing, 2) clinoptilolite standard, 3) clinoptilolite mixed with acetaminophen for 24 hours)

The results in figure 3.1.4 show that the unit cells  $a$ ,  $b$  and  $c$  all exhibit a significant change in their lattice parameters between samples 1 and 3. However, only for the unit cell  $a$  and  $b$  and angle  $\beta$  show a lattice parameter change between samples 2 and 3. As all these changes mentioned above are larger than the calculated standard error, it suggests Clinoptilolites channel pores are expanding and contracting to accommodate Acetaminophen molecules.

The  $R_{wp}$  values for the three Pawley fits [Figure 3.1.5] are shown in table 3.1.3.

Table 3.1.3 – The  $R_{wp}$  values of the Pawley fits in figure 3.1.5

XRD Pattern	$R_{wp}$ %
1) Clinoptilolite with zero mixing time	10.919
2) Clinoptilolite standard	10.926
3) Clinoptilolite mixed with Acetaminophen	11.423

The  $R_{wp}$  values are all similar for the samples in table 3.1.3. With a fairly low average of 11.09% [Table 3.1.3] the Pawley fit results are not seen as a poor fit. By using figure 3.1.5 the impurities causing the poor fit can be identified. This is because the tick marks at the bottom of each XRD pattern collected should match up with a peak [Figure 3.1.5]. If a peak with no matching blue line is visible, then an impurity has caused that particular peak. The peak at 20-22° 2 $\theta$  and the peak 34-36° 2 $\theta$  [Figure 3.1.5] are assumed to be caused from impurities in the original sample of clinoptilolite, as the peaks are visible in all three diffraction patterns. There are no clear impurity peaks found in the XRD pattern “Clinoptilolite mixed with Acetaminophen for 24 hours” [Figure 3.1.5] that can be thought to have been caused by acetaminophen and account for the slightly larger  $R_{wp}$  value [Table 3.1.3].

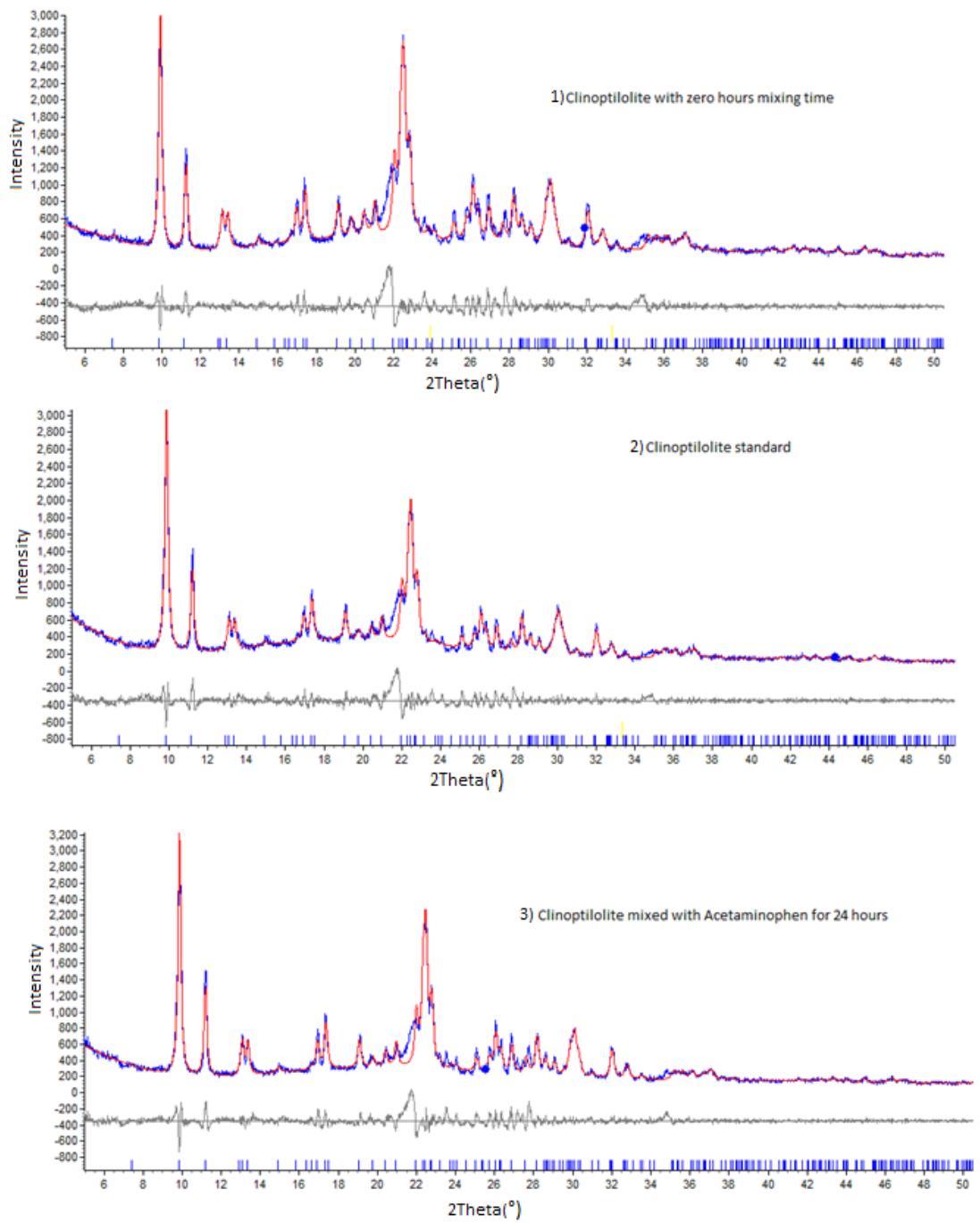


Figure 3.1.5 – Pawley fits obtained for 1) clinoptilolite with zero hours mixing 2) clinoptilolite standard 3) clinoptilolite mixed with acetaminophen for 24 hours

### 3.1.4 Na-Ibuprofen XRD Results

The XRD patterns show a slight intensity change between 10 and 12° 2 $\theta$  and between 20 and 25° 2 $\theta$  [Figure 3.1.6]. When comparing the 3 samples [Figure 3.1.6], the intensity of peak 2 relative to peak 1 decreases down the table [Table 3.1.4]; however, peak 3 does not follow this trend but does exhibit the biggest intensity change. Peak 3 is also the only peak to increase in intensity (relative to peak 1) [Figure 3.1.6] [Table 3.1.4] as peak 3 in XRD pattern A increases by 13.2% in XRD pattern C.

The diffraction patterns in figure 3.1.6 are also analysed using the Pawley fit method with the same refinement parameters used previously. The Pawley fit results highlight that the unit cells *a* and *b* have the biggest parameter change. The lattice parameters for unit cell *a* [Figure 3.1.8] shows the largest change between samples 1 and 3, as well as, sample 2 and 3, with an approximate decrease of 55.5%. Unit cell *b* shows the next biggest change, along with the only increase in change, between samples 1 and 3 and samples 2 and 3. Furthermore, the change for unit cell *c* between samples 2 and 3 are non-significant as they are within error. The lattice parameter changes [Figure 3.1.8] could be caused by clinoptilolites main pore altering in size and structure to accommodate for the uptake of Na-ibuprofen, especially with figure 3.1.8 showing clinoptilolites *a*-axis decreasing and *b*-axis increasing between samples 2 and 3.

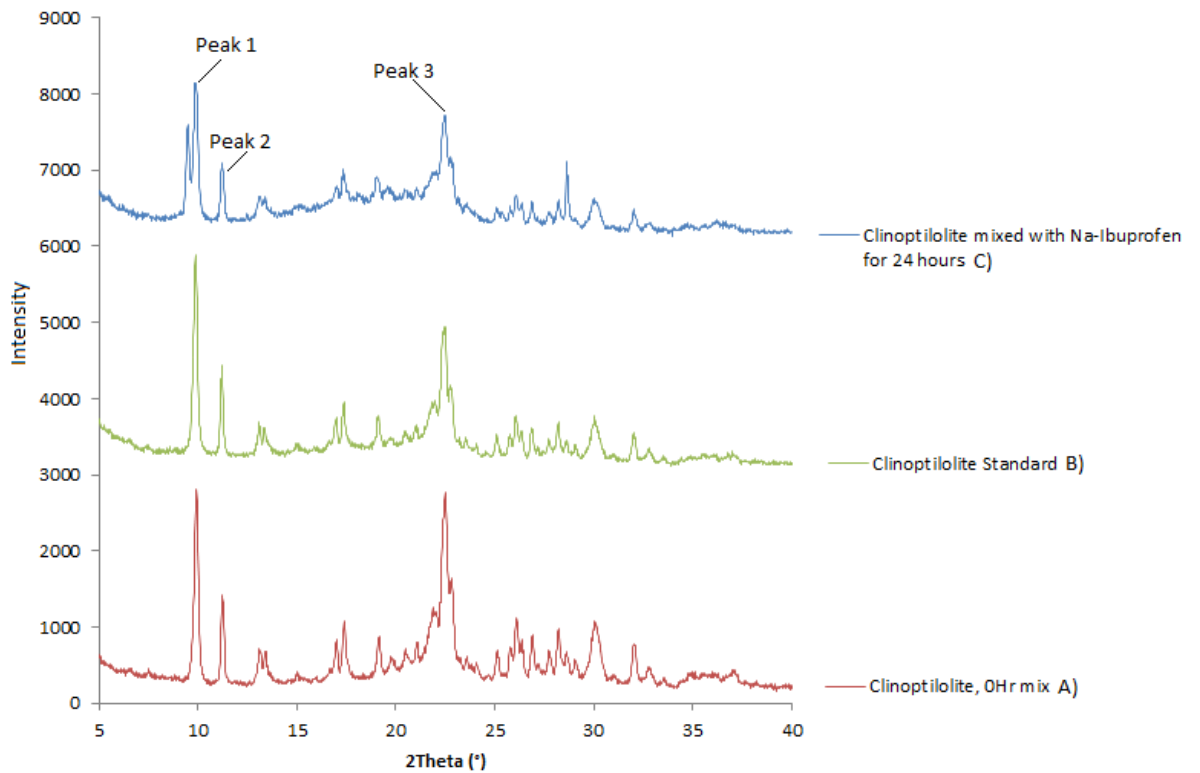


Figure 3.1.6 – Comparison of the XRD pattern of clinoptilolite adsorbed with Na-ibuprofen against the XRD pattern of the clinoptilolite standard and the XRD pattern of clinoptilolite with zero mixing time. XRD patterns and peaks labelled with reference to table 3.1.4

Table 3.1.4 – Intensity changes of peak 2 and 3, relative to peak 1, for all for the three XRD patterns in Figure 3.1.6

	Peak 1 Intensity (%)	Peak 2 Intensity (%)	Peak 3 Intensity (%)
<b>Clinoptilolite with zero mixing time (A)</b>	100.0	46.3	92.9
<b>Clinoptilolite standard (B)</b>	100.0	44.6	62.4
<b>Clinoptilolite mixed with Na-ibuprofen (C)</b>	100.0	42.2	71.9

Table 3.1.5 – The  $R_{wp}$  values of the Pawley fits in figure 3.1.7

XRD Pattern	$R_{wp}$ %
1) Clinoptilolite with zero mixing time	10.919
2) Clinoptilolite standard	10.926
3) Clinoptilolite mixed with Na-ibuprofen	12.000

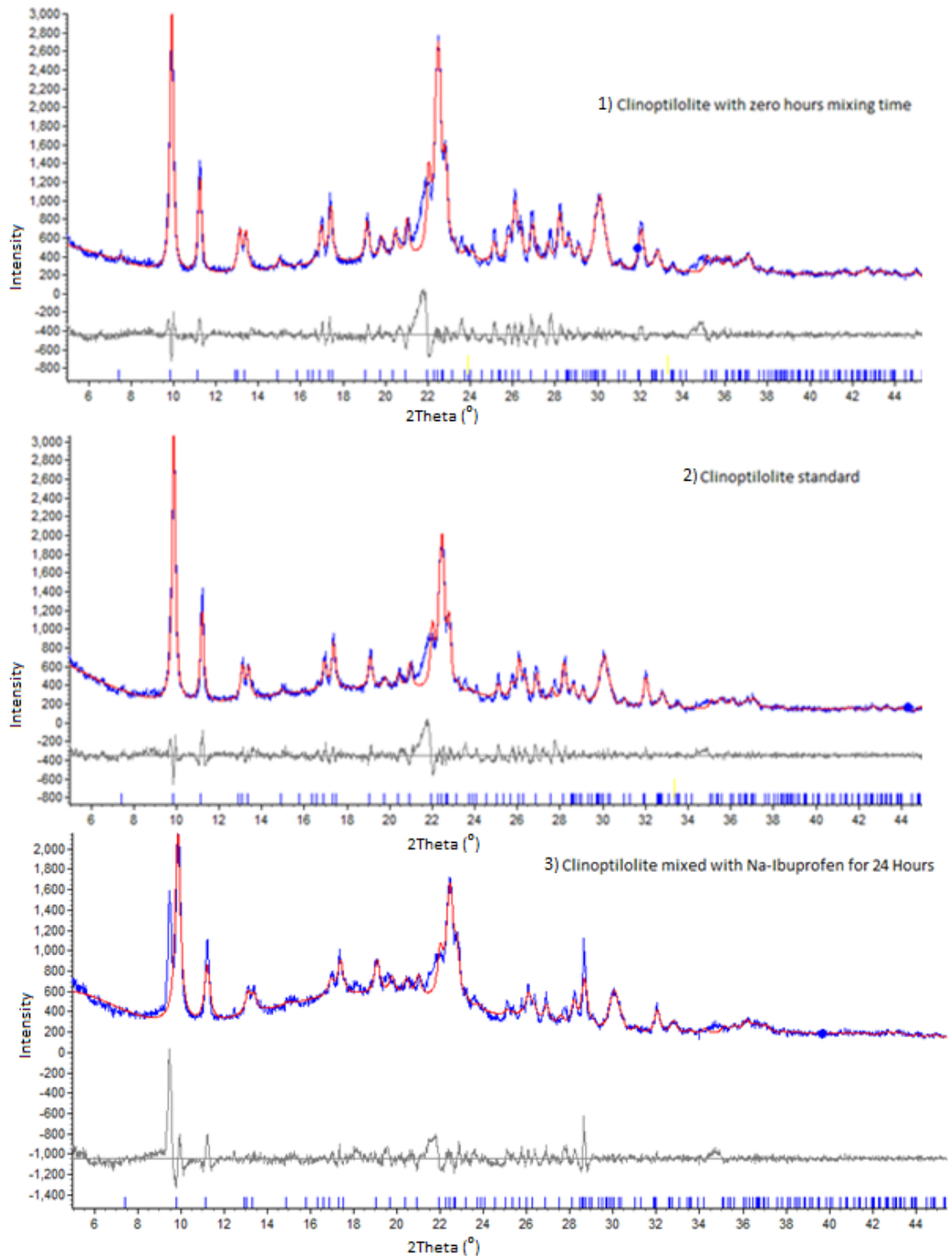


Figure 3.1.7 – Pawley fits for 1) clinoptilolite with zero hours mixing time 2) clinoptilolite standard 3) clinoptilolite with Na-ibuprofen

There is an impurity present in the ‘Clinoptilolite mixed with Na-Ibuprofen for 24 hours’

Pawley fit [Figure 3.1.7] at approximately  $9^\circ 2\theta$ . It was first thought the impurity was caused by Na-Ibuprofen, however, when comparing the diffraction pattern of ‘Clinoptilolite mixed

with Na-Ibuprofen” against the diffraction pattern of Na-Ibuprofen there were no matching peak. Furthermore, the diffraction pattern database could not confirm the impurity peak to be caused by degradation products of Na-Ibuprofen such as: hydratropic acid, 4-ethylbenzaldehyde, 4-(1-carboxyethyl)benzoic acid, 1-(4-isobutylphenyl)-1-ethanol, 2-[4-(1-hydroxy-2-methylpropyl)phenyl]propanoic acid, 1-isobutyl-4-vinylbenzene, 4-isobutylphenol [179].

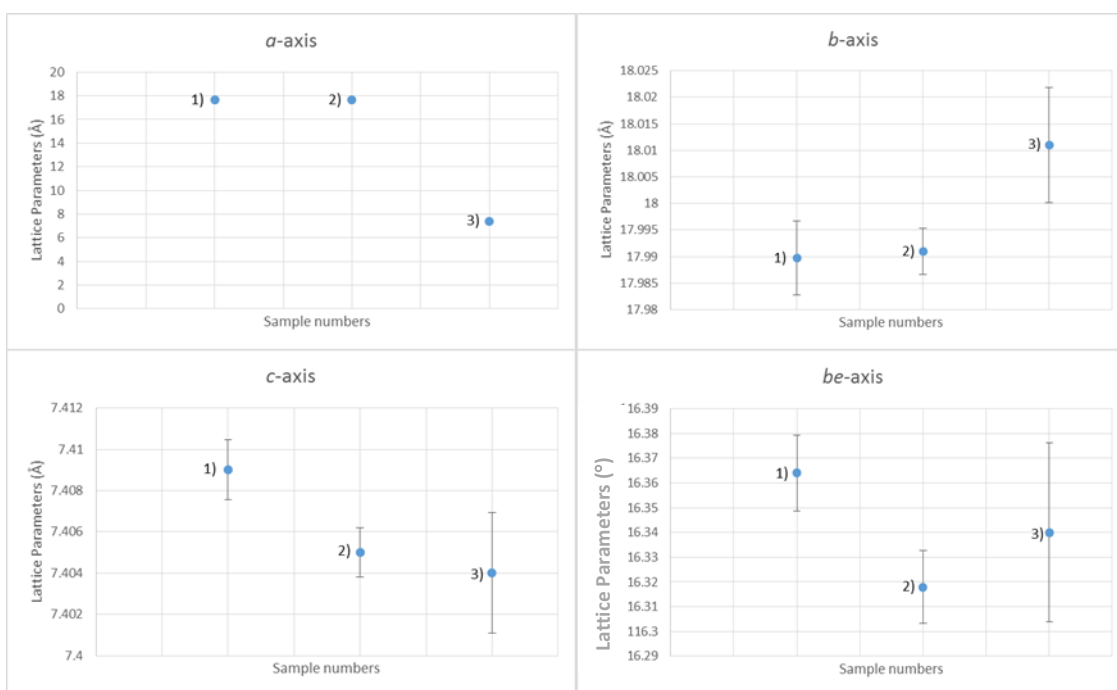


Figure 3.1.8– Change in the unit cell lattice parameters of clinoptilolite before and after adsorption (1) clinoptilolite with no mixing, 2) clinoptilolite standard, 3) clinoptilolite mixed with Na-ibuprofen for 24 hours)

## 3.2 Adsorption by Japanese Clinoptilolite

The first two adsorptions performed in section 3.1 were repeated with a different absorbent; clinoptilolite obtained from Japan. As mentioned earlier natural zeolite can vary in elemental composition with change in geographical location. A change in elemental composition could potentially affect clinoptilolite's adsorption capacity. Therefore, further adsorption experiments were carried out with natural clinoptilolite obtained from a different location, with HPLC and XRD analysis to determine the affinity of the new clinoptilolite.

### 3.2.1 HPLC Results

The HPLC results attained [Table 3.2.1], show the remaining concentrations of the drugs in solution and the percentage of drug adsorbed by Japanese clinoptilolite. When comparing the HPLC result tables [Table 3.1.1] [Table 3.2.1] the results obtained show that both clinoptilolite samples have a higher affinity towards the adsorption of Na-ibuprofen.

The HPLC results also show that the Moroccan clinoptilolite has a higher adsorption capacity for acetaminophen compared to Japanese clinoptilolite [Table 3.1.1] [Table 3.2.1]. Nevertheless, the overall HPLC results show that both clinoptilolite samples have the ability to adsorb acetaminophen and Na-ibuprofen [Table 3.1.1] [Table 3.2.1].

Table 3.2.1 – Percentage of drug uptake by Japanese clinoptilolite determined by HPLC

<b>Drug Adsorbed</b>	<b>Drug Uptake (%)</b>	<b>Concentration Remaining in Solution (M)</b>
Acetaminophen	12.64	$4.4 \times 10^{-3}$
Na-Ibuprofen	54.11	$2.3 \times 10^{-4}$

### 3.2.2 XRD Results for Acetaminophen

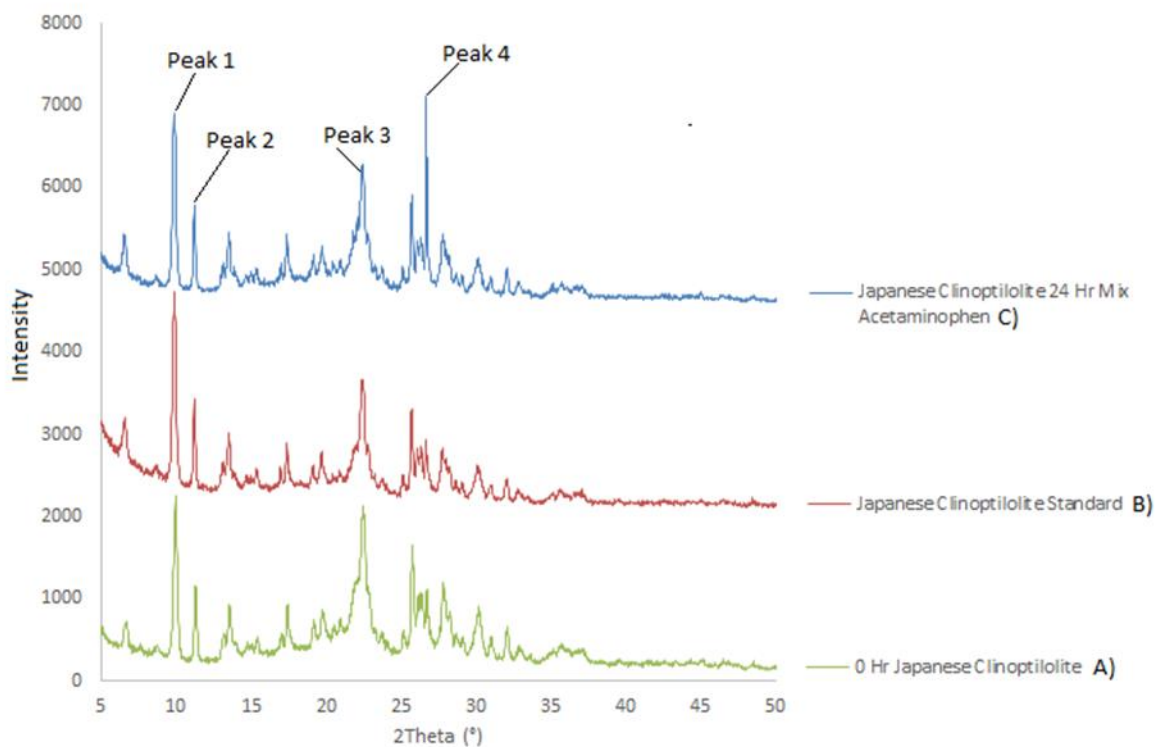


Figure 3.2.1 – Comparison of the XRD pattern of Japanese clinoptilolite adsorbed with acetaminophen against the XRD pattern of the Japanese clinoptilolite standard and the XRD pattern of Japanese clinoptilolite with zero mixing time. XRD patterns and peaks labelled with reference to table 3.2.2

Table 3.2.2 – Intensity changes of peak 2, 3 and 4, in respect to peak 1, for all for the three XRD patterns in Figure 3.2.1

	<b>Peak 1 Intensity (%)</b>	<b>Peak 2 Intensity (%)</b>	<b>Peak 3 Intensity (%)</b>	<b>Peak 4 Intensity (%)</b>
<b>Japanese Clinoptilolite with zero mixing time (A)</b>	100.0	46.4	86.2	37.2
<b>Japanese Clinoptilolite standard (B)</b>	100.0	47.7	56.0	24.0
<b>Japanese Clinoptilolite mixed with Acetaminophen (C)</b>	100.0	49.1	65.6	94.0

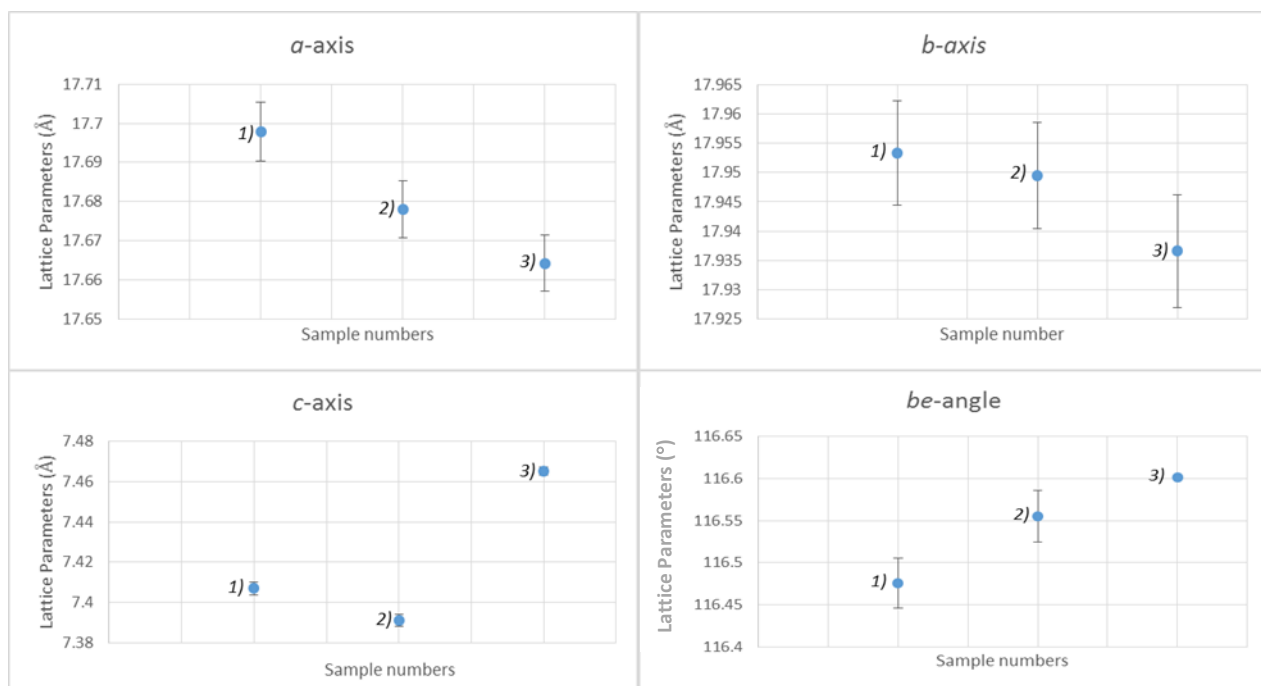


Figure 3.2.2 – Change in the unit cell lattice parameters of Japanese clinoptilolite before and after adsorption (1) Japanese clinoptilolite with no mixing, 2) Japanese clinoptilolite standard, 3) Japanese clinoptilolite mixed with acetaminophen for 24 hours)

The diffraction patterns of Japanese clinoptilolite before and after adsorption of acetaminophen are shown in figure 3.2.1. The XRD patterns show a slight intensity change between 10 and 12° 2 $\theta$  and between 20 and 30° 2 $\theta$  [Figure 3.2.1]. The greatest intensity change is displayed by peak 4 [Table 3.2.2] [Figure 3.2.1] between XRD pattern A and C with peak intensity increasing by 60.43%. XRD patterns from figure 3.1 display less changes in peak intensity changes than those in figure 3.2.1, which is interesting when you compare them to the HPLC results [Table 3.2.1] [Table 3.1.1]. It would be expected that the diffraction patterns in figure 3.2.1 would have had less peak intensity changes [Table 3.2.2] than figure 3.1.2 [Table 3.1.2], as less acetaminophen was absorbed according to the HPLC results obtained [Table 3.2.1] [Table 3.1.1].

The Pawley fit results show that the only significant lattice parameter changes were between samples 2 and 3 along the  $c$ -axis and for unit cell angle  $be$ , as the recorded

changes are outside of the estimated error [Figure 3.2.2]. The results could also be interpreted to show no change in pore size due to low uptake of acetaminophen [Table 3.2.1], as there is are no significant changes displayed by unit cells *a* and *b*.

Table 3.2.3 – The  $R_{wp}$  values of the Pawley fits in figure 3.2.3

XRD Pattern	$R_{wp}$ %
1) Japanese Clinoptilolite with zero mixing time	12.964
2) Japanese Clinoptilolite standard	12.391
3) Japanese Clinoptilolite mixed with Acetaminophen	15.297

With the  $R_{wp}$  values being relatively low [Table 3.2.3], it shows the XRD patterns fit relatively well to the structural model, however, table 3.2.3 displays the highest  $R_{wp}$  value recorded so far. It was originally thought that adsorbed acetaminophen had caused the high  $R_{wp}$  but with visual aid [Figure 3.2.3] it was clear that the impurity was not acetaminophen, as all the noticeable unticked peaks are present in all three Pawley fits.

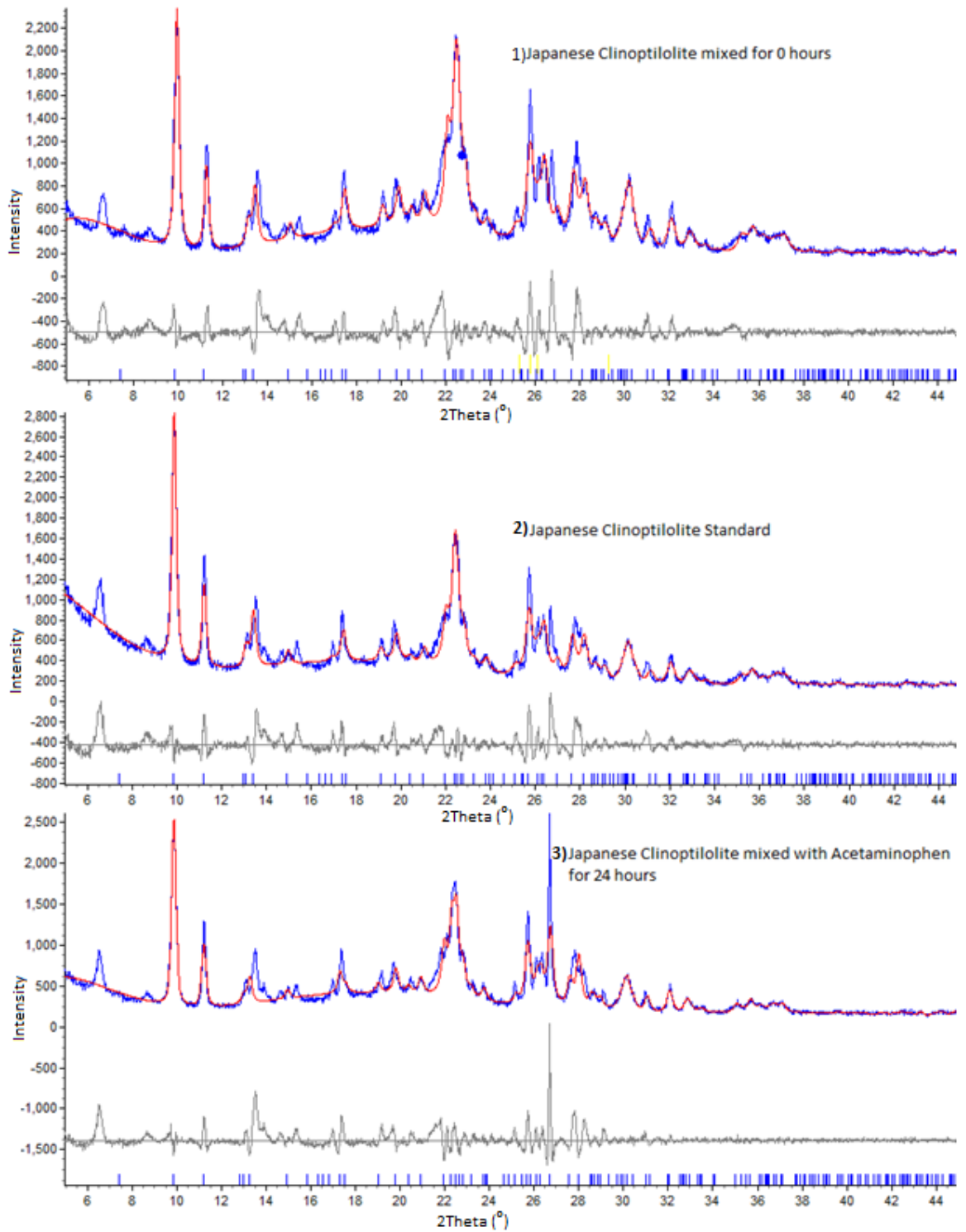


Figure 3.2.3 – Pawley fits obtained for 1) Japanese clinoptilolite mixed for 0 hours 2) Japanese clinoptilolite standard 3) Japanese clinoptilolite mixed with acetaminophen for 24 hours

### 3.2.3 XRD Results for Na-Ibuprofen

The unit cells  $a$  and  $b$  [Figure 3.2.5] have similar results to figure 3.2.2 with lattice parameter changes between samples 2 and 3 being within error. However, if the drug was adsorbed into the pores, it was assumed that there would be significant changes seen in figure 3.2.5, especially as there was a high percentage drug uptake of 54.11% [Table 3.2.1]. However, as there is no significant lattice parameter changes, it can be assumed the drug is small enough to not alter the pore size shape, or the drug has adsorbed to the samples surface.

The Pawley fit for “Japanese clinoptilolite mixed with Na-Ibuprofen for 24 hours” [Figure 3.2.6] has the same impurity as the “Clinoptilolite mixed with Na-Ibuprofen for 24 hours” [Figure 3.1.7] at approximately  $9^\circ 2\theta$ . As this impurity is not seen when acetaminophen is used, therefore, it can be assumed Na-ibuprofen is somehow causing this peak to appear.

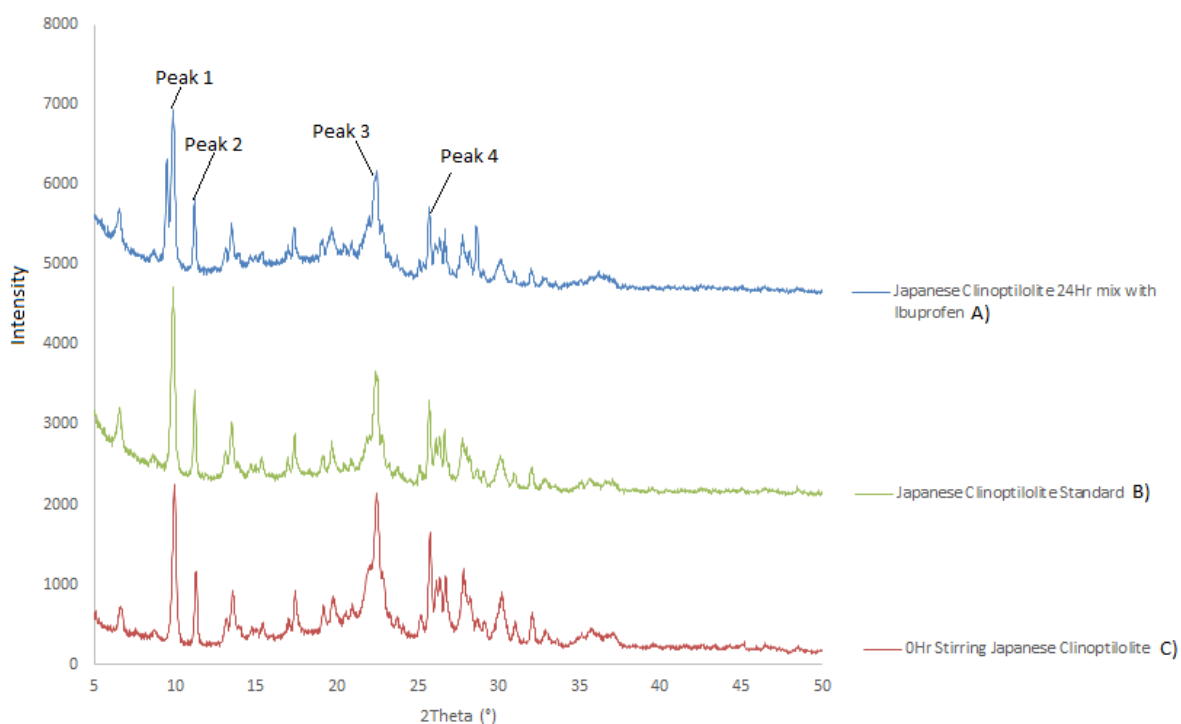


Figure 3.2.4 – Comparison of the XRD pattern of Japanese clinoptilolite adsorbed with Na-ibuprofen against the XRD pattern of the Japanese clinoptilolite standard and the XRD pattern of Japanese clinoptilolite with zero mixing time. XRD patterns and peaks labelled with reference to table 3.2.4

Table 3.2.4 – Intensity changes of peak 2, 3 and 4, relative to peak 1, for all of the three XRD patterns in Figure 3.2.4

	Peak 1 Intensity (%)	Peak 2 Intensity (%)	Peak 3 Intensity (%)	Peak 4 Intensity (%)
Japanese Clinoptilolite with zero mixing time (A)	100.0	46.4	86.2	66.2
Japanese Clinoptilolite standard (B)	100.0	47.7	56.0	45.9
Japanese Clinoptilolite mixed with Na-Ibuprofen(C)	100.0	45.4	57.0	42.3

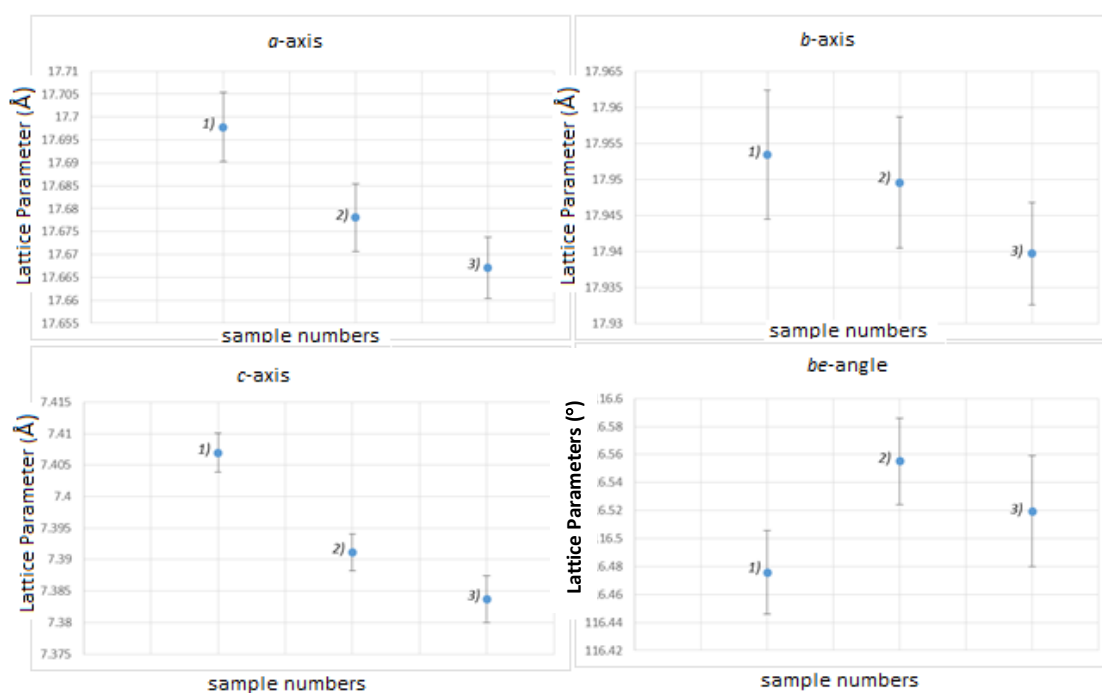


Figure 3.2.5 – Change in the unit cell lattice parameters of Japanese clinoptilolite before and after adsorption (1) Japanese clinoptilolite with no mixing, 2) Japanese clinoptilolite standard, 3) Japanese clinoptilolite mixed with Na-ibuprofen for 24 hours)

Table 3.2.5 – The  $R_{wp}$  values of Pawley fits in figure 3.2.6

XRD Pattern	$R_{WP}$ %
1) Japanese Clinoptilolite with zero mixing time	12.964
2) Japanese Clinoptilolite standard	12.391
3) Japanese Clinoptilolite mixed with Na-Ibuprofen	12.488

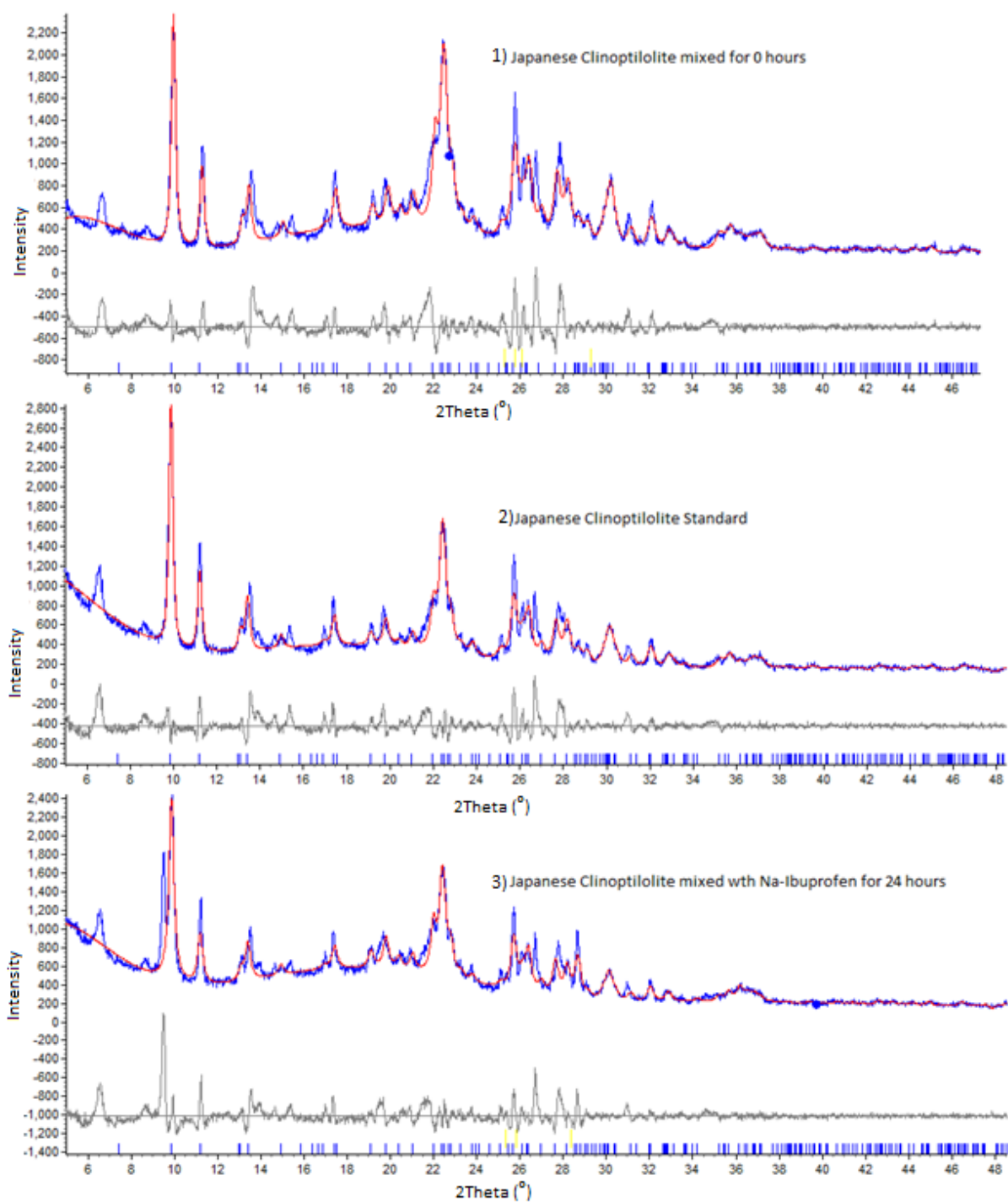


Figure 3.2.6 – Pawley fits obtained for 1) Japanese clinoptilolite mixed for 0 hours 2) Japanese clinoptilolite Standard 3) Japanese clinoptilolite mixed with Na-ibuprofen for 24 hours

### 3.3 Ion-Exchange of Clinoptilolite

In the last decade, natural zeolites have attracted great attention as ecologically advantageous and affordable materials that are abundant and inexpensive. Importantly, they can be modified to adjust and even tailor their adsorptive possibilities. Rakić *et al.* [155] ion-exchanged clinoptilolite with the following heavy metals: Mn(II), Ni(II), Cu(II), and Zn(II), as they formed stable complexes with N and O-donor groups present in their chosen pharmaceuticals; salicylic acid, acetylsalicylic acid and atenolol. The results showed clinoptilolite ion-exchanged with Cu to have a high adsorption capacity. For this reason, Japanese clinoptilolite and Moroccan clinoptilolite were ion-exchanged with Fe(III), Cu(II) and  $\text{NH}_4^+$ . Both clinoptilolite samples were ion-exchanged with  $\text{NH}_4^+$ , as they form stable bonds with the hydrogen atoms present in both pharmaceuticals.

#### 3.3.1 SEM-EDX Results

Chemical analysis of the clinoptilolite samples were performed, before and after ion-exchange, using a scanning electron microscope in conjunction with an energy-dispersive X-ray spectroscopy. An average elemental composition of the samples was obtained by a data collection at 5 different areas on the samples surface. The results attained confirm that all ion-exchanges were successful [Table 3.3.1] [Table 3.3.2].

Table 3.3.1 – Results of EDX analyses for each of the four clinoptilolite samples in wt%. The chemical compositions correspond to average values obtained from 5 area measurements (1-2mm<sup>2</sup>)

Elements Detected	Results for Clinoptilolite (Wt%)	Clinoptilolite Ion-exchanged with Copper (Wt%)	Clinoptilolite Ion-exchanged with Iron (Wt%)	Clinoptilolite Ion-exchanged with Ammonia (Wt%)
Si	30.5	31.9	27.4	33.3
Al	6.9	6.7	5.6	7.1
O	43.6	41.8	44.5	43.9
Fe	2.2	3.0	6.6	1.1
Cu	1.0	5.9	0.9	0.6
N	8.2	7.3	11.7	12.2
Na	1.8	0.4	0.5	0.6
Ca	1.2	0.8	0.83	0.2
K	2.7	2.2	1.8	1.1

Table 3.3.2- Results of EDX analyses for each of the four Japanese clinoptilolite samples in wt%. The chemical compositions correspond to average values obtained from 5 area measurements (1-2mm<sup>2</sup>)

Elements Detected	Results for Japanese Clinoptilolite (Wt%)	Japanese Clinoptilolite Ion-exchanged with Copper (Wt%)	Japanese Clinoptilolite Ion-exchanged with Iron (Wt%)	Japanese Clinoptilolite Ion-exchanged with Ammonia (Wt%)
Si	33.3	31.7	32.6	33.8
Al	6.5	6.5	6.6	6.5
O	43.1	41.5	43.5	44.2
Fe	1.3	1.4	4.3	0.9
Cu	0.8	6.1	0.7	0.7
N	10.0	9.5	10.9	12.0
Na	1.9	0.7	0.8	0.7
Ca	0.7	0.6	0.6	0.3
K	2.5	2.0	2.1	0.9

### 3.3.2 HPLC Results

Importantly, these results [Table 3.3.3 – Table 3.3.6] clearly show that adsorption capacity of clinoptilolites can be enhanced by the addition of different ions: all cation-exchanged samples adsorb higher amount of Na-ibuprofen than the parent zeolite. However, contrary to Na-ibuprofen adsorption [Table 3.3.3- Table 3.3.6], the acetaminophen exhibited lower adsorption capacities than the original clinoptilolite [Table 3.3.1]. The variances in drug uptake demonstrates how the presence of a certain cation influences the adsorption capacity of the zeolite and how zeolites can be modified towards uptake of a particular pharmaceutical. It is also worth mentioning that the best adsorptions achieved were from the Cu-exchanged clinoptilolites [Table 3.3.3 – Table 3.3.6], which was also observed by Rakić *et al* [155].

Table 3.3.3 – Percentage uptake of Acetaminophen by clinoptilolite samples determined by HPLC

	<b>Drug Uptake (%)</b>	<b>Concentration Remaining in Solution (M)</b>
Clinoptilolite ion-exchanged with Cu	21.66	$3.92 \times 10^{-3}$
Clinoptilolite ion-exchanged with Fe	10.97	$4.45 \times 10^{-3}$
Clinoptilolite ion-exchanged with NH <sub>4</sub>	10.65	$4.47 \times 10^{-3}$

Table 3.3.4 – Percentage uptake of Acetaminophen by Japanese clinoptilolite samples determined by HPLC

	<b>Drug Uptake (%)</b>	<b>Concentration Remaining in Solution (M)</b>
Japanese Clinoptilolite ion-exchanged with Cu	15.04	$4.25 \times 10^{-3}$
Japanese Clinoptilolite ion-exchanged with Fe	13.11	$4.34 \times 10^{-3}$
Japanese Clinoptilolite ion-exchanged with NH <sub>4</sub>	14.19	$4.29 \times 10^{-3}$

Table 3.3.5 – Percentage uptake of Na-ibuprofen by clinoptilolite samples determined by HPLC

	<b>Drug Uptake (%)</b>	<b>Concentration Remaining in Solution (M)</b>
Clinoptilolite ion-exchanged with Cu	60.87	$1.96 \times 10^{-4}$
Clinoptilolite ion-exchanged with Fe	55.07	$2.46 \times 10^{-4}$
Clinoptilolite ion-exchanged with NH <sub>4</sub>	57.77	$2.11 \times 10^{-4}$

Table 3.3.6 – Percentage uptake of Na-ibuprofen by clinoptilolite samples determined by HPLC

	<b>Drug Uptake (%)</b>	<b>Concentration Remaining in Solution (M)</b>
Japanese Clinoptilolite ion-exchanged with Cu	60.70	$1.97 \times 10^{-4}$
Japanese Clinoptilolite ion-exchanged with Fe	50.77	$2.46 \times 10^{-4}$
Japanese Clinoptilolite ion-exchanged with NH <sub>4</sub>	52.48	$2.38 \times 10^{-4}$

### 3.3.3 XRD Results for Cu-exchanged Clinoptilolite Samples

A significant change in the XRD pattern C [Figure 3.3.2] is seen between 5 and 10° 2θ and 25 and 30° 2θ, with the addition of 4 new peaks. The addition of the same 4 peaks is also seen in [Figure 3.3.3] but there are no additional peaks present in the acetaminophen samples. It was originally thought that the additional peaks were caused by Na-ibuprofen precipitating from solution, however, when compared to the Na-ibuprofen XRD pattern it was apparent the 4 peaks were not caused from adsorbed Na-ibuprofen [Figure 3.3.2] [Figure 3.3.3].

Identification of the substance causing all the new peaks was not possible, however, the diffraction pattern for copper propanoate matched the peak at approximately  $6^\circ$   $2\theta$  [Figure 3.3.5] [Figure 3.3.2]. The blue tick marks in figure 3.3.5 represent peaks from the copper propanoate diffraction pattern. It is thought that during the adsorption experiment, Na-ibuprofen has decomposed to form a propanoate ion which forms a complex with the copper ions, which has caused peak 2 [Figure 3.3.2] [Figure 3.3.3]. It can be assumed that the other 3 peaks found in Na-ibuprofen adsorption diffraction patterns [Figure 3.3.2] [Figure 3.3.3] are caused by other degradation products of Na-ibuprofen forming complexes with clinoptilolite cations.

For the acetaminophen adsorptions, the changes in peak intensities are highlighted in figure 3.3.1 and figure 3.3.4. The Cu-exchanged, Moroccan, clinoptilolite displays the largest intensity changes [Table3.3.8] in comparison to the intensity changes experienced by the Cu-exchanged, Japanese, clinoptilolite [Table 3.3.7]. Which relates to the HPLC results obtained from the acetaminophen adsorptions [Table 3.3.3] [Table 3.3.4], as the variance in intensity changes in table 3.3.8 could be caused from the higher uptake of acetaminophen [Table3.3.3].

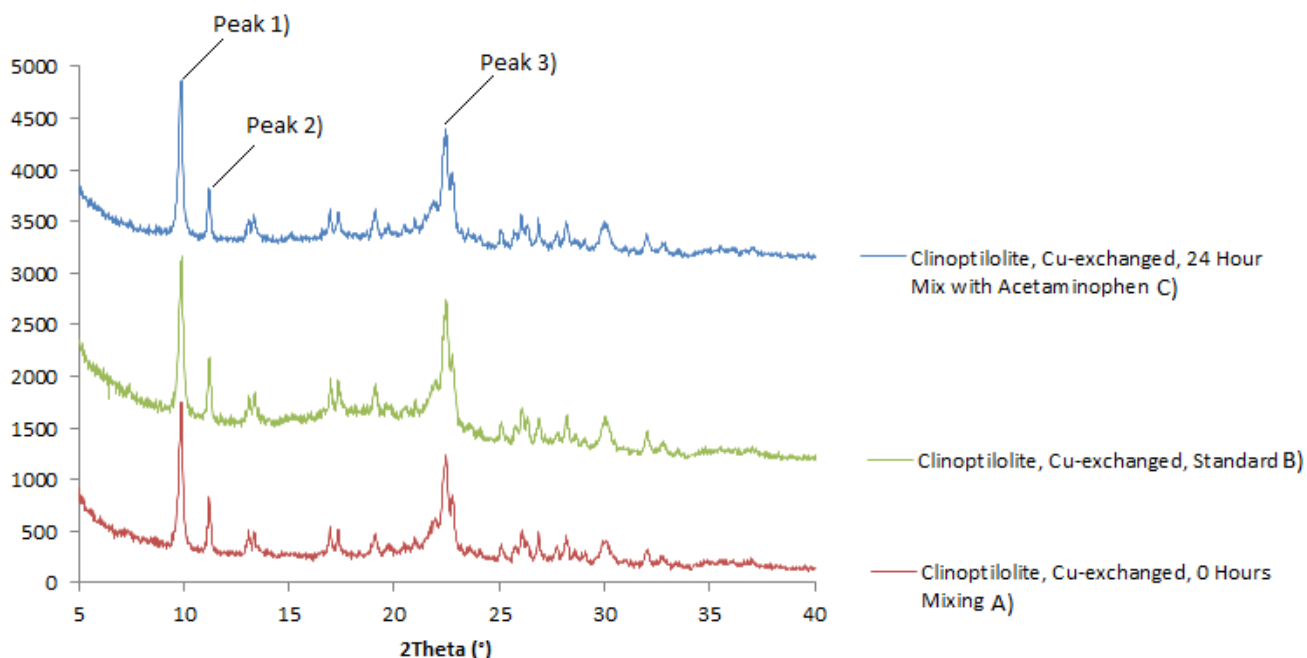


Figure 3.3.1 – Comparison of the XRD pattern of clinoptilolite Cu-exchanged adsorbed with acetaminophen against the XRD pattern of the clinoptilolite Cu-exchanged standard, and the XRD pattern of clinoptilolite with zero mixing time. XRD patterns and peaks labelled with reference to table 3.3.8

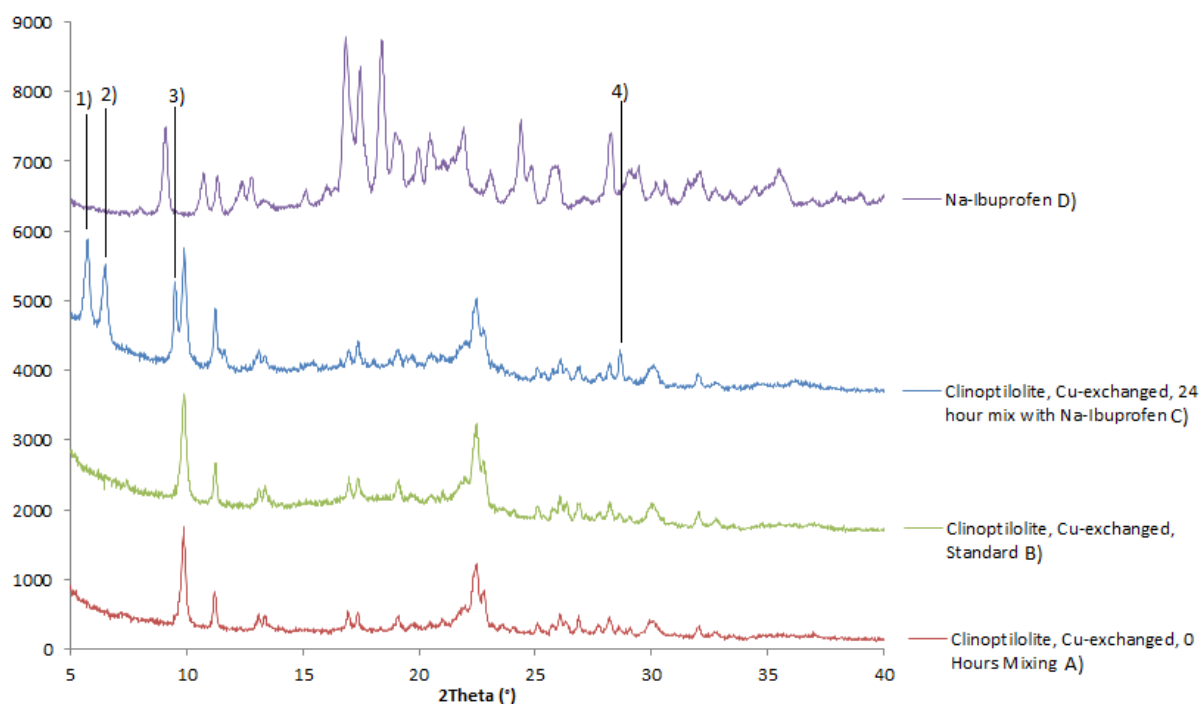


Figure 3.3.2 – Comparison of the XRD pattern of clinoptilolite Cu-exchanged adsorbed with Na-ibuprofen against the XRD pattern of the clinoptilolite Cu-exchanged standard, the XRD pattern of clinoptilolite with zero mixing time and the XRD pattern of Na-ibuprofen.

Table 3.3.7 – Intensity changes of peak 2, 3 and 4, relative to peak 1, for all of the three XRD patterns in Figure 3.3.4

	<b>Peak 1 Intensity (%)</b>	<b>Peak 2 Intensity (%)</b>	<b>Peak 3 Intensity (%)</b>
<b>Japanese Clinoptilolite, Cu-exchanged, with zero mixing time (A)</b>	100	37.3	74.4
<b>Japanese Clinoptilolite, Cu-exchanged, standard (B)</b>	100	35.4	71.5
<b>Japanese Clinoptilolite, Cu-exchanged, mixed with Acetaminophen (C)</b>	100	36.3	71.7

Table 3.3.8 – Intensity changes of peak 2, 3 and 4, relative to peak 1, for all of the three XRD patterns in Figure 3.3.1

	<b>Peak 1 Intensity (%)</b>	<b>Peak 2 Intensity (%)</b>	<b>Peak 3 Intensity (%)</b>
<b>Clinoptilolite, Cu-exchanged, with zero mixing time (A)</b>	100	35.8	65.8
<b>Clinoptilolite, Cu-exchanged, standard (B)</b>	100	39.9	84
<b>Clinoptilolite, Cu-exchanged, mixed with Acetaminophen (C)</b>	100	29.8	71.8

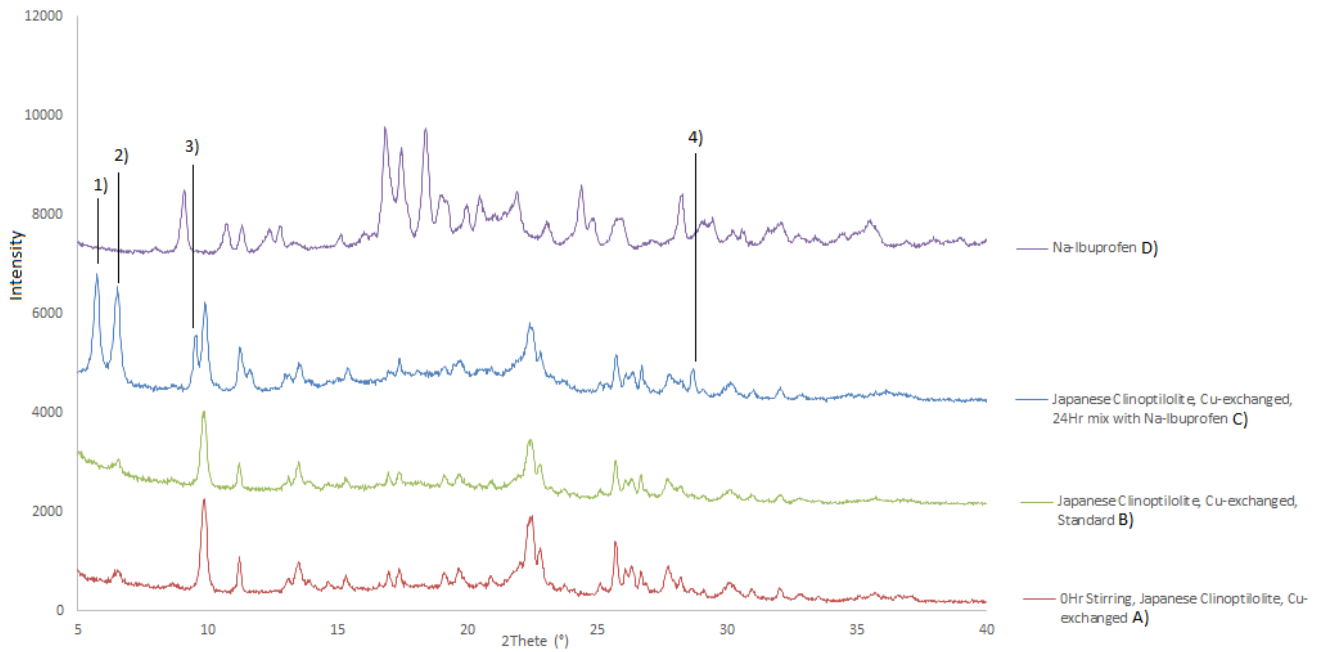


Figure 3.3.3 – Comparison of the XRD pattern of Japanese clinoptilolite Cu-exchanged adsorbed with Na-ibuprofen against the XRD pattern of the Japanese clinoptilolite Cu-exchanged standard, the XRD pattern of Japanese clinoptilolite with zero mixing time and the XRD pattern of Na-ibuprofen.

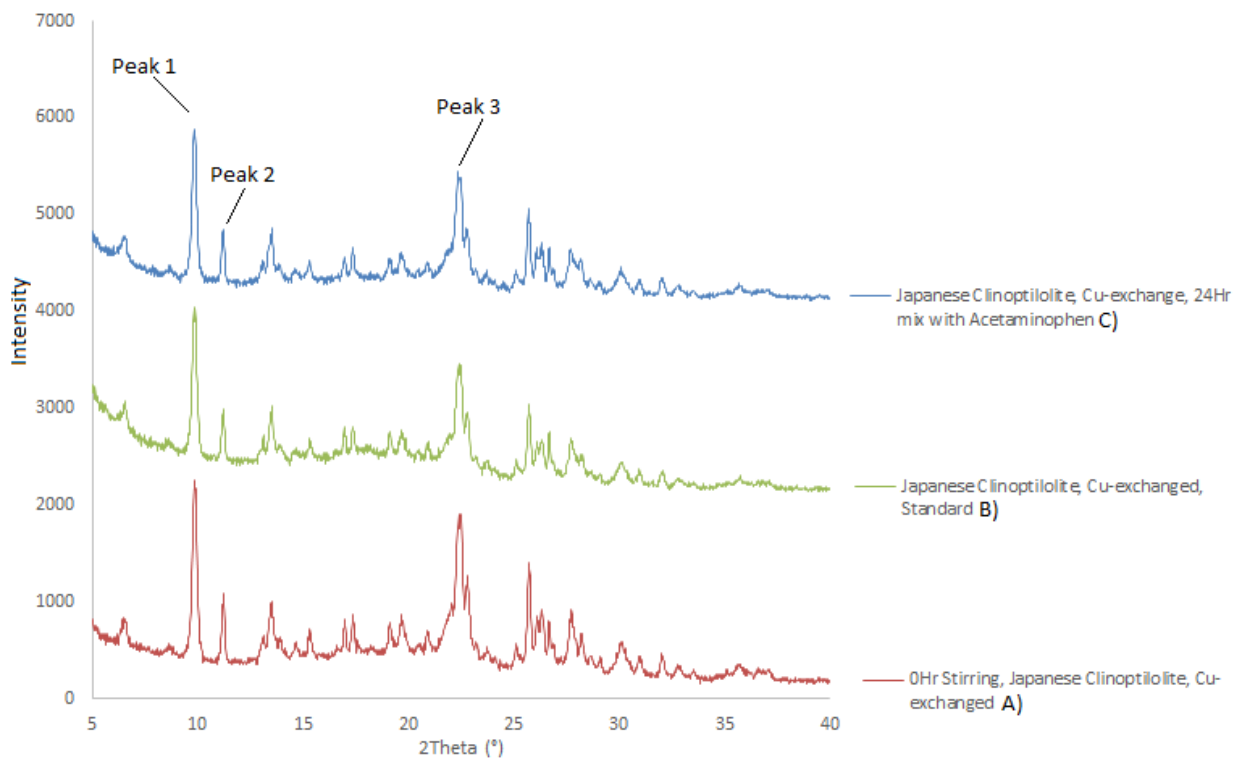


Figure 3.3.4 – Comparison of the XRD pattern of Japanese clinoptilolite Cu-exchanged adsorbed with acetaminophen against the XRD pattern of the Japanese clinoptilolite Cu-exchanged standard, and the XRD pattern of Japanese clinoptilolite with zero mixing time. XRD patterns and peaks labelled with reference to table 3.3.7

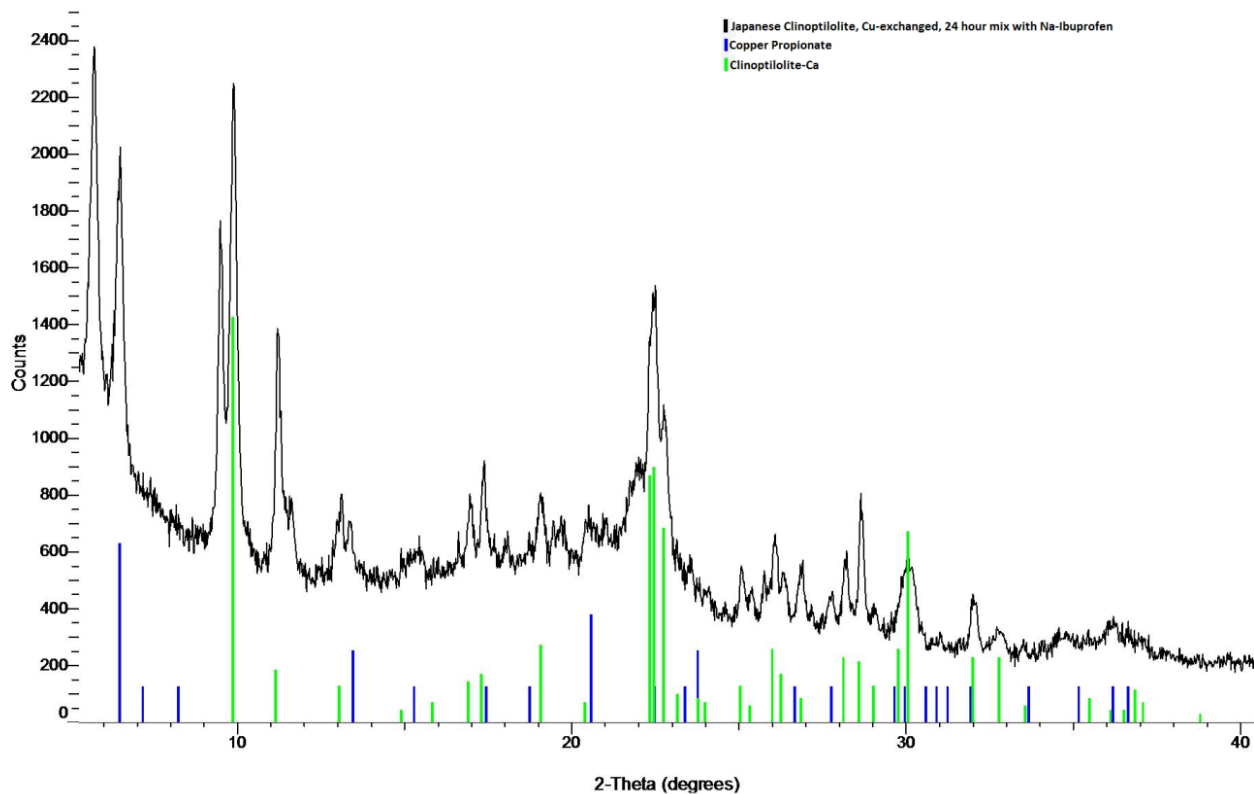


Figure 3.3.5 – Identification of new peaks found in the diffraction pattern of Japanese clinoptilolite Cu-exchanged adsorbed with Na-ibuprofen. The diffraction pattern of Copper propionate is represented by the blue lines and the green lines represent the diffraction pattern from clinoptilolite

Results from figure 3.3.6 to figure 3.3.9 all show substantial change in lattice parameters between samples 2 and 3 for unit cell axis  $a$  and  $b$ . This change in lattice parameters for the  $a$  and  $b$ -axis could be from the pores altering shape to accommodate the drug inside, particularly as the Cu-exchange Clinoptilolite samples have achieved highest drug uptake recorded so far [Tables 3.3.3 – Table 3.3.6].

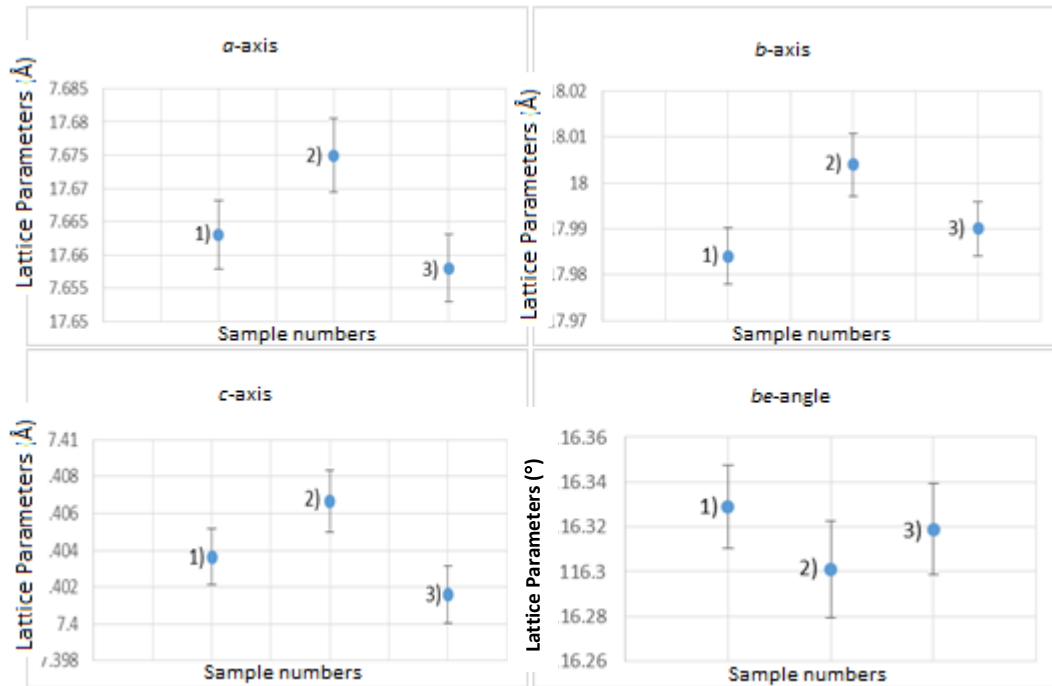


Figure 3.3.6 – Change in the unit cell lattice parameters of Cu-exchanged clinoptilolite before and after adsorption (1) Cu-exchanged clinoptilolite with no mixing, 2) Cu-exchanged, clinoptilolite standard, 3) Cu-exchanged, clinoptilolite mixed with acetaminophen for 24 hours

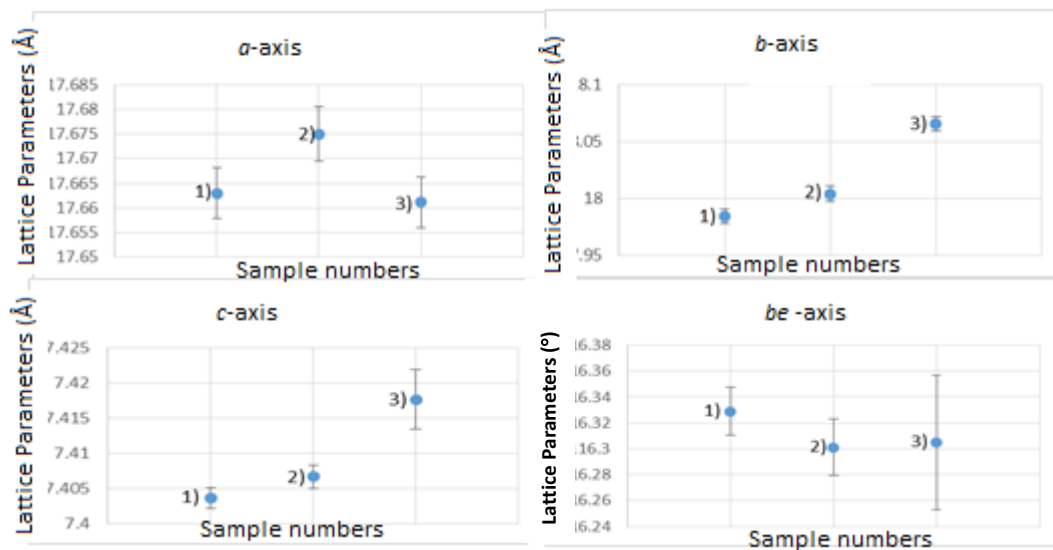


Figure 3.3.7 – Change in the unit cell lattice parameters of Cu-exchanged clinoptilolite before and after adsorption (1) Cu-exchanged clinoptilolite with no mixing, 2) Cu-exchanged, clinoptilolite standard, 3) Cu-exchanged, clinoptilolite mixed with Na-ibuprofen for 24 hours

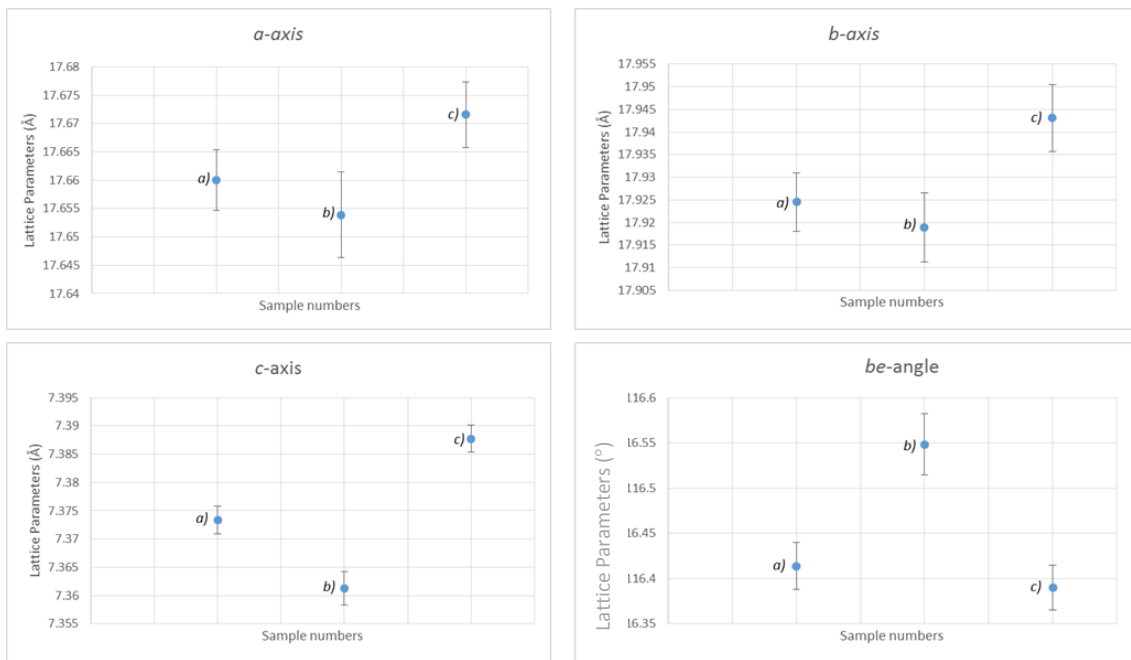


Figure 3.3.8 – Change in the unit cell lattice parameters of Cu-exchanged, Japanese clinoptilolite before and after adsorption (1) Cu-exchanged, Japanese clinoptilolite with no mixing, 2) Cu-exchanged, Japanese clinoptilolite standard, 3) Cu-exchanged, Japanese clinoptilolite mixed with acetaminophen for 24 hours

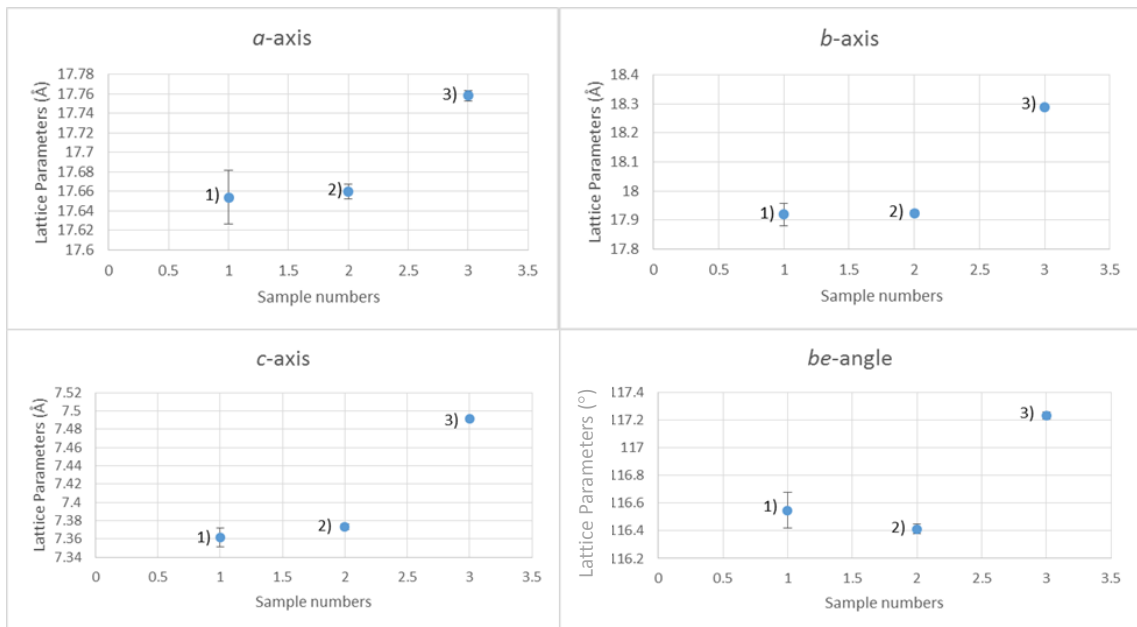


Figure 3.3.9 – Change in the unit cell lattice parameters of Cu-exchanged, Japanese clinoptilolite before and after adsorption (1) Cu-exchanged, Japanese clinoptilolite with no mixing, 2) Cu-exchanged, Japanese clinoptilolite standard, 3) Cu-exchanged, Japanese clinoptilolite mixed with Na-ibuprofen for 24 hours

Table 3.3.9 - The  $R_{wp}$  values of the Pawley fits in figure 3.3.11

XRD Pattern	$R_{WP}$ %
Clinoptilolite, Cu-exchanged, with zero mixing time (1)	9.018
Clinoptilolite, Cu-exchanged, standard (2)	6.811
Clinoptilolite, Cu-exchanged, mixed with Acetaminophen (3)	8.518
Clinoptilolite, Cu-exchanged, mix with Na-Ibuprofen (4)	12.129

Table 3.3.10 - The  $R_{wp}$  values of the Pawley fits in figure 3.3.12

XRD Pattern	$R_{WP}$ %
Japanese Clinoptilolite, Cu-exchanged, with zero mixing time (1)	11.181
Japanese Clinoptilolite, Cu-exchanged, standard (2)	9.499
Japanese Clinoptilolite, Cu-exchanged, mixed with Acetaminophen (3)	11.842
Japanese Clinoptilolite, Cu-exchanged, mix with Na-Ibuprofen (4)	16.991

The highest  $R_{wp}$  values recorded for all Cu-exchanged samples are from both clinoptilolite samples absorbed with Na-ibuprofen [Table 3.3.9] [Table 3.3.10]. This is due to the impurity peaks between  $5$  and  $10^\circ 2\theta$  and  $25$  and  $30^\circ 2\theta$  along with the high background noise [Figure 3.3.10] [Figure 3.3.11].

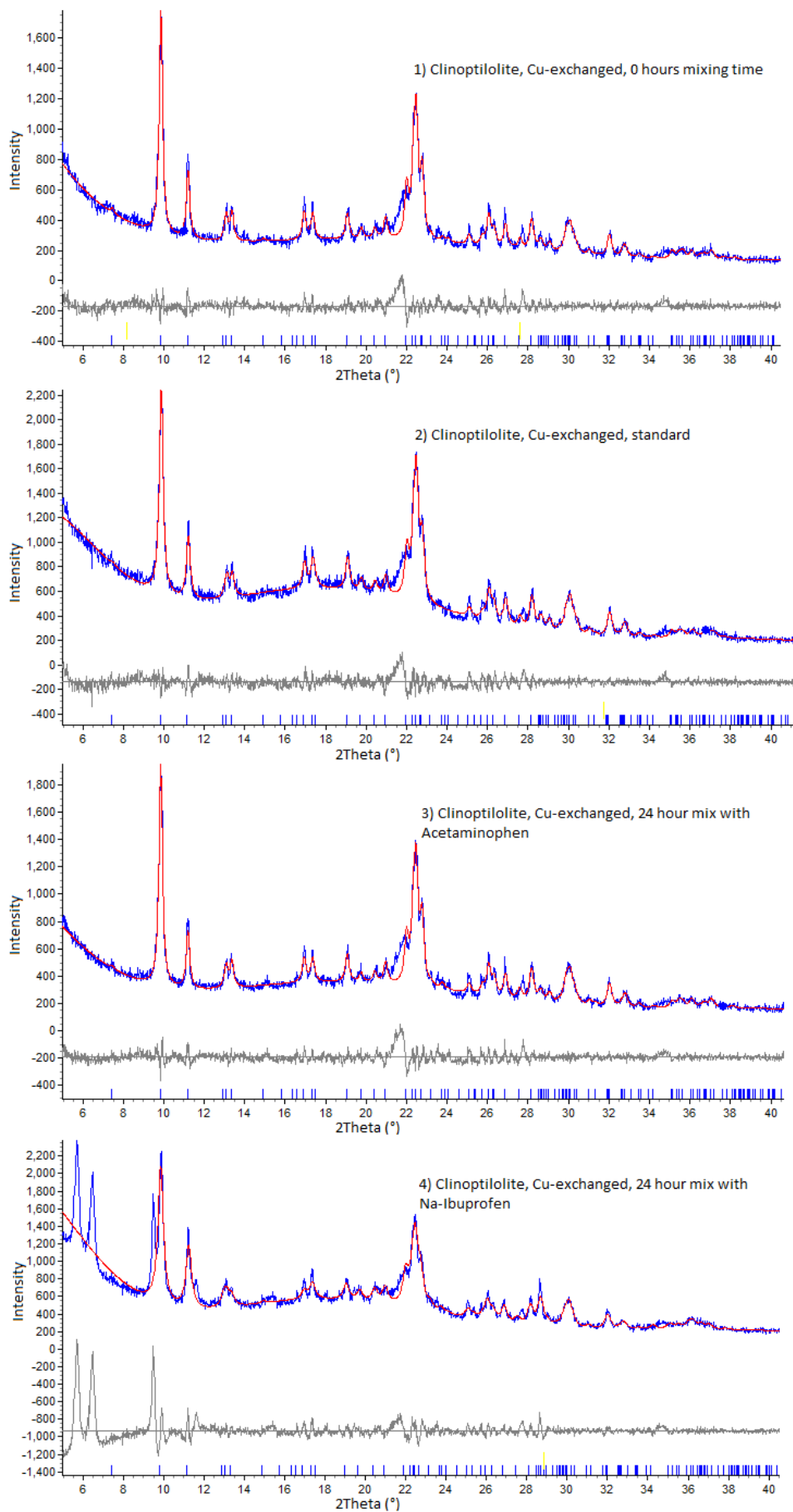


Figure 3.3.10 – Pawley fits for 1) clinoptilolite, Cu-exchanged, 0 hours mixing time, 2) clinoptilolite, Cu-exchanged, standard, 3) clinoptilolite, Cu-exchanged, 24 hour mix with acetaminophen, 4) clinoptilolite, 24 hour mix with Na-ibuprofen

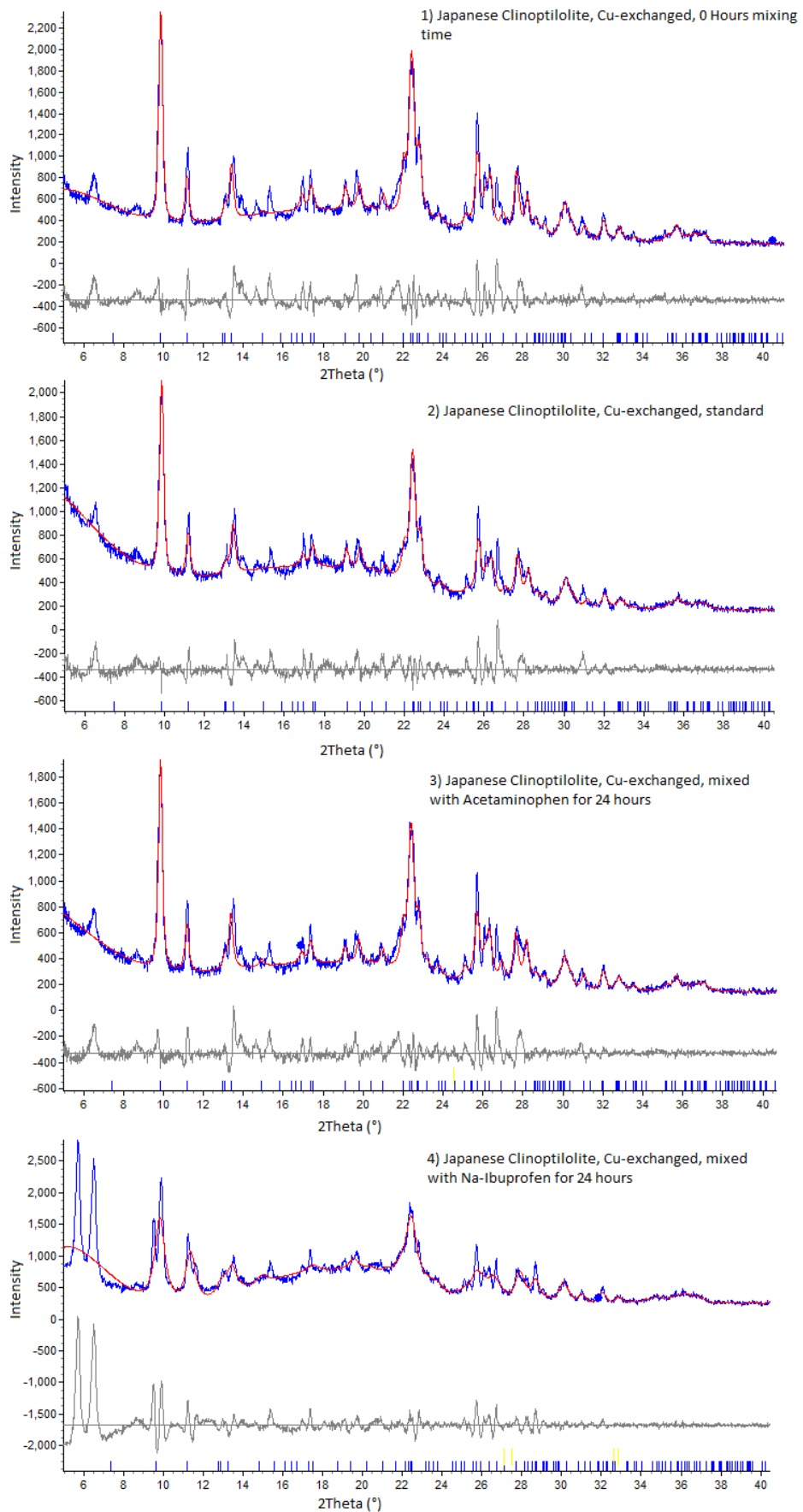


Figure 3.3.11 - Pawley fits for 1) Japanese clinoptilolite, Cu-exchanged, 0 hours mixing time, 2) Japanese Clinoptilolite, Cu-exchanged, standard, 3) Japanese clinoptilolite, Cu-exchanged, 24 hour mix with acetaminophen, 4) Japanese clinoptilolite, 24 hour mix with Na-ibuprofen

### 3.4 Adsorption using Zeolite Beta

Adsorption experiments were performed exactly as described in section 3.3, however, zeolite beta hydrogen (BEA-H) and zeolite beta ammonia (BEA-NH<sub>4</sub>) were used as the adsorbent. BEA zeolites were selected as the adsorbents due to its large pores and defective structures, both characteristic appear to be ideal for the adsorption of drugs with moderate molecular dimensions.

#### 3.4.1 Ion-exchange

In this study BEA-H and BEA-NH<sub>4</sub> were used as the initial adsorbents. The only difference between the two starting adsorbents were the cations present. Both zeolites were ion-exchanged with Fe(III), Cu(II) and NH<sub>4</sub><sup>+</sup>. The ion-exchanges were performed on both zeolites because the starting cations may have different binding affinities towards the zeolite, thus, after ion-exchange the initial zeolites may have different quantities of the new cation. The difference in the amount of cations has the potential to effect the zeolites adsorption capacity. However, it is also possible that after ion-exchange the two initial zeolites to be co-ordinated with similar amounts of the same cation. If this were the case, it is thought the adsorption results should be similar.

Chemical analysis of the BEA samples was performed, before and after ion-exchange, using an SEM-EDX. An average elemental composition of the samples was obtained by a data collection at 5 different areas on the samples surface. The results attained confirm that all ion-exchanges were successful [Table 3.4.1] [Table 3.4.2].

Table 3.4.1- Results of EDX analyses for each of the four BEA-H samples in wt%. The chemical compositions correspond to average values obtained from 5 area measurements (1-2mm<sup>2</sup>)

Elements detected	Results for BEA-H (Wt %)	Results for BEA-H, Ion-exchanged with Cu (Wt %)	Results for BEA-H, Ion-exchanged with Fe (Wt %)	Results for BEA-H, Ion-exchanged with NH <sub>4</sub> (Wt %)
Si	46.4	41.7	40.5	38.5
Al	0.8	0.6	2.4	1.6
O	42.8	46.9	46.4	41.8
Fe	0.5	0.2	2.8	1.4
Cu	0.8	0.6	0.7	3.2
N	8.8	10.0	8.9	15.5

Table 3.4.2- Results of EDX analyses for each of the three BEA-NH<sub>4</sub> samples in wt%. The chemical compositions correspond to average values obtained from 5 area measurements (1-2mm<sup>2</sup>)

Elements detected	Results for BEA-NH <sub>4</sub> (Wt %)	Results for BEA-NH <sub>4</sub> , Ion-exchanged with Cu (Wt %)	Results for BEA-NH <sub>4</sub> , Ion-exchanged with Fe (Wt %)
Si	40.5	36.5	34.8
Al	3.8	3.2	2.7
O	45.3	45.5	43.9
Fe	0.4	0.3	7.2
Cu	0.7	3.6	0.9
N	9.4	10.9	10.5

EDX results showed that BEA-NH<sub>4</sub> ion-exchanged to a greater extent with Cu(II) and Fe(III) more so than BEA-H [Table 3.4.1] [Table 3.4.2]. The results also showed that ion-exchange with Fe(III) was more successful with BEA-NH<sub>4</sub> than BEA-H. As 7.2% Fe was detected in BEA-NH<sub>4</sub> ion-exchange with Fe(III) compared to the 2.8% detected in the BEA-H ion-exchanged with Fe (III) [Table 3.4.1] [Table 3.4.2]. Additionally, the Fe-exchanged sample for BEA-NH<sub>4</sub> is above the ion-exchange capacity. The higher quantity is thought to be caused by the formation of finely dispersed intra-zeolite ferric oxide clusters.

### 3.4.2 HPLC Results

The HPLC results obtained [Table 3.4.5] [Table 3.4.6], show that all the BEA samples have similar adsorption affinities towards acetaminophen of approximately 12%. This is also the case for the Na-ibuprofen adsorptions, with all the BEA samples absorbing approximately 23% [Table 3.4.3] [Table 3.4.4]. As there is little variance in drug uptake, it can be assumed that pharmaceuticals in question, can bind to each cation with similar binding affinities.

The highest percentage uptake of acetaminophen and Na-ibuprofen is exhibited by all BEA samples ion-exchanged with Fe [Table 3.4.3 - Table 3.4.6]. Furthermore, the HPLC results show that BEA has a higher affinity towards Na-ibuprofen [Table 3.4.3] [Table 3.4.4] compared to acetaminophen [Table 3.4.5] [Table 3.4.6], this was also the case for all the clinoptilolite adsorptions [Table 3.0] [Table 3.2.1] [Table 3.3.3] [Table 3.3.4] [Table 3.3.5] [Table 3.3.6]. However, BEA showed relatively low uptake of Na-ibuprofen, with an approximate adsorption of 23% [Table 3.4.3] [Table 3.4.4], compared to the 60% uptake displayed by Clinoptilolite [Table 3.3.5] [Table 3.3.6].

Furthermore, the HPLC results show that the BEA-NH<sub>4</sub> samples ion-exchanged with Fe, achieved higher drug uptake for both pharmaceuticals [Table 3.4.4] [Table 3.4.6], when compared to the adsorption results achieved by the BEA-H samples ion-exchanged with Fe [Table 3.4.3] [Table 3.4.5]. It is thought that this slight difference in adsorptions is due to the quantities of Fe cations present. As the EDX results show [Table 3.4.1] [Table 3.4.2] that after ion-exchange with Fe, that there are more Fe cations present in the BEA-NH<sub>4</sub> sample than the BEA-H sample. Therefore, it is thought that BEA-NH<sub>4</sub> achieved higher adsorption results [Table 3.4.4] [Table 3.4.6] as it contained more Fe cations for the drugs to bind to.

Table 3.4.3 – Percentage uptake of Na-Ibuprofen by Beta Hydrogen (X) samples determined by HPLC

	<b>Drug uptake (%)</b>	<b>Concentration Remaining</b>
<b>Beta Hydrogen (X)</b>	23.97	$3.802 \times 10^{-4}$
<b>X, Ion-exchanged with Cu</b>	21.84	$3.908 \times 10^{-4}$
<b>X, Ion-exchanged with Fe</b>	25.60	$3.720 \times 10^{-4}$
<b>X, Ion-exchanged with NH<sub>4</sub></b>	22.02	$3.899 \times 10^{-4}$

Table 3.4.4 – Percentage uptake of Na-Ibuprofen by Beta Ammonia (Y) samples determined by HPLC

	<b>Drug uptake (%)</b>	<b>Concentration Remaining</b>
<b>Beta Ammonia (Y)</b>	21.90	$3.905 \times 10^{-4}$
<b>Y, Ion-exchanged with Cu</b>	22.51	$3.875 \times 10^{-4}$
<b>Y, Ion-exchanged with Fe</b>	28.93	$3.554 \times 10^{-4}$

Table 3.4.5 – Percentage uptake of Acetaminophen by Beta Hydrogen (X) samples determined by HPLC

	<b>Drug uptake (%)</b>	<b>Concentration Remaining</b>
<b>Beta Hydrogen (X)</b>	11.35	$4.43 \times 10^{-3}$
<b>X, Ion-exchanged with Cu</b>	11.12	$4.44 \times 10^{-3}$
<b>X, Ion-exchanged with Fe</b>	13.77	$4.31 \times 10^{-3}$
<b>X, Ion-exchanged with NH<sub>4</sub></b>	11.53	$4.42 \times 10^{-3}$

Table 3.4.6 – Percentage uptake of Acetaminophen by Beta Ammonia (Y) samples determined by HPLC

	<b>Drug uptake (%)</b>	<b>Concentration Remaining</b>
<b>Beta Ammonia (Y)</b>	13.90	$4.31 \times 10^{-3}$
<b>Y, Ion-exchanged with Cu</b>	12.68	$4.37 \times 10^{-3}$
<b>Y, Ion-exchanged with Fe</b>	14.43	$4.28 \times 10^{-3}$

### 3.4.3 XRD results for BEA-NH<sub>4</sub> Ion-exchanged with Fe

The pore size of BEA is big enough to accommodate acetaminophen and Na-ibuprofen, therefore, BEA pores would not express any structure change during pharmaceutical adsorption. The changes in lattice parameters between the standard sample (2) and the drug adsorbed sample (3) [Figure 3.4.1] [Figure 3.4.2] are all within calculated error. The error is caused by defects site (Si(OH)<sub>x</sub> groups) present in BEAs framework. Therefore, it cannot be confirmed that no substantial changes have occurred to the BEA unit cells [Figure 3.4.1] [Figure 3.4.2].

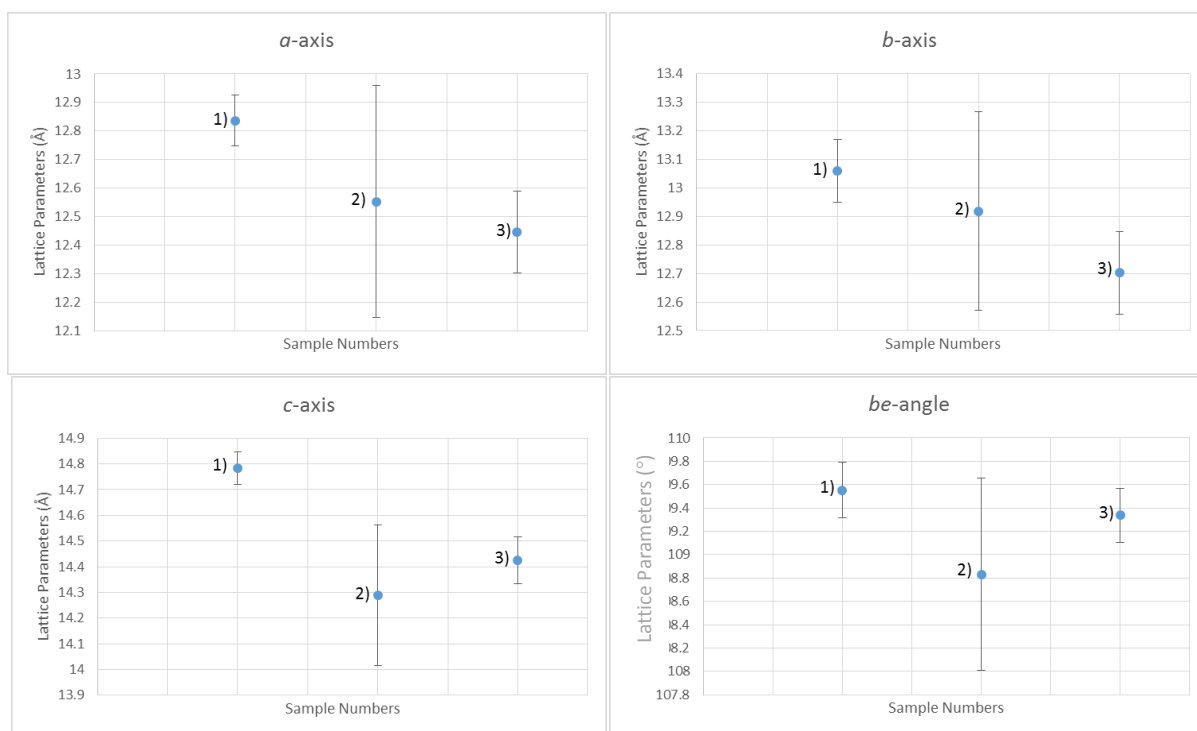


Figure 3.4.1– Change in the unit cell lattice parameters of Fe-exchanged, BEA-NH<sub>4</sub> before and after adsorption (1) Fe-exchanged, BEA-NH<sub>4</sub> with no mixing, 2) Fe-exchanged, BEA-NH<sub>4</sub> standard, 3) Fe-exchanged, BEA-NH<sub>4</sub> mixed with acetaminophen for 24 hours

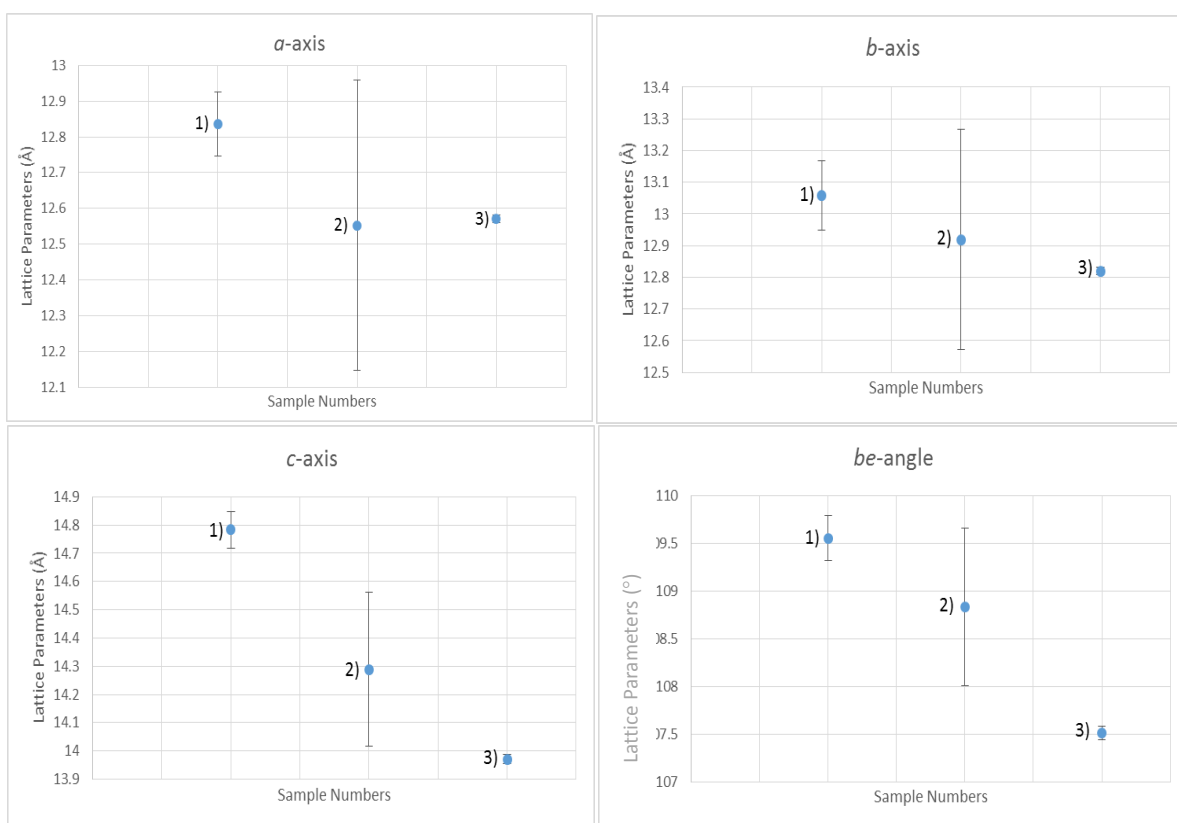


Figure 3.4.2– Change in the unit cell lattice parameters of Fe-exchanged, BEA-NH<sub>4</sub> before and after adsorption (1) Fe-exchanged, BEA-NH<sub>4</sub> with no mixing, 2) Fe-exchanged, BEA-NH<sub>4</sub> standard, 3) Fe-exchanged, BEA-NH<sub>4</sub> mixed with Na-ibuprofen for 24 hours

Table 3.4.7 - The  $R_{wp}$  values of the Pawley fits in figure 3.4.3

XRD Pattern	$R_{WP}$ %
BEA-NH <sub>4</sub> , Fe-exchanged, with zero mixing time (1)	5.676
BEA-NH <sub>4</sub> , Fe-exchanged, standard (2)	5.557
BEA-NH <sub>4</sub> , Fe-exchanged, mixed with Acetaminophen (3)	5.522
BEA-NH <sub>4</sub> , Fe-exchanged, mix with Na-Ibuprofen (4)	13.529

The  $R_{wp}$  values for “BEA-NH<sub>4</sub>, Fe-exchanged, mixed with Na-Ibuprofen” has the highest  $R_{wp}$  value of 13.529% [Table 3.4.7]. It is still seen as a “good fit”, however, all the other  $R_{wp}$  values in table 3.4.7 are all a lot lower with approximately 5%. It is thought the error is due to the Pawley fit trying to match the impurity peaks to BEA peaks. This is very clear at around 10° 2θ [Figure 3.4.3] in the Pawley fit for “3) BEA-NH<sub>4</sub>, Fe-exchanged, mixed with Na-Ibuprofen” as the BEA peak is too narrow to be matched with the impurity peak.

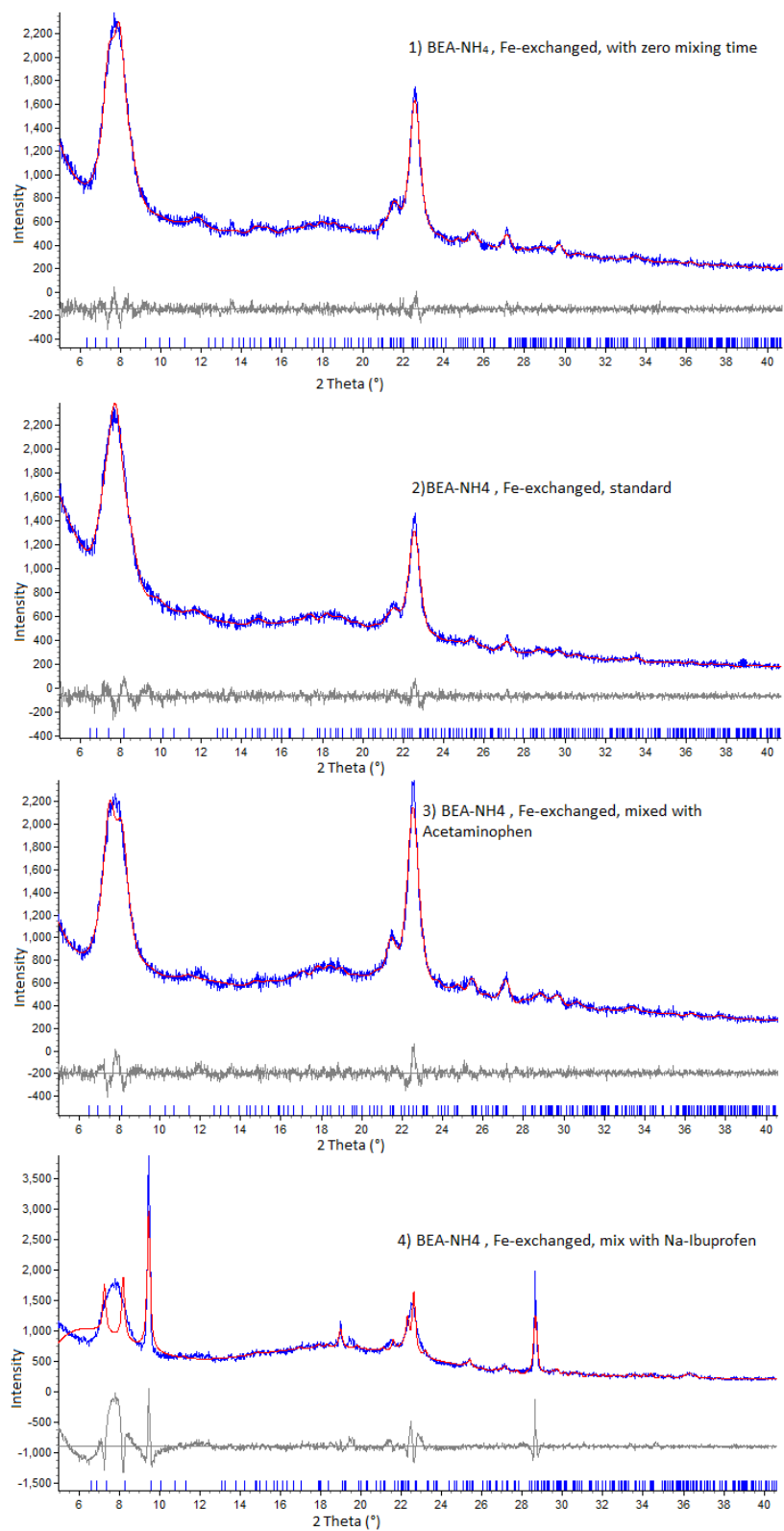


Figure 3.4.3– Pawley fits obtained for (1) Fe-exchanged, BEA-NH<sub>4</sub> with no mixing, 2) Fe-exchanged, BEA-NH<sub>4</sub> standard, 3) Fe-exchanged, BEA-NH<sub>4</sub> mixed with acetaminophen for 24 hours and 4) Fe-exchanged, BEA-NH<sub>4</sub> mixed with Na-ibuprofen for 24 hours

Identification of the substance causing the new peak at approximately  $9^\circ 2\theta$  [Figure 3.4.3] is thought to be copper acetate hydroxide hydrate. The blue lines in figure 3.4.4 represent the peaks from the copper acetate hydroxide hydrate diffraction pattern. Figure 3.4.4 shows three peaks that match up, however, the intensity for blue line at approximately  $28^\circ 2\theta$  is not an exact match. It is thought that copper acetate hydroxide hydrate is another degradation product formed from Na-ibuprofen, similar to the copper propanoate ion identified earlier [3.3.5]. Although this species is co-ordinated to copper, it is possible it could be co-ordinated to the iron cat ions.

### Adsorption of Na-Ibuprofen by Zeolite Beta Ammonia, Ion-exchanged with Fe

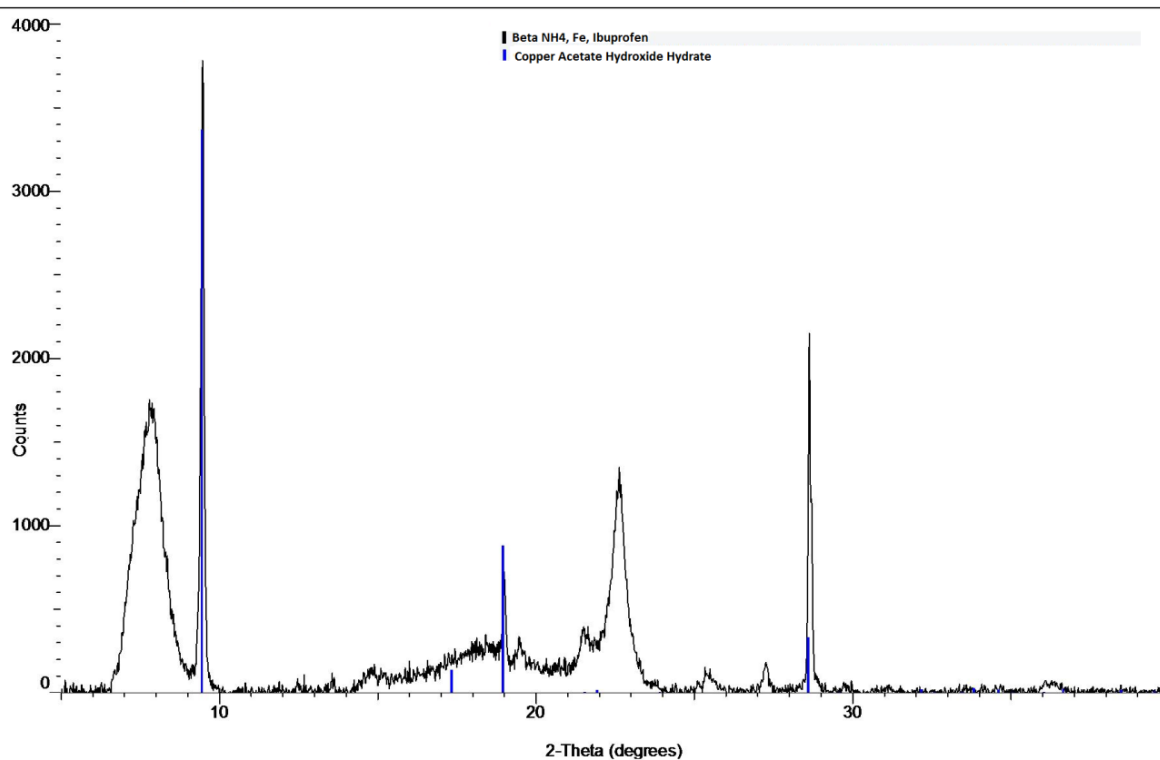


Figure 3.4.4 – Identification of new peaks found in the diffraction pattern of Na-Ibuprofen adsorbed by BEA-NH<sub>4</sub>, ion-exchanged with Fe. The diffraction pattern of copper acetate hydroxide hydrate is represented by the blue lines

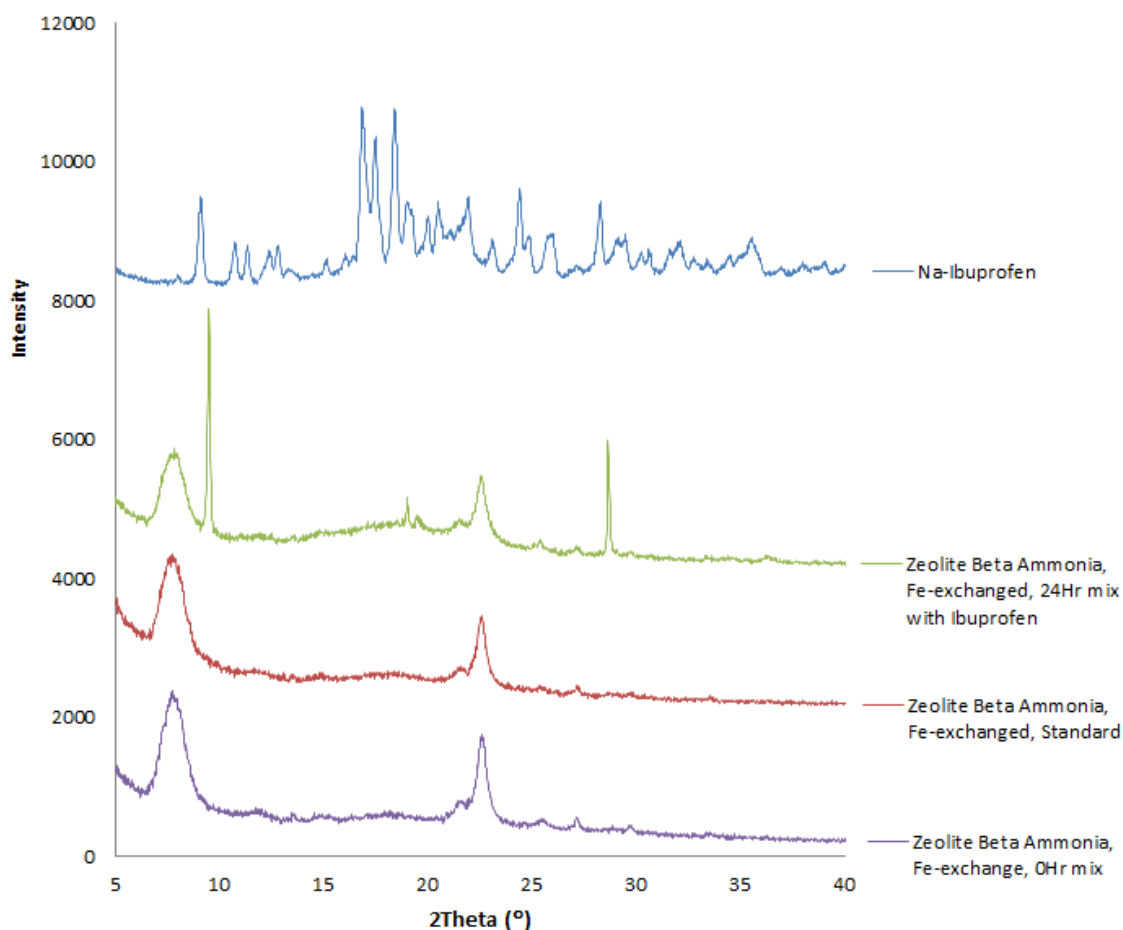


Figure 3.4.5 – Comparison of the diffraction pattern of BEA-NH<sub>4</sub> Fe-exchanged adsorbed with Na-ibuprofen against the XRD pattern of BEA-NH<sub>4</sub> Fe-exchanged, standard, the diffraction pattern of BEA-NH<sub>4</sub> Fe-exchanged, with zero mixing time, and the diffraction pattern of Na-ibuprofen

The XRD diffraction pattern for of BEA-NH<sub>4</sub> Fe-exchanged adsorbed with acetaminophen [Figure 3.4.5] does not contain any peaks which are thought to be caused by acetaminophen related impurities. However, the peak present between 20 and 25° 2θ noticeably varies with its peak intensities before and after adsorption [Figure 3.4.5] that could be caused by the uptake of acetaminophen.

The R<sub>wp</sub> value for “BEA-NH<sub>4</sub> Fe-exchanged, mixed with acetaminophen (3)” shows the Pawley fit to be a relatively good [Table 3.4.7]. Along with figure 3.4.3 it shows there is no impurity peaks in the diffraction pattern to be caused by acetaminophen. The low uptake of acetaminophen at 14.43% [Table 3.4.6] could be the reason why there are only slight peak intensity variances [Figure 3.4.5].

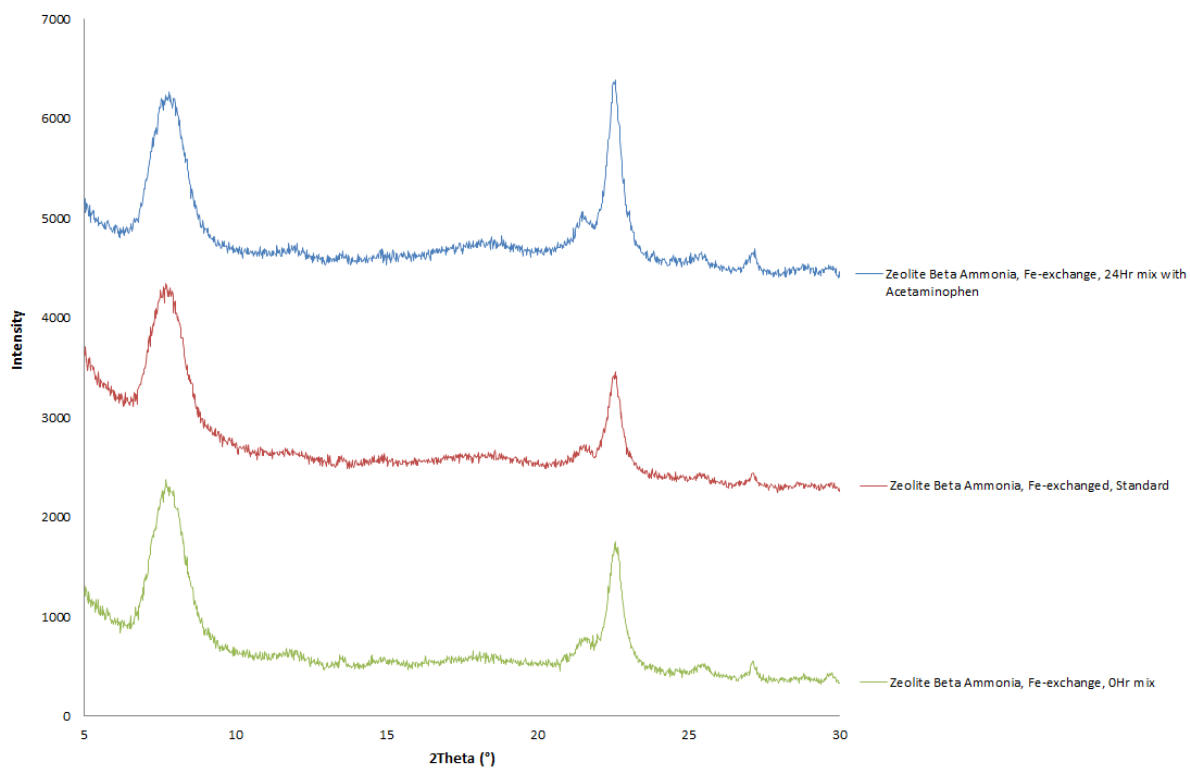


Figure 3.4.6 – Comparison of the diffraction pattern of BEA-NH<sub>4</sub> Fe-exchanged adsorbed with Acetaminophen against the diffraction pattern of BEA-NH<sub>4</sub> Fe-exchanged, standard and the diffraction pattern of BEA-NH<sub>4</sub> Fe-exchanged, with zero mixing time

### 3.5 <sup>29</sup>Si MAS NMR Results

29-Si MAS NMR was performed to determine the silicon to aluminium ratio (Si:Al) of the following zeolites; clinoptilolite, Japanese clinoptilolite, BEA-H and BEA-NH<sub>4</sub> were determined using 29-Si MAS NMR. The results are tabulated below in table 3.5.1.

*Table 3.5.1. – Si:Al results for the four initial zeolites as supplied without modification*

<b>Zeolite</b>	<b>Si:Al</b>
Clinoptilolite	3.75
Japanese Clinoptilolite	4.48
BEA-H	3.43
BEA-NH <sub>4</sub>	3.21

The Si:Al ratio can be used to determine the number of cations in the zeolites framework. As each Al atom brings one negative charge to be compensated by the adequate cation, thus, the Si:Al ratio strongly influences the adsorptive properties of zeolites.

The 29-Si MAS NMR results [Table 3.5.1] show the clinoptilolite samples to have a higher Si:Al ratio than the BEA samples. These results are inconsistent with the information provided by the supplier [Table 3.5.1] as BEA is a ‘high silica’ zeolite with a Si:Al ratio  $\geq 10$  [180]. BEA’s lower Si:Al ratio results indicates the presence of some defect silanol (Si(OH)<sub>x</sub>) groups in the BEA sample. As the ratio of tetrahedral silicon and aluminium in the zeolite framework can be directly calculated from the line intensities in a 29-Si MAS NMR by the following equation assuming that the Al-Al avoidance rule of Lowenstein is obeyed and Si(OH)<sub>x</sub> signals are not included in the bands:

$$(Si:Al)_{NMR} = \sum I_{Si(nAl)} / \sum_4^n I_{Si(nAl)} \quad \text{summation is from } n = 0 \text{ to } n = 4$$

*Equation 3.1 – Equation for Si:Al ratio*

The resulting Si:Al may strongly under estimate the actual Si:Al ratio as defect sites (Si(OH)<sub>x</sub> groups) are generally present in the zeolite framework [181]

With clinoptilolite having the lower Si:Al ratio it is expected that clinoptilolite's framework would contain more cations. As a result, clinoptilolite should perform better at adsorbing pharmaceuticals with polar functional groups. Consequently, the HPLC results show the clinoptilolite samples to have a higher percentage drug uptake for both acetaminophen and Na-ibuprofen [Table 3.1.1] [Table 3.2.1] [Table 3.3.3 – 3.3.6]. Therefore, it is believed that adsorption results are influenced by the adsorbents pore shape and size, as well as, the number of cations present.

### 3.6 BET Results

If the drug was adsorbed into the zeolites pore it is thought the pores volume would decrease. Therefore, BET analysis was performed on the two clinoptilolites, before and after drug adsorption, in order to determine if the drug is in the pore by comparing the pore volumes [Table 3.6.1 - Table 3.6.2]. Dehydration was performed at 100°C under vacuum, rather than 300°C, so the majority of water is removed and to prevent the breakdown of the drug adsorbed.

*Table 3.6.1 – BET results showing the micropore volume (cm<sup>3</sup>/g) for the following samples: 1) Moroccan clinoptilolite standard, 2) Moroccan clinoptilolite adsorbed with acetaminophen and 2) Moroccan clinoptilolite adsorbed with Na-ibuprofen*

<b>Moroccan Clinoptilolite Sample:</b>	<b>Micropore Volume (cm<sup>3</sup>/g)</b>
<i>1) Standard</i>	0.003
<i>2) Adsorbed with Acetaminophen</i>	0.001
<i>3) Adsorbed with Na-Ibuprofen</i>	0.002

*Table 3.6.2 –BET results showing the micropore volume (cm<sup>3</sup>/g) for the following samples: 1) Japanese clinoptilolite standard, 2) Japanese clinoptilolite adsorbed with acetaminophen and 2) Japanese clinoptilolite adsorbed with Na-ibuprofen*

<b>Japanese Clinoptilolite Sample:</b>	<b>Micropore Volume (cm<sup>3</sup>/g)</b>
<i>1) Standard</i>	0.003
<i>2) Adsorbed with Acetaminophen</i>	0.001
<i>3) Adsorbed with Na-Ibuprofen</i>	0.002

From the BET results obtained [Table 3.6.1 - Table 3.6.2] it is believed that that cations found in clinoptilolites pores binds to functional groups of acetaminophen and Na-ibuprofen. As both Moroccan and Japanese clinoptilolite samples have an approximate pore volume of 0.003 cm<sup>3</sup> /g [Table 3.6.1 - Table 3.6.2], which decrease in size after drug uptake. For both clinoptilolite samples, the pore volume is smallest after adsorption of acetaminophen with an approximate size of 0.001 cm<sup>3</sup>/g [Table 3.6.1 - Table 3.6.2].

The pore volume also decreases after adsorption of Na-ibuprofen, for both samples, with approximate volume of 0.002 cm<sup>3</sup>/g [Table 3.6.1 - Table 3.6.2]. From the HPLC results

obtained, it was initially thought the smaller pore volumes would have been exhibited by the clinoptilolite samples absorbed with Na-ibuprofen, due to the HPLC results showing both clinoptilolite samples to adsorb more Na-ibuprofen [Table 3.1.1] [Table 3.2.1] [Table 3.3.3 – Table 3.3.6]. However, as this is not the case, it is now thought that the larger pore volume is due to the adsorption of Na-ibuprofen and the formation of degradation products, such as the propanoate ion. However, we do not know if the products are degrading in the water or if clinoptilolite is enhancing the degradation. None the less, the smaller pore volume after adsorption indicates clinoptilolite adsorbs acetaminophen and Na-ibuprofen into its pores.

## Chapter 4: Conclusion and Future work

This work focused on the adsorption of the pharmaceuticals; acetaminophen and Na-ibuprofen by clinoptilolite and zeolite BEA. The study included how the adsorption capacity was effected by cation-exchange and from the altered elemental composition of natural clinoptilolite that was attained from different geographical locations.

The results indicated that clinoptilolite was more efficient in the removal of the analgesics in question. However, it should be highlighted that both analgesics appeared to be absorbed into clinoptilolites pores, even though the drugs dimensions appear to be larger than the pore dimensions. In contrary, BEA achieved lower adsorption results even though the dimensions of its pores appear to be suitable for adsorption. These results are similar to Martucci *et al.* [182] who investigated the absorbance of three antibiotics; erythromycin (ERY), carbamazepine (CBZ) and levofloxacin (FLX) by using zeolite Y, mordenite (MOR) and ZSM-5. They expected little to no adsorption of ERY by zeolite Y as the drug dimensions appeared to be too large to pass through the zeolites 12-ring windows that are restricting access to the large cage. However, zeolite Y achieved the best adsorption results for ERY, whereas, the zeolites MOR and ZSM-5 did not absorb CBZ, even though both materials had larger and more suitable channel dimensions.

The modified zeolites by cation-exchange showed different adsorption capacities in comparison to the initial zeolite. More importantly, the results obtained show how the presence of different cations can adjust or even be used to tailor specific adsorptions. It was found that the addition of Cu(II) cations to natural clinoptilolite specifically enhanced the adsorption of Na-ibuprofen. The differences in ion-exchange selectivity has prompted the idea of further investigations with different cations to find the optimum modification. Future work could include the sorption of the metallic cations: Zn(II), Mn(II) and Ni(II). Rakić *et al.* [155]

sorbed these metallic cations into clinoptilolite to enhance adsorption of salicylic acid, acetylsalicylic acid and atenolol, as the metal cations form stable complexes with N- and O-donor groups present in their chosen pharmaceuticals. As both Na-ibuprofen and acetaminophen contain N- and O- donor groups it would be interesting if we could achieve similar adsorption results.

Furthermore, the results also proved that drug adsorption can be altered with the use of a natural zeolite attained from different geographical locations. It was found that the different elemental compositions of the two clinoptilolite effected the amount of pharmaceutical adsorbed. As clinoptilolite from Morocco achieved overall highest adsorptions. Future work could focus on investigating the adsorption capacities of clinoptilolite attained from different geographical locations, such as; Australia or Turkey. As the clinoptilolite used to adsorb nuclear waste in Sellafield, England, is obtained from one specific mine due to this particular clinoptilolite having a high selectivity towards  $\text{Cs}^+$  ions.

The overall results obtained show that both clinoptilolite and BEA can be used to remove the investigated analgesics by adsorption. However, as clinoptilolite achieved the highest adsorption results it would be of interest to see if it had similar adsorption affinities towards other drugs such as naproxen and diclofenac. A recent study [183] used clinoptilolite from California as a surface modified natural zeolite as a carrier for sustained diclofenac release. The study concluded that clinoptilolite made a very versatile drug carrier since molecules with different chemical properties can be potentially loaded in or on the zeolite. As clinoptilolite surface is easily modified, it broadens the range of ways in which the material can be applied, therefore, the research group is continuing their focus on the pharmaceutical application of clinoptilolite.

Additionally, the work presented here could also further investigate the location of the drugs after adsorption. As it is not clear whether the drugs are located at the zeolites surface or inside the pores. Particularly, as clinoptilolite has showed to form interactions with

pharmaceuticals at its surface [183], as well as, inside its pores [155]. Extended X-ray adsorption fine structure (EXAFS) spectroscopy could potentially be used to identify the location of the drug after adsorption, due to EXAFS analysing specific local areas only. Future work would specifically look at the local area surrounding the Cu cations before and after adsorption, due Cu-exchanged Clinoptilolite exhibited the highest drug adsorption. Analysis by EXAFS could determine if the drug is forming a stable complex with Cu cations present by looking at changes exhibited by the arrangement of atoms surrounding the cation before and after adsorption.

Further characterisation of the zeolites content could be done by the physicochemical technique thermogravimetric analysis (TGA). TGA is an analytical technique in which the effect of heat on the mass of a sample with time is studied to obtain quantitative information. TGA can obtain information about various parameters, namely mass, enthalpy, magnetic and electrical properties. Thermal events are usually recorded by observing the change in the thermal property as the temperature is varied to give a thermal analysis curve or a thermogram. The thermal events which can lead to some important quantitative information can be melting, phase transition, decomposition and glass transition. Thermogravimetry, in particular, would be able to provide the change in mass of the sample as the temperature is varied. When the sample is heated from ambient to 1000°C, under an atmosphere of O<sub>2</sub> or N<sub>2</sub>, characteristic weight losses can be obtained which may yield important information regarding the zeolites uptake of the drug. It is expected that the thermogram of the pure drug to be a different shape when compared to the thermogram of the drug loaded zeolite. This change would show the presence of drug in confined environments verses the free drug [184].

Lastly, the BET results obtained have shown the pore volume of the clinoptilolite absorbed with acetaminophen to be smaller than clinoptilolite absorbed with Na-ibuprofen. This is particularly interesting as HPLC results have shown clinoptilolite to absorb more Na-ibuprofen, therefore, it was initially thought that the pore volume of clinoptilolite absorbed with Na-

ibuprofen would have the smaller volume. As this is not the case, future work would involve the study of the potential degradation products of Na-ibuprofen and if clinoptilolite is catalysing the degradation upon adsorption. It is thought that clinoptilolite is forming complexes with degradation products as it is conveying a larger pore volume. Furthermore, one of the degradation products could be a propanoate ion, as it was found to have matching diffraction peaks to the “clinoptilolite Cu-exchanged absorbed with Na-ibuprofen” sample. To identify other possible degradation products future work could include high performance liquid chromatography, in conjunction with a mass spectrometer (HPLC-MS) analyse of adsorption experiment samples taken at variable time intervals. By identifying the degradation products it would be possible to determine a degradation mechanism.

## Chapter 5: References

[1] J. Hollender, H. Singer, Ch.S. Mcardell, Dangerous Pollutants (Xenobiotics) in Urban Water Cycle, NATO Science for Peace and Security Series, Series C: Environmental Security, Springer, Dordrecht, 2008, 103–116.

[2] H. Yamamoto, Y. Nakamura, S. Moriguchi, Y. Nakamura, Y. Honda, I. Tamura, Y. Hirata, A. Hayashi, J. Sekizawa, Persistence and partitioning of eight selected pharmaceuticals in the aquatic environment: Laboratory photolysis, biodegradation, and sorption experiments., *Water Res.*, 2009, 43, 351-362.

[3] M. S. Diaz-Cruz, M. J. Lopez de Alda, D. Barceló, Environmental behavior and analysis of veterinary and human drugs in soils, sediments and sludge., *Trends in Analytical Chemistry*, 2003, 22, 340–351.

[4] A. Almeida, V. Calisto, V. I. Esteves, R. J. Schneider, A. M. V. M. Soares, E. Figueria, R. Freitas, Presence of the pharmaceutical drug carbamazepine in coastal systems: effects on bivalves., *Aquat., Toxicol.*, 2014, 156, 74-87.

[5] B. Quinn, W. Schmidt, K. O'Rourke, R. Hernan, Effects of the pharmaceuticals gemfibrozil and diclofenac on biomarker expression in the zebra mussel (*Dreissena polymorpha*) and their comparison with standardised toxicity tests, *Chemosphere*, 2011, 84, 657-663.

[6] A. B. Caracciolo, E. Topp and P. Grenni, Pharmaceuticals in the environment: biodegradation and effects on natural microbial communities, A review. *J. Pharm. Biomed. Anal.*, 2015, 106, 25–36.

[7] M. E. Valdes, M. V. Ame, M. D. L. A. Bistoni, D. A. Wunderlin, Occurrence and bioaccumulation of pharmaceuticals in a fish species inhabiting the Suquia River basin, *Sci. Total Environ.*, 2014, 472, 389–396.

- [8] A. Zenker, M. Rita, F. Prestinaci, P. Bottoni and M. Carere, Bioaccumulation and biomagnification potential of pharmaceuticals with a focus to the aquatic environment, *J. Environ. Manage.*, 2014, 133, 378- 387.
- [9] S.K. Khetan, T.J. Collins, Human pharmaceuticals in the aquatic environment: a challenge to Green Chemistry, *Chem. Rev.*, 2007, 107, 2319–2364.
- [10] M. Klavairoti, D. Mantzavinos, D. Kassinos, Removal of residual pharmaceuticals from aqueous systems by advanced oxidation processes, *Environ. Int.*, 2009, 35, 402–417.
- [11] J. Neuwoehner, B.I. Escher, The pH-dependent toxicity of basic pharmaceuticals in the green algae *Scenedesmus vacuolatus* can be explained with a toxicokinetic ion-trapping model, *Aquat. Toxicol.*, 2011, 101, 266–275.
- [12] V. Fessard, L. Le Hégarat, A strategy to study genotoxicity: application to aquatic toxins, limits and solutions., *Anal. Bioanal. Chem.*, 2010, 397, 1715–1722.
- [13] S.T. Glassmeyer, D.W. Kolpin, E.T. Furlong, M.J. Focazio, Fate of Pharmaceuticals in the Environment and in Water Treatment Systems, CRC Press, Boca Raton, 2008, 3–51.
- [14] P. Bottoni, S. Caroli, A. Barra Caracciolo, Pharmaceuticals as Priority water contaminants, *Toxicol. Environ. Chem.*, 92, 2010, 549– 565.
- [15] M. Carballa, F. Omil, J.M. Lema, M. Llompарт, C. Garcia-Jares, Behavior of pharmaceuticals, cosmetics and hormones in a sewage treatment plant, *Water Res.* 38, 2004, 2918–2926.
- [16] C. Prasse, M.P. Schlusener, R. Schulz, Th.A. Ternes, Antiviral Drugs in Wastewater and Surface Waters: A New Pharmaceutical Class of Environmental Relevance, *Environ. Sci. Technol.*, 44, 2010, 1728–1735.
- [17] A. Garcia-Ac, P.A. Segura, Ch. Gagnon, S. Sauve, Determination of bezafibrate, methotrexate, cyclophosphamide, orlistat and enalapril in waste and surface waters using on-

line solid-phase extraction liquid chromatography coupled to polarity-switching electrospray tandem mass spectrometry, *J. Environ. Monit.*, 2009, 11, 830–838

[18] J. Corcoran, M.J. Winter, Ch.R. Tyler, Pharmaceuticals in the aquatic environment: A critical review of the evidence for health effects in fish, *Rev. Toxicol.*, 40, 2010, 287–304.

[19] C.G. Daughton, Contaminants of Emerging Concern in the Environment: Ecological and Human Health considerations, ACS Symposium Series, 2010, 9–68.

[20] J. L. Tambosi, L.Y. Yamanaka, H.J. José, R.F.P.M. Moreira, Recent research data on the removal of pharmaceuticals from sewage treatment plants (STP), *Quim. Nova*, 33, 2010, 411–420.

[21] D. J. Lapworth, N. Baran, M. E. Stuart, R. S. Ward, Emerging organic contaminants in groundwater: A review of sources, fate and occurrence, *Environ. Pollut.*, 2012, 163, 287-303.

[22] Distribution of Pharmaceutical Residues in the Environment Issues in Environmental Science and Technology No. 41 Pharmaceuticals in the Environment Edited by R.E. Hester and R.M. Harrison r The Royal Society of Chemistry 2016 Published by the Royal Society of Chemistry, [www.rsc.org](http://www.rsc.org)

[23] European Commission, Accompanying the document Proposal for a Decision of the European Parliament and of the Council on a General Union Environment Action Programme to 2020 “Living well, within the limits of our planet,” 2012.

[24] R. P. Deo, Pharmaceuticals in the surface water of the USA: A review. *Curr. Environ. Health Rep.* 2014, 1, 113–122.

[25] C. Yan, Y. Yang, J. Zhou, M. Liu, M. Nie, H. Shi, L. Gu, Antibiotics in the surface water of the Yangtze Estuary: occurrence, distribution and risk assessment, *Environ. Pollut.*, 2013, 175, 22–29.

- [26] C. Fernández, M. González-Doncel, J. Pro, G. Carbonell, J. V. Tarazona, Occurrence of pharmaceutically active compounds in surface waters of the Henares-Jarama-Tajo river system (Madrid, Spain) and a potential risk characterization. *Sci. Total Environ.*, 2010, 408, 543–551.
- [27] P. Guerra, M. Kim, A. Shah, M. Alaei, S. A. Smyth, Occurrence and fate of antibiotic, analgesic/anti-inflammatory, and antifungal compounds in five wastewater treatment processes, *Sci. Total Environ.*, 2014, 235–243.
- [28] T. Okuda, N. Yamashita, H. Tanaka, H. Matsukawa, K. Tanabe, Development of extraction method of pharmaceuticals and their occurrences found in Japanese wastewater treatment plants, *Environ. Int.*, 2009, 35, 815–820.
- [29] O. Golovko, V. Kumar, G. Fedorova, T. Randak, R. Grabic, Removal and seasonal variability of selected analgesics/anti-inflammatory, anti-hypertensive/cardiovascular pharmaceuticals and UV filters in wastewater treatment plant, *Chemosphere*, 2014, 111, 418–426.
- [30] X. Li, W. Zheng, W. R. Kelly, Occurrence and removal of pharmaceutical and hormone contaminants in rural wastewater treatment lagoons, *Sci. Total Environ.*, 2013, 445–446, 22–28.
- [31] R. López-Serna, A. Jurado, E. Vázquez-Sunñe, J. Carrera, M. Petrović, D. Barceló, Occurrence of 95 pharmaceuticals and transformation products in urban groundwaters underlying the metropolis of Barcelona, Spain, *Environ. Pollut.*, 2001, 174, 305–315.
- [32] X. Peng, W. Ou, C. Wang, Z. Wang, Q. Huang, J. Jin, J. Tan, Occurrence and ecological potential of pharmaceuticals and personal care products in groundwater and reservoirs in the vicinity of municipal landfills in China, *Sci. Total Environ.*, 2014, 490, 889–898.
- [33] S. Bayen, H. Zhang, M. M. Desai, S. K. Ooi, B. C. Kelly, Occurrence and distribution of pharmaceutically active and endocrine disrupting compounds in Singapore's marine

environment: influence of hydrodynamics and physical-chemical properties, *Environ. Pollut.*, 2013, 182, 1–8.

[34] D. A. Alvarez, K. A. Maruya, N. G. Dodder, W. Lao, E. T. Furlong and K. L. Smalling, *Mar. Pollut. Bull.*, 2014, 81, 347–354.

[35] M. J. Benotti, R. A. Trenholm, B. J. Vanderford, J. C. Holady, B. D. Stanford and S. A. Snyder, *Environ. Sci. Technol.*, 2009, 43, 597–603.

[36] K. McClellan and R. U. Halden, *Water Res.*, 2010, 44, 658–668.

[37] C. Wu, A. L. Spongberg, J. D. Witter and B. B. M. Sridhar, *Ecotoxicol. Environ. Saf.*, 2012, 85, 104–109.

[38] M. S. Díaz-Cruz, M. J. López de Alda and D. Barceló, *TrAC, Trends Anal. Chem.*, 2003, 22, 340–351.

[39] D. J. Fairbairn, M. E. Karpuzcu, W. A. Arnold, B. L. Barber, E. F. Kaufenberg, W. C. Koskinen, P. J. Novak, P. J. Rice and D. L. Swackhamer, *Sci. Total Environ.*, 2015, 505, 896–904.

[40] T. Christian, R. J. Schneider, H. A. Farber, D. Skutlarek, M. T. Meyer and H. E. Goldbach, *Acta Hydrochim. Hydrobiol.*, 2003, 1, 36–44.

[41] W. C. Li, *Environ. Pollut.*, 2014, 187, 193–201.

[42] R. Aznar, C. Sánchez-Brunete, B. Albero, J. A. Rodríguez, J. L. Tadeo, *Environ. Sci. Pollut. Res.*, 2014, 21, 4772–4782.

[43] M. E. Valdés, M. V. Amé, M. D. L. A. Bistoni, D. A. Wunderlin, *Sci. Total Environ.*, 2014, 472, 389–396.

- [44] E. A. M. Gilroy, J. S. Klinck, S. D. Campbell, R. McInnis, P. L. Gillis, S. R. de Solla, *Sci. Total Environ.*, 2014, 487, 537–544.
- [45] P. Bottoni and S. Caroli, *J. Pharm. Biomed. Anal.*, 2014, 106, 3–24.
- [46] F.-A. Weber, A. Carius, G. Grüttner, H. Silke, I. Ebert, A. Hein, A. Küster, J. Rose, J. Koch-Jugl and H.-C. Stolzenberg, *Pharmaceuticals in the environment – the global perspective Occurrence, effects, and potential cooperative action under SAICM, 2014, Report, available at <http://www.pharmaceuticals-in-the-environment.org>.*
- [47] M. Farré, I. Ferrer, A. Ginebreda, M. Figueras, L. Olivella, L. Tirapu, M. Vilanova, D. Barcelo, Determination of drugs in surface water and wastewater samples by liquid chromatography-mass spectrometry: methods and preliminary results including toxicity studies with *Vibrio fischeri*. *J Chromat A*, 2001, 938:187–197.
- [48] R. Andreozzi, M. Raffaele, P. Nicklas, *Pharmaceuticals in STP effluents and their solar photodegradation in the aquatic environment. Chemosphere*, 2003, 50:1319–1330.
- [49] C. Metcalfe, X-S. Miao, B.G. Koenig, J. Struger, *Distribution of acidic and neutral drugs in surface waters near sewage treatment plants in the lower Great Lakes, Canada. Environ Toxicol Chem*, 2003, 22:2881–2889.
- [50] T. Ternes, Occurrence of drugs in German sewage treatment plants and rivers. *Water Res.*, 1998, 32:3245–3260.
- [51] S. Weigel, U. Berger, E. Jensen, R. Kallenborn, H. Thoresen, H. Hühnerfuss, Determination of selected pharmaceuticals and caffeine in sewage and seawater from Tromsø/Norway with emphasis on ibuprofen and its metabolites. *Chemosphere.*, 2004, 56:583–592.
- [52] D. Bendz, N. Paxéus, T.R. Ginn, F.J. Loge, Occurrence and fate of pharmaceutically active compounds in the environment, a case study: Höje River in Sweden. *J Hazard Mater.*, 2005, 122:195–204.

- [53] M. Ahel, I. Jelić, Phenazone Analgesics in Soil and Groundwater below a Municipal Solid Waste Landfill. In: Daughton CG and Jones-Lepp T (eds), American Chemical Society, Symposium series 791, Washington, DC, 2001, 100–115.
- [54] T. Heberer, I.M. Verstraeten, M.T. Meyer, A. Mechlinski, K. Reddersen K, Occurrence and fate of pharmaceuticals during bank filtration - preliminary results from investigations in Germany and the United States. *Water Resour Update.*, 2001, 120, 4–17.
- [55] J.V. Holm, K. Rügge, P.L. Bjerg, T.H. Christensen, Occurrence and distribution of pharmaceutical organic compounds in the groundwater downgradient of a landfill (Grinsted, Denmark). *Environ SciTechnol.*, 1995, 29(5): 1415–1420.
- [56] K. Reddersen, T. Heberer, U. Dünnbier, Identification and significance of phenazone drugs and their metabolism in ground- and drinking water. *Chemosphere.*, 2002, 49, 539–544.
- [57] F. Sacher, F.T. Lange, H.J. Brauch, I. Blankenhorn, Pharmaceuticals in groundwaters. Analytical methods and results of a monitoring program in Baden-Württemberg, Germany. *J Chromat A.*, 2001, 938:199–210.
- [58] T. Ternes, Pharmaceuticals and Metabolites as Contaminants of the Aquatic Environment. In: Daughton CG and Jones-Lepp T (eds), American Chemical Society, Symposium series 791, Washington D.C, 2001, 39–54.
- [59] G.R. Boyd, H. Reemtsma, D.A. Grimm, S. Mitra, Pharmaceuticals and personal care products (PPCPs) in surface and treated waters of Louisiana, USA and Ontario, Canada. *Sci Tot Environ.* 2003, 311:135–149.
- [60] J.M Skadsen, B.L. Rice, D.J. Meyering, The occurrence and fate of pharmaceuticals, personal care products and endocrine disrupting compounds in a municipal water use cycle: a case study in the city of Ann Arbor. *Water Utilities and Fleis & VandenBrink Engineering, Inc., City of Ann Arbor.*, 2004

- [61] P.E. Stackelberg, E.T Furlong, M.T Meyer, S.D. Zaugg, A.K. Henderson, D.B. Reissman, Persistence of pharmaceutical compounds and other organic wastewater contaminants in a conventional drinking-water-treatment plant. *Sci Total Environ.* 2004, 329, 99–113.
- [62] D. Fatta, A. Nikolaou, A. Achilleous, S. Meric, Analytical methods for tracing pharmaceutical residues in water and wastewater. *Trends in Analytical Chemistry.*, 2007, 26, 515-553.
- [63] D. Taylor, *Pharmaceuticals in the Environment, Issues I Environmental Science and Technology*, 2015, 1 – 33.
- [64] M. L. Richardson, J. M. Bowron, The fate of pharmaceutical chemicals in the aquatic environment, *J Pharm Pharmacol*, 1985, 37, 1-12.
- [65] B. Roig, *Pharmaceuticals in the environment, current knowledge and needs assessment to reduce pressure and impact*, vol 1, IWA publishing, 2010, 1-256.
- [66] J.P. Sumpter. *Pharmaceuticals in the Environment: Moving from a Problem to a Solution.*, 1998, 11-22
- [67] J.P. Sumpter, A.C. Johnson, Reflections on endocrine disruption in the aquatic environment: From known knowns to unknown unknowns (and many things in between). *J Environ Monit.*, 2008, 10, 1476–1485
- [68] Jobling S, Nolan M, Tyler CR, Brighty G, Sumpter JP (1998) Widespread sexual disruption in wild fish. *Environ Sci Technol* 32, 2498–2506
- [69] C.R. Tyler, S. Jobling, Roach, sex, and gender-bending chemicals: The feminization of wild fish in English rivers. *Bioscience*, 2008, 58, 1051–1059

[70] J.P. Sumpter. Pharmaceuticals in the Environment: Moving from a Problem to a Solution., 1998, 11-22

[https://www.google.co.uk/url?sa=t&rct=j&q=&esrc=s&source=web&cd=1&ved=0ahUKEwj5I7Xc2rXPAhUGnRoKSHzC-cQFggeMAA&url=http%3A%2F%2Fwww.springer.com%2Fcd%2Fcontent%2Fdocument%2Fcd\\_a\\_downloaddocument%2F9783642051982-c1.pdf%3FSGWID%3D0-0-45-923445-p173948303&usg=AFQjCNHbaDH1BWYvxKhbEfKBg65Ri\\_TVbQ](https://www.google.co.uk/url?sa=t&rct=j&q=&esrc=s&source=web&cd=1&ved=0ahUKEwj5I7Xc2rXPAhUGnRoKSHzC-cQFggeMAA&url=http%3A%2F%2Fwww.springer.com%2Fcd%2Fcontent%2Fdocument%2Fcd_a_downloaddocument%2F9783642051982-c1.pdf%3FSGWID%3D0-0-45-923445-p173948303&usg=AFQjCNHbaDH1BWYvxKhbEfKBg65Ri_TVbQ) Last Accessed:30.09.16

[71] D.J. Caldwell, F. Mastrocco, T.H. Hutchinson, R. Lange, D. Heijerick, C. Janssen, P.D.

Anderson, J.P. Sumpter, Derivation of an aquatic predicted no-effect concentration for the synthetic hormone, 17 $\alpha$ -ethinyl estradiol. Environ Sci Technol., 2008, 42, 7046–7054

[72] R. Länge, T.H. Hutchinson, C.P. Croudace, F. Siegmund, H. Schweinfurth, P. Hampe, G.H.

Panter, J.P. Sumpter, Effects of the synthetic oestrogen 17 $\alpha$ -ethinylestradiol over the life-cycle of the fathead minnow (*Pimephales promelas*). Environ Toxicol Chem., 2001, 20, 1216–1227

[73] J.P. Nash, D.E Kime, L.T.M van der Ven, P.W. Wester, F. Brion, G. Maack, P. Stahlschmidt-

Allner, C.P Tyler, Long-term exposure to environmental concentrations of the pharmaceutical 17 $\alpha$ -ethinylestradiol cause reproductive failure in fish. Environ Health Perspect, 2001, 112, 1725–1733

[74] C. E. Corcoran, E. Nellesmann, R. Baker, D. Bos, H. Savelli, Sick water? The central role of waste-water management in sustainable development, 2010, 1-88.

[75] B. Huerta, D. Barceló, S. Mozaz-Rodríguez, Pharmaceuticals in biota in the aquatic

environment: Analytical methods and environmental implications, Anal. Bioanal. Chem., 2012, 404, 2611–2624.

[76] M. Sun, S. Gan, D. Yin, H. Liu, W. Yang, Application of nano-filtration membrane in the purification process of Tylosin, Chin. J. Antibiot., 2000, 25, 172–174.

- [77] W. Zhang, G. H. He, P. Gao, G.H. Chen, Development and characterization of composite nanofiltration membranes and their application in concentration of antibiotics, *Sep. Purif. Technol.*, 2003, 30, 27–35.
- [78] A.S. Mestre, J. Pires, J.M.F. Nogueira, A.P. Carvalho, Activated carbons for the adsorption of ibuprofen, *Carbon*, 2007, 45, 1979–1988.
- [79] T. Ternes, M. Meisenheimer, D. Mcdowell, F. Sacher, H.J. Brauch, B. Haist-Gulde, Removal of pharmaceuticals during drinking water treatment, *Environ. Sci. Technol.* 2002, 36, 3855–3863.
- [80] Y. Yoon, P. Westerhoff, S.A. Snyder, M. Esparza, HPLC- fluorescence detection and adsorption of bisphenol A, 17 $\beta$ -estradiol, and 17 $\alpha$ -ethynyl estradiol on powdered activated carbon, *Water Res.*, 2003, 37, 3530–3537.
- [81] S. Snyder, S. Adham, A.M. Redding, F.S. Cannon, J. Decarolis, J. Oppenheimer, E.C. Wert, Y. Yoon, Role of membranes and activated carbon in the removal of endocrine disruptors and pharmaceuticals, *Desalination*, 2007, 202, 156–181.
- [82] C. Stoquart, P. Servais, P.R. Be rube, B. Barbeau, Hybrid membrane processes using activated carbon treatment for drinking water: A review, *J. Membr. Sci.*, 2012, 1–12.
- [83] K. K mmerer, Ed. *Pharmaceuticals in the Environment: Sources, Fate, Effects and Risks* 3rd ed.; Springer: Berlin, 2008.
- [84] K. K mmerer, A. Al-Ahmed, V. Mersch-Sundermann, Biodegradability of some antibiotics, elimination of the genotoxicity and affection of wastewater bacteria in a simple test, *Chemosphere*, 2000, 40, 701–710.
- [85] B. Halling-S rensen, H.C. L tzhof, H.R. Andersen, F. Ingerslev, Environmental risk assessment of antibiotics: Comparison of mecillinam, trimethoprim and Ciprofloxacin, *J. Antimicrob. Chemother.*, 2000, 46, 53–58.

- [86] M. Klavarioti, D. Mantzavinos, D. Kassinos, Removal of residual pharmaceuticals from aqueous systems by advanced oxidation processes, *Environ. Int.*, 2009, 35, 402–417.
- [87] R. F. Dantes, S. Contreras, C. Sans, S. Esplugas, Sulfamethoxazole abatement by means of ozonation, *J. Hazard. Mater.*, 2008, 150, 790–794.
- [88] E.G. Helmig, J. D. Fettig, L. Cordone, P.S. Suri Rominder, API removal from pharmaceutical manufacturing wastewater - Results of process development, pilot-testing, and scale-up, *WEFTEC.05, Conf. Proc., Annu. Tech. Exhib. Conf.*, 78<sup>th</sup>, 2005, 207–226.
- [89] A. Balcioglu, M. Otker, Treatment of pharmaceutical wastewater containing antibiotics by  $O_3$  and  $O_3/H_2O_2$  processes, *Chemosphere.*, 2003, 50, 85–95.
- [90] N. Nakada, H. Shinohara, A. Murata, K. Kiri, S. Managakia, N. Sato, H. Takada, Removal of selected pharmaceuticals and personal care products (PPCPs) and endocrine-disrupting chemicals (EDCs) during sand filtration and ozonation at a municipal sewage treatment plant, *Water Res.*, 2007, 41, 4373–4382.
- [91] I.A. Alaton, S. Dogruel, E. Baykal, G. Gerone, Combined chemical and biological oxidation of penicillin formulation effluent, *J. Environ. Manage.*, 2004, 73, 155–163.
- [92] E.U. Cokgor, I.A. Alaton, O. Karahan, S. Dogruel, D. Orhon, Biological treatability of raw and ozonated penicillin formulation effluent, *J. Hazard. Mater.*, 2004, 116, 159–166.
- [93] I. Sireś, E. Brillas, Remediation of water pollution caused by pharmaceutical residues based on electrochemical separation and degradation technologies: A review, *Environ. Int.*, 2012, 40, 212–229.
- [94] J.R. Domínguez, T. González, P. Palo, Electrochemical Degradation of a Real Pharmaceutical Effluent, *Water, Air, Soil Pollut.*, 2012, 223, 2685–2694.

- [95] E. Brillas, I. Sires, C. Arias, P. Cabot, F. Centellas, R.M. Rodriguez, J.A. Garrido, Mineralization of paracetamol in aqueous medium by anodic oxidation with a boron-doped diamond electrode, *Chemosphere.*, 2005, 58, 399–406.
- [96] D.L. Bish, D.W. Ming, *Natural zeolites: Occurrence, Properties, Applications*, 2001, 45, 519–550
- [97] S. Ozaydin, G. Kocar, A. Hepbasli, Natural zeolites in energy applications, *Energy Sources Part A: Recovery Utilization and Environmental Effects*, 2006, 28, 1425–1431
- [98] A. J. Celestain, J. D. Kubicki, J. Hanson, A. Clearfield, J. B. Parise, The mechanism responsible for extraordinary Cs Ion Selectivity in Crystalline Silicotitanate, *J. Am. Chem. Soc.*, 2008, 130, 11689 - 11694
- [99] S. Wanga, P.B. Yuelian, Natural zeolites as effective adsorbents in water and wastewater treatment, *Chemical Engineering Journal*, 2010, 156, 11–24
- [100] S. M. Auerbach, A. Carrado, P. K. Dutta, *Handbook of Zeolite Science and Technology. Vol 1*. CRC Press; 2013, 1- 1204
- [101] P. A. Jacobs, E. M. Flanigen, J. C. Jansen, H. van Bekkum, *Introduction to zeolite science and practice*, 2<sup>nd</sup> Ed., Amsterdam, Elsevier Science, 2001, 509-510
- [102] ZEOCHEM Molecular Sieves, Last Accessed: : 08.08.2016  
[http://www.zeochem.ch/dev/html/molecular\\_sieves.html](http://www.zeochem.ch/dev/html/molecular_sieves.html)
- [103] R. Xu, W. Pang, J. Yu, Q. Huo, J. Chen, *Chemistry of Zeolites and Related Porous Materials: Synthesis and Structure*, Wiley, 2007, 13-15
- [104] J.S. Magee, M. M. Mitchell, *Fluid Catalytic Cracking: Science and Technology*, Elsevier Science, 1993, 41-45

- [105] J. L. Guthrie, H. Kessler, *Catalysis and Zeolites: Fundamentals and applications*, Springer, 1999, 1-52
- [106] V. Solinas, R. Monaci, B. Marongui, L. Forni, Isomerisation of 1-methylnaphthalene over synthetic zeolites, *Journal of Catalysis*, 1984, 9, 109-117
- [107] E. F. Sousa-Aguiar, A. J. C. Mota, M. L. M. Valle, Catalytic Cracking of Decalin Isomers over ReHY-zeolites with different sizes, *Journal of Molecular Catalysis A: Chemical*, 1996, 104, 267-271
- [108] N. Mori, S. Nishiyama, S. Tsuruya, M. Massi, Deactivation of Zeolites in n-hexane cracking, *Applied Catalysis*, 1991, 74, 37-52
- [109] A. Nock, R. Rudham, Enhanced Cracking Activity of Dealuminated Y Zeolites, *Zeolites*, 1987, 7, 481-484
- [110] K. Reddy, C. Song, Synthesis of Mesoporous Zeolites and Their Application for Catalytic Conversion of Polycyclic Aromatic Hydrocarbons, *Catalysis Today*, 1996, 31, 137-144
- [111] H. Starch, U. Lohse, H. Thamm, W. Schirmer, Adsorption Equilibria of Hydrocarbons on Highly Dealuminated Zeolites, *Zeolites*, 1986, 6, 74 - 90
- [112] G. Cerri, M. Farina, A. Brundu, A. Dakovic, P. Giunchedi, E. Gavini, G. Rassa, Natural Zeolites for Pharmaceutical Formulations: Preparation and Evaluation of a Clinoptilolite-based material, *Microporous and Mesoporous Materials*, 2016, 223, 58 -67
- [113] P. Gallezot, R. Beaumont, D. Barthomeuf, Crystal Structure of a Dealuminated Y-type zeolite, *Journal of Physical Chemistry*, 1974, 78, 1550 - 1553
- [114] J. Millic, A. Dakovic, G. Krajisnik, *Advanced healthcare materials*. Vol 1. Hoboken: John Wiley & Sons, Inc; 2014:403

- [115] M. Vallet-Regi, A. Ramila, R.P. del Real, J. Perez-Pariente, A new property of MCM-41, Drug delivery system, Chem. Mater., 2001, 13, 308-311
- [116] T. Sismanoglu, S. Pura, Adsorption of Aqueous Nitrophenols on Clinoptilolite, Colloids and Surfaces, 2001, 180, 1-6
- [117] IZA Commission on Natural Zeolites, Clinoptilolite, Last Accessed: 08.08.16  
<http://www.iza-online.org/natural/Datasheets/Clinoptilolite/clinoptilolite.htm>
- [118] G. Cerri, M. Farina, A. Brundu, A. Dakovic, P. Giunchedi, E. Gavini, G. Rassu, Natural zeolites for pharmaceutical formulations: Preparation and Evaluation of a Clinoptilolite-based Material, Microporous and Mesoporous Materials, 2016, 223, 58-67
- [119] Z. Li, T. Burt, R.S. Bowman, Sorption of Ionizable Organic Solutes by Surfactants Modified Zeolite, Environmental Science & Technology, 2000, 19, 3756-3760
- [120] S. Yaper, M. Yilmaz, Removal of Phenol by Montmorillonite, Clinoptilolite and Hydrotalcite, Adsorption, 2004, 10, 287-298
- [121] P. Misaelides, Application of natural zeolites in environmental remediation: A short review, Microporous Mesoporous Materials, 2011, 144, 15-18
- [122] L. Pasti, E. Sarti, A. Cavazzini, N. Marchetti, F. Dondi, A. Martucci, Factors affecting drug adsorption on beta zeolites, J. Sep. Sci. 2013, 36, 1604–1611
- [123] A. Corma, M. Moliner, A. Cantin, M. J. Diaz-Cabanas, J. L. Jorda, D. Zhang, J. Sun, K. Jansson, S. Hovmoller, X. Zou, Synthesis and structure of polymorph B of Beta zeolite, Chem. Mater, 2008, 20, 3218 - 3223
- [124] J. M. Newsam, M. M. J. Treacy, W. T. Koetsier, C. B. De Gruyter, Structural Characterization of Zeolite Beta, Mathematical, Physical and Engineering Sciences, 1988, 420, 375-405

- [125] H. M. Otker, I. Akmehmet-Balcioglu, Adsorption and degradation of enrofloxacin, a veterinary antibiotic on natural zeolite, *J Hazard Mater*, 2005, 251-258
- [126] S. N. Mohseni, A. A. Amooey, H. Tashakkorian, A. I. Amouei, Removal of dexamethasone from aqueous solutions using modified clinoptilolite zeolite (equilibrium and kinetic), *Int. J. Environ. Sci. Technol*, 2016, 13, 2261–2268
- [127] M. Sindia, Rivera-Jimenez, J. Atruro, Hernandez-Maldonado, Nickel(II) grafted MCM-41: A novel sorbent for the removal of Naproxen from water, *Microporous and Mesoporous Materials*, 2008, 116, 246–252
- [128] T. Xuan Bui, H. Choi, Adsorptive removal of selected pharmaceuticals by mesoporous silica SBA-15, *Journal of Hazardous Materials*, 2009, 168, 602–608
- [129] A. Martucci, L. Pasti, N. Marchetti, A. Cavazzini, F. Dondi, A. Alberti, Adsorption of pharmaceuticals from aqueous solutions on synthetic zeolites, *Microporous and Mesoporous Materials*, 2012, 148, 174–183
- [130] How does Ibuprofen work, Last Accessed: 30.09.16 <http://www.rsc.org/learn-chemistry/resources/chemistry-in-your-cupboard/nurofen/2>
- [131] The OTC marker in Britain, *The Pharmaceutical Journal*, Dawn Connelly, Last Modified: 24.04.16, Last Accessed: 30.09.16 <http://www.pharmaceutical-journal.com/news-and-analysis/features/sales-of-over-the-counter-medicines-in-2015-by-clinical-area-and-top-50-selling-brands/20200923.article>
- [132] A. Nikolaou, S. Meric, D. Fatta, Occurrence patterns of pharmaceuticals in water and wastewater environments, *Anal Bioanal Chem*, 2007, 387, 1225 - 1234
- [133] R. Bushra, N. Aslam, An overview of clinical pharmacology of Ibuprofen, *Oman Med J.*, 2010, 25, 155-1661

- [134] T. Heberer, Occurrence, fate, and removal of pharmaceutical residues in the aquatic environment: a review of recent research data, *Toxicology Lett.*, 2002,131, 5-17
- [135] D. W. Kolpin, E. T. Furlong, M. T. Meyer, E. M. Thurman, S. D. Zaugg, L. B. Barber, H. T. Buxton, Pharmaceuticals, hormones, and other organic wastewater contaminants in US streams, 1999–2000: a national reconnaissance, *Environ. Sci. Technol.*, 2002, 36, 1202–1211.
- [136] S. D. Richardson, Water analysis: Emerging contaminants and current issues, *Anal. Chem.*, 2007, 79, 4295-4324.
- [137] F. Pomati, A. G. Netting, D. Calamari, B. A. Neilan, Effects of erythromycin, tetracycline and ibuprofen on the growth of *Synechocystis* sp. and *Lemna minor*, *Aquat. Toxicol.*, 2004, 67, 387–396
- [138] T. Roizman, Ibuprofen side effects with longterm use, Last Modified: 2011 Retrieved from: <http://www.livestrong.com/article/102201-ibuprofen-side-effects-longterm-use> Last Accessed: 29/08/2016
- [139] B. C. Lourenção, R. A. Medeiros, R. C. Rocha-Filho, L. H. Mazo, O. F. Oilho, Simultaneous voltammetric determination of paracetamol and caffeine in pharmaceutical formulations using a boron-doped diamond electrode, *Talanta*, 2009, 78, 748–752.
- [140] M. Solé, J. P. Shaw, P. E. Frickers, J. W. Readman, T. H. Hutchinson, Effects on feeding rate and biomarker responses of marine mussels experimentally exposed to propranolol and acetaminophen, *Anal. Bioanal. Chem.*, 2010, 396, 649–656.
- [141] L. Yang, L. E. Yu, M.B. Ray, Degradation of paracetamol in aqueous solutions by TiO<sub>2</sub> photocatalysis, *Water Res.*, 2008, 42, 3480–3488.
- [142] J. J. Xu, B. S. Hendriks, J. Zhao, D. Graaf, Multiple effects of acetaminophen and p38 inhibitors: towards pathway toxicology, *FEBS Lett.*, 2008, 582, 1276–1282.

- [143] M. Grung, T. Kallqvist, S. Sakshaug, S. Skurtviet, K. V. Thomas, Environmental assessment of Norwegian priority pharmaceuticals based on the EMEA guideline, *Ecotoxicol Environ. Safe*, 2008, 71, 328-340.
- [144] A. M. Brind, Drugs that damage the liver, *Medicine*, 2007, 35, 26–30.
- [145] J. A. Hinson, A. B. Reid, S. S. McCullough, L. P. James, Acetaminophen-induced hepatotoxicity: role of metabolic activation, reactive oxygen/nitrogen species, and mitochondrial permeability transition, *Drug Metab. Rev.*, 2004, 36, 805–822.
- [146] H. Jaeschke, M. L. Bajt, Intracellular signaling mechanisms of acetaminophen-induced liver cell death, *Toxicol. Sci.*, 2001, 89, 31–41.
- [147] L. F. Prescott, Kinetics and metabolism of paracetamol and phenacetin, *Br. J. Clin. Pharmacol.*, 1980, 10, 291S–298S.
- [148] M. Patel, B. K. Tang, W. Kalow, Variability of acetaminophen metabolism in Caucasians and Orientals, *Pharmacogenetics*, 1992, 2, 38–45.
- [159] M. Grung, T. Kallqvist, S. Sakshaug, S. Skurtviet, K.V. Thomas, *Ecotox Environ Safe*, 2008, 71, 328-340.
- [150] T.A. Ternes, Occurrence of drugs in German sewage treatment plants and rivers, *Water Res.*, 1998, 32, 3245–3260.
- [151] D.W. Kolpin, E.T. Furlong, M.T. Meyer, E.M. Thurman, D.S. Zaugg, L.B. Barber, H.T. Buxton, Pharmaceuticals, hormones, and other organic wastewater contaminants in US streams, 1999–2000: a national reconnaissance, *Environ. Sci. Technol.*, 2002, 36, 1202–1211.
- [152] P. H. Roberts, K.V. Thomas, The occurrence of selected pharmaceuticals in wastewater effluent and surface waters of the lower Tyne catchment, *Sci. Total Environ.*, 2006, 356, 143–153.

[153] What is Adsorption?, International Adsorption Society, Last Viewed: 28.09.16

<http://ias.vub.ac.be/What%20is%20adsorption.html>

[154] T. X. Bui, V. H. Pham, S. T. Le, H. Choi, Adsorption of pharmaceuticals onto trimethylsilylated mesoporous SBA-15, Journal of Hazardous Materials ,2013, 254-255, 345–353

[155] V. Rakic, N. Rajic, A. Dakovic, A. Auroux, The adsorption of salicylic acid, acetylsalicylic acid and atenolol from aqueous solutions onto natural zeolites and clays: Clinoptilolite, bentonite and kaolin, microporous and Mesoporous Materials, 2013, 166, 185-194

[156] A. Clearfield, J. Reibenspies, N. Bhuvanesh, Principles and Applications of Powder Diffraction, Sussex: Wiley, 2008, 73-78

[157] C. Hammond, The Basics of Crystallography and Diffraction, New York: Oxford Science Publications, 1997, 125- 130

[158][http://www.softmatter.physik.unimuenchen.de/teaching/fortgeschrittenenpraktikum/sa\\_xs/R2b\\_Work\\_Instructions.pdf](http://www.softmatter.physik.unimuenchen.de/teaching/fortgeschrittenenpraktikum/sa_xs/R2b_Work_Instructions.pdf) Last viewed: 28.09.16

[159] C. Housecroft, Inorganic Chemistry, 4<sup>th</sup> ed., Essex: Pearson, 2012, 121-124

[160] V. Pecharsky, P. Zavalij, Fundamentals of Powder Diffraction and Structural Characterization of Materials, New York: Springer, 2003, 306-307

[161] A.K. Cheetham, P. Day, Solid State Chemistry Techniques, Oxford: Oxford Science Publications, 1988, 47-52

- [162] R. E. Dinnebier, S. J. Billinge, Powder diffraction: Theory and practice. Cambridge: Royal Society of Chemistry, 2008, 1-101
- [163] J. Evans, Pawley fitting, Last Modified: 09.04.16, Last Accessed: 28.09.16,  
[https://community.dur.ac.uk/john.evans/topas\\_workshop/tutorial\\_tio2pawley.htm](https://community.dur.ac.uk/john.evans/topas_workshop/tutorial_tio2pawley.htm)
- [164] B. Toby, R factors in Rietveld analysis: How good is good enough?, Advanced Photon Source, 2005, Last Accessed: 28.09.16 [http://x-ray.ucsd.edu/mediawiki/images/6/61/Toby\\_Rfactors.pdf](http://x-ray.ucsd.edu/mediawiki/images/6/61/Toby_Rfactors.pdf)
- [165] U. Kolb, K. Shankland, L. Meshi, A. Avilov, W. David, Uniting Electron Crystallography and Powder Diffraction, Springer, 2012, 22
- [166] O. McPolin, An Introduction to HPLC for Pharmaceutical Analysis, Mourne Training services, 2009, 41, 1-7
- [167] R. Terrill, An Introduction to High Performance Liquid Chromatography, 2003, Last Accessed: 15.08.2016  
<http://www.chemistry.sjsu.edu/rterrill/ped/55/Lab/HPLC%20analysis%20from%20155.pdf>
- [168] J. A. Martens, P. A. Jacobs, E. M. Flanigen, J. C. Jason, Introduction to Zeolite Science and Practice, Studies in surface science and catalysis, 2001, 137, 633 - 671
- [169] <http://www.shodex.com/en/kouza/f.html> Last viewed: 17.08.2016

[170] Introduction to IR Spectroscopy, Last Modified: 03.01.16, Last Viewed: 18.08.16

[http://www.rsc.org/learn-chemistry/wiki/Introduction\\_to\\_IR\\_spectroscopy](http://www.rsc.org/learn-chemistry/wiki/Introduction_to_IR_spectroscopy)

[171] Spectra School, RSC, Last viewed: 18.08.16 [http://www.rsc.org/learn-](http://www.rsc.org/learn-chemistry/collections/spectroscopy/introduction#IRSpectroscopy)

[chemistry/collections/spectroscopy/introduction#IRSpectroscopy](http://www.rsc.org/learn-chemistry/collections/spectroscopy/introduction#IRSpectroscopy)

[172] A. West, Solid State Chemistry and its Applications, John Wiley: United Kingdom, 2014, 298-299

[173] M. A. Hemminga, Introduction to NMR, Trends in Food Science and Technology, 1992, 3, 179 - 186

[174] L. Reimer, Scanning Electron Microscopy, 2<sup>nd</sup> ed., Heidelberg: Springer, 1988, 2-10

[175] N. Valery, Shake-out Among the Microscope Makers, New Scientist, September 1972, 498

[176] Fourier Transform-Infrared Spectroscopy (FTIR), Materials Evaluated and Engineering, INC., Last Accessed: 28.09.16 <http://www.mee-inc.com/hamm/energy-dispersive-x-ray-spectroscopyeds/>

[177] Introduction to BET (Brunauer, Emmett and Teller), Particle Analytical, Last viewed: 28.09.16 <http://particle.dk/methods-analytical-laboratory/surface-area-bet-2/>

[178] G. Attard, C. Barnes, Surfaces, Oxford Chemistry Primers, Oxford New York, 2009, 6-7

- [179] G. Caviglioli, P. Valeria, P. Brunella, C. Sergio, A. Attilia, B. Gaetano, Identification of degradation products of ibuprofen arising from oxidative and thermal treatments, *J Pharm Biomed Anal.*, 2002 ,15, 499-509.
- [180] C. Naccache, Y. B. Tarrit, In: F. R. Riberio, A. E. Rodrigues L. D. Rollmann, C. Naccache (Eds.), *Zeeolite Science and Technology* Martinus Nijhoff Publishers, The Hague, 1984
- [181] T. I. Korányi, K. Föttinger, H. Vinek, J. B. Nagy, Characterization of aluminum sitting in MOR and BEA zeolites by  $^{27}\text{Al}$ ,  $^{29}\text{Si}$  NMR and FTIR spectroscopy, 2005, 158, 765-772
- [182] A. Martucci, L. Pasti, N. Marchetti, A. Cavazzini, F. Dondi, A. Alberit, Adsorption of pharmaceuticals from aqueous solutions on synthetic zeolites, *Microporous and Mesoporous Materials*, 2012, 148, 174-183
- [183] B. de Gennaro, L. Catalanotti, P. Cappelletti, A. Langella, M. Mercurio, C. Serri, M. Biondi, L. Mayol, Surface modified natural zeolite as a carrier for sustained diclofenac release: A preliminary feasibility study, *Colloids and Surfaces B: Biointerfaces*, 2015, 130, 101–109
- [184] A. Datt, Applications of mesoporous silica and zeolites for drug delivery, 2012, 22-23, last accessed: 20.05.17 <http://ir.uiowa.edu/cgi/viewcontent.cgi?article=3443&context=etd>